

Aus der Elisabeth-Klinik Bigge
Fachklinik für Orthopädie und Rheumatologie
Leiter : Professor Dr. Dr. Axel Wilke
des Fachbereich Medizin der Philipps-Universität Marburg
in Zusammenarbeit mit dem Universitätsklinikum Gießen und Marburg GmbH
Standort Marburg



Acoustic Emission Measurement System in Diagnostic of Cartilage Injuries of the Knee

Inaugural-Dissertation zur Erlangung des Doktorgrades der gesamten
Humanmedizin
Dr.med.
dem Fachbereich Medizin der Philipps-Universität Marburg
vorgelegt von

Cristina Zolog
aus Cluj-Napoca, Rumänien

Marburg 2011

Angenommen vom Fachbereich Medizin der Philipps-Universität Marburg am:
09.03.2011

Gedruckt mit Genehmigung des Fachbereichs.

Dekan: Prof. Dr. med. Matthias Rothmund
Referent: Priv. Doz. Dr. med. Stefan Endres
Vorsitzender : PD Dr. Skwara
Korreferent: Prof. Dr. Dr. Heverhagen

Contents

1. INTRODUCTION.....	8
2. ANATOMY OF THE KNEE.....	9
Hyaline / Articular cartilage.....	11
3. IMAGING OF THE KNEE.....	16
3.1. Radiographic examination of the knee.....	16
3.2. Radionuclide imaging.....	20
3.3. Arthrography.....	21
3.4. Ultrasound.....	22
3.5. Magnetic resonance imaging (MRI).....	23
3.5.1. Bone disorders.....	24
3.5.2. Articular disorders.....	26
3.5.3. Soft tissue disorders and synovial disorders.....	27
4. RELEVANT BIOMECHANICS OF THE KNEE.....	29
4.1. Kinematics.....	29
4.2. Kinetics.....	38
4.2.1. Statics of the tibiofemoral joint.....	38
4.2.2. Dynamics of the tibiofemoral joint.....	40
5. AIM OF THE STUDY.....	47
6. ACOUSTIC EMISSION MEASUREMENT SYSTEM FOR THE ORTHOPEDICALLY DIAGNOSTIC OF THE KNEE JOINT.....	48
7. MATERIAL AND METHODS.....	56
8. RESULTS.....	60
9. DISCUSSIONS.....	76
10. CONCLUSIONS.....	85
11. REFERENCES.....	87

Acknowledgments

Ehrenwörtliche Erklärung

Verzeichnis akademischer Lehrer

Curriculum vitae

Zusammenfassung in deutscher Sprache

Mittels eines speziell entwickelten Gerätes (Bonedias - Bone Diagnostic System) konnte am menschlichen Kniegelenk durch eine Roll-Gleitbewegung (Kniebeuge) eine physiologische Schallemission akustisch sichtbar gemacht werden. In der vorliegenden Studie wurden über 100 Patienten untersucht, einen Tag vor einer geplanten Operation (Arthroskopie oder Knieendoprothese) untersucht, um eine mögliche Korrelation zwischen der akustischen Schallemission mit den intraoperativen pathologischen Befunden zu prüfen. Über 100 Patienten wurden evaluiert. Analogien zwischen den intraoperativen gefundenen Knorpelschaden und dem Alter, dem Geschlecht, der Länge des Oberschenkels, der Dicke des Oberschenkels, dem Body Mass Index und der Fehlstellung des Kniegelenkes wurden mituntersucht.

Das Ziel dieser Studie ist die Evaluation eines nicht invasivem Untersuchungsverfahrens zur Beurteilung von Knorpelschadens am Kniegelenk, auch schon im Anfangsstadium. Bislang wurden teure oder invasive Diagnoseverfahren benutzt um Schädigungen im menschlichen Knie bewerten zu können. Die Schallemissionsanalyse ist ein nicht-invasives, kostengünstiges Verfahren, das typische Signalmusters anbietet und die in der Zusammenschau mit den klinischen Befunden Hinweise auf vorliegende Knorpelläsionen erlaubt.

Die Ergebnisse dieser Studie zeigen über 60% Übereinstimmung zwischen Schallemissionsanalyse und den fortgeschrittenen Knorpeldefekte (typ III und IV nach Outerbridge). Von höherem Stellenwert sind die Ergebnisse mit 50% Übereinstimmung für die Knorpelläsionen Typ 0, I und II nach Outerbridge, mit den Schallemissionen-Signalen. Die typischen Schallsignale, die mit den intraoperativen Befunde (arthroskopische Befunde) korrespondiert werden können, zeigen die Bedeutung dieses Verfahren für die Diagnostik der beginnenden Knorpelschaden. Diese Methode ist noch nicht ausgereift. Die Ergebnisse der Schallemission sind statistisch nicht eindeutig der Knorpelschaden im Stadium 0-II zuzuordnen (50%). Dennoch bietet der Einsatz in viele Fällen weitere Informationen an, die in der Zusammenschau der klinischen Befundergebnisse in Zukunft in der weiteren Einschätzung der diagnostischen und therapeutischen Vorgehensweise benutzt werden können. Das Verfahren ist noch nicht ideal um Schallsignale zweifelsfrei mit intra-arthroskopischen Befunde

nebeneinanderzustellen. Jeder Patient muss separat untersucht und ausgewertet werden, was relativ viel Zeit in Anspruch nimmt: 20-30 Minuten für die Schallemissionsuntersuchung, klärende Fragen und klinische Tests, sowie weitere 15 Minuten für die Auswertung der Signale und den Vergleich mit den intraoperativen Befunden. Im Rahmen einer wissenschaftlichen Studie ist dieser Zeitaufwand akzeptabel, kaum jedoch für die tägliche Praxis. Eine verfeinerte standardisierte Auswertung nach weiteren, größeren Studien könnte wichtige Vorteile und Gewinne bezüglich der Bestimmung von Knie-Knorpelschäden in frühen Stadien ergeben.

Zusammenfassend bietet diese Studie maßgebliche Informationen über die Rolle der Schallemissionsanalyse bei Knorpelerkrankungen am Kniegelenk an, Informationen die für die zukünftige Studien benutzt werden können. Dieses Verfahren ist günstig und nicht-invasiv, zeitaufwändig und benötigt weitere Verbesserungen, damit die Methode hilfreich in der Diagnostik der früheren Stadien der Knorpelläsionen im alltäglichen Gebrauch angewendet werden kann.

Abstract

The measurement system BONEDIAS (Bone Diagnostic System) was developed as a non-invasive diagnostic method, based on the analysis on the acoustic emission from the knee joint. Knee squats of a patient will release acoustic emission in high temporal resolution and well correlated to the angle of knee flexion. The physician will get the relevant information concerning arthritic lesions in the knee joint (well characterized acoustic emission, singular events without a follow up of further emission), acoustic emission due to elevated intra-articular friction caused by e.g. cartilage lesions, inappropriate surface roughness, a lack of synovial fluid or crack initiation in the femur. Over 100 patients were analyzed with the measurement system BONEDIAS, afterwards the results were compared with the intra-operative views (arthroscopy and arthroplasty of the knee). Other parameters were studied, concerning the relation between the age and the sex of the subjects, the length of the femur, thigh thickness, the body mass index, the anatomical axis of the knee and the appearance and severity of the cartilage lesions.

The study was made with the purpose to see if there was a correspondence between the cartilage disorders, the intraoperative views (arthroscopy and the arthroplasty of the knee) and the acoustic emission measurements, performed one day before the surgery. Because there aren't at this moment cheap and standards methods who can determine the early cartilage injuries, this study is supposed (concording with the results) to open new ideas and new advantages in the diagnostic of this often disease, using the acoustic emission measurement system.

The results obtained, 50% correspondence for the gr. 0, I and II Outerbridge lesions are more important, more significant than the other results, with over 60% correspondence for the advanced osteoarthritis. The obtained acoustic emission signals, corresponding to the intra-arthroscopic findings showed the importance of this method to identify the early cartilage injuries. The method is not perfect and the results (50%) are not really statistically significant, so that we can introduce this method on a large scale, but offers important information that should be used in the future. Also, there isn't a perfect method to compare the acoustic emission signals with the intra-arthroscopic findings. Every patient was analysed separately and with his corresponding measurement compared, that means a lot of time (20 – 30 minutes for the measurement and the other questions and clinical tests and another 15 minutes to analyse the signals

and compare them with the intra-operative findings). For a study this can be accepted, but for clinical every day use maybe not. A standard interpretation and analyse method, maybe after clinical large trials, if such a method can be developed, could bring big advantages for the early determination of the cartilage injuries.

In conclusion, the study had offered important informations about the importance of accoustic emission measurements, that can be used for the future studies and with some improvements, this method , cheap and non-invasive, but at this moment a little beat time-consuming, can be helpful in the diagnose of the early cartilage injuries.

1. INTRODUCTION

The measurement system BONEDIAS (Bone Diagnostic System) was developed as a non-invasive diagnostic method, based on the analysis on the acoustic emission from the knee joint.

BONEDIAS

Method of fracture diagnostic / German Patent P4422451.6

Training system with a device of performing a procedure that stimulates the bone growth / EU Patent 0821929

BONEDIAS Brand owner Nr. 304 64 589

Patent application DE 10254065 A1 2004.06.03

Owner of the patent B.Ziegler, Dr. H.-J. Schwalbe

Knee squats of a patient will release acoustic emission in high temporal resolution and well correlated to the angle of knee flexion. The physician will get the relevant information concerning arthritic lesions in the knee joint (well characterized acoustic emission, singular events without a follow up of further emission), acoustic emission due to elevated intra-articular friction caused by e.g. cartilage lesions, inappropriate surface roughness, a lack of synovial fluid or other defects (a plethora of continuous emission), crack initiation in the femur (a burst type of acoustic emission followed by continuous emission, which is typical of relaxation phenomena in the crack banks). Over 100 patients were analyzed with the measurement system BONEDIAS, afterwards the results were compared with the intra-operative views (arthroscopy and arthroplasty of the knee). Other parameters were studied, concerning the relation between the age and the sex of the subjects, the length of the femur, thigh thickness, the body mass index, the anatomical axis of the knee and the appearance and severity of the cartilage lesions.

2. ANATOMY OF THE KNEE

The anatomy of the knee can be examined on a number of levels from the microscopic to gross and using a variety of techniques, including physical examination, anatomic dissection, radiographic and cross-sectional imaging and arthroscopic examination. Some important aspects concerning the anatomy of the knee will be presented below, emphasizing my object of study, the articular cartilage.

The knee joint consists of three bony structures – the femur, tibia and patella – that form three distinct and partially separated compartments: the medial, lateral and patellofemoral compartments. [52]

The patella is the largest sesamoid bone in the body and sits in the femoral trochlea. The articulation between the patella and femoral trochlea forms the anterior or patellofemoral compartment. The architecture of the distal femur is complex. Furthermore, this area serves as the attachment site of numerous ligaments and tendons. The lateral condyle is slightly wider than the medial condyle at the center of the intercondylar notch. Anteriorly, the condyles are separated by a groove: the femoral trochlea. The sulcus represents the deepest point in the trochlea. Relative to the midplane between the condyles, the sulcus lies slightly laterally.

The intercondylar notch separates the two condyles distally and posteriorly. The lateral wall of the notch has a flat impression, where the proximal origin of the anterior cruciate ligament (ACL) arises. On the medial wall of the notch is a larger site where the posterior cruciate ligament (PCL) originates. The mean width of the notch is narrowest at the distal end and widens proximally (1,8 to 2,3 cm); in distinction, the height of the notch is greatest at the midportion (2,4cm) and decreases proximally (1,3cm) and distally (1,8cm).

The lateral condyle has a short groove just proximal to the articular margin, in which lies the tendinous origin of the popliteus muscle. This groove separates the lateral epicondyle from the joint line. The lateral epicondyle is a small but distinct prominence to which attaches the lateral (fibular) collateral ligament (LCL). On the medial condyle the prominent adductor tubercle is the insertion site of the adductor magnus. The medial epicondyle lies anteriorly and distally to the adductor tubercle and is a C-shaped ridge with a central depression or sulcus. Rather than originating from the ridge, the medial collateral ligament (MCL) originates from the sulcus. The epicondylar axis passes through the center of the sulcus of the medial epicondyle and the prominence of the

lateral epiconyle. This line serves as an important reference line in total knee replacement. Measurements of the width of distal femur along the transepicondylar axis suggest that women have narrower femurs than males relative to the anteroposterior dimension. (Fig. 2.1. and 2.2.) [52]

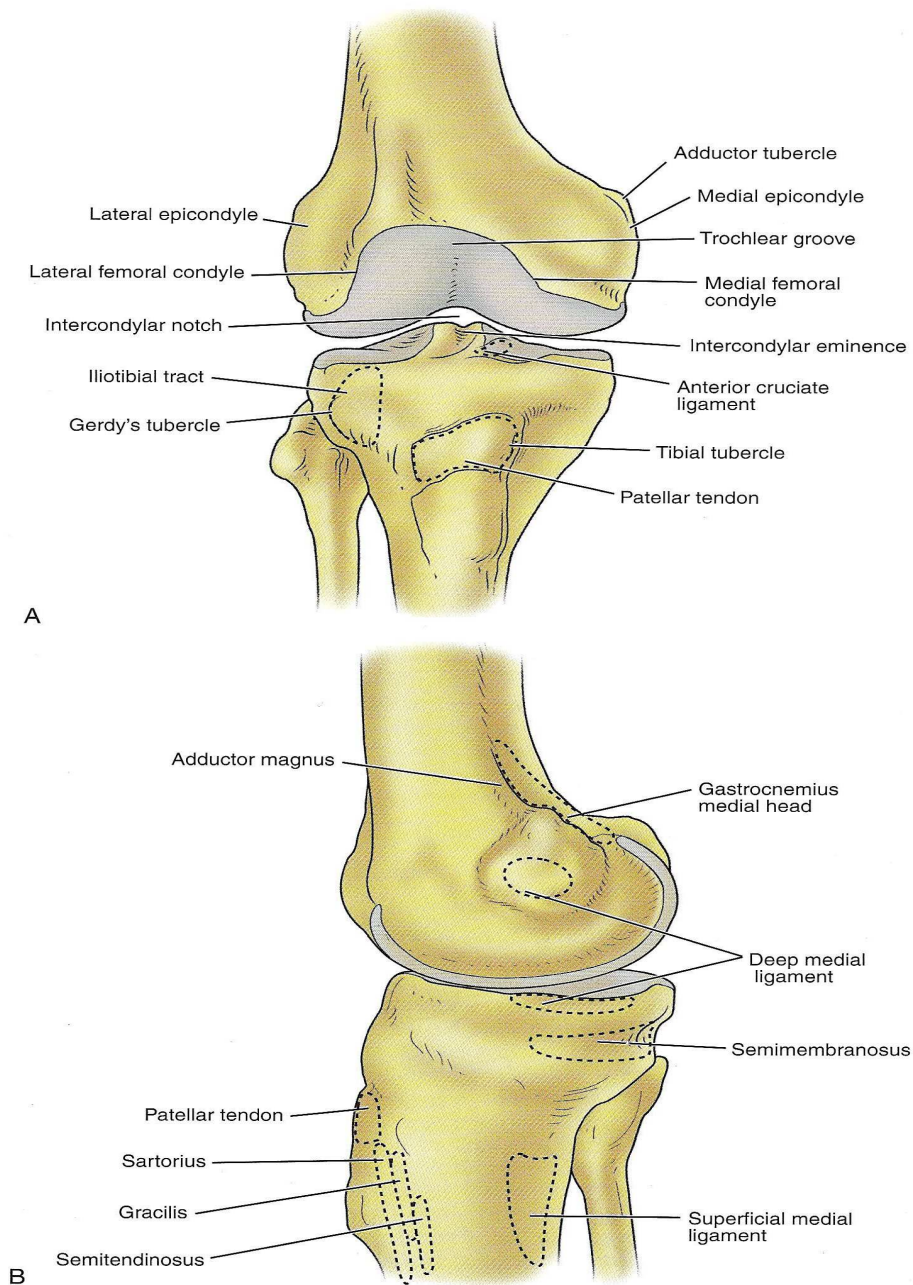


Illustration continued on following page

Figure 2.1.. Bony landmarks with ligament and tendon attachment sites on the anterior (A), medial (B).

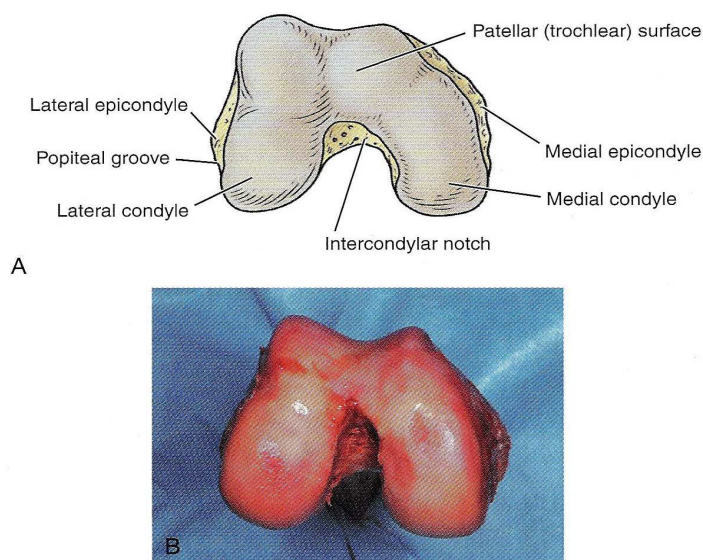


Figure 2.2. A) Bony architecture of the distal femur; B) Anatomic specimen of the distal femur. The femoral trochlea separates the lateral and medial femoral condyles. The deepest point lies slightly offset to the lateral side. The anterior aspect of the lateral condyle is more prominent than the medial side.

In a macerated skeleton, inspection of the tibial plateau suggests that the femoral and tibial surfaces do not conform at all. The larger medial tibial plateau is nearly flat and has a squared-off posterior aspect that is quite distinct on a lateral radiograph. In distinction, the articular surface of the narrower lateral plateau borders on convexity. Both have a posterior inclination with respect to the shaft of the tibia of approximately 10 degrees. However, the lack of conformity between the femoral and tibial articular surfaces is more apparent than real. In the intact knee, the menisci enlarge the contact area considerably and increase the conformity of the joint surfaces. The median portion of the tibia between the plateau is occupied by an eminence: the spine of the tibia. Anteriorly there is a depression, the anterior intercondylar fossa, to which, from anterior to posterior, the anterior horn of the medial meniscus, the ACL, and the anterior horn of the lateral meniscus are attached. Behind this region are two elevations: the medial and lateral tubercles. They are divided by a gutter-like depression: the intertubercular sulcus. Approximately 2 to 3 cm lateral to tibial tubercles is Gerdy's tubercle, which is the insertion site of the iliotibial band (ITB). [52]

Hyaline / Articular cartilage

Articular cartilage is a specialized connective tissue composed of hydrated proteoglycans within a matrix of collagen fibrils. Proteoglycans are complex

glycoproteins that are made up of a central protein core to which are attached glycosaminoglycan chains. The structure of hyaline cartilage is not uniform, but rather can be divided into distinct zones based on the arrangement of collagen fibrils and the distribution of chondrocytes. The density of chondrocytes is highest close to the subchondral bone and decreases toward the articular surface. Calcification occurs in a distinct basophilic zone at the deepest level of chondrocyte proliferation termed the tidemark. Beneath this region is a zone of calcified cartilage that anchors the cartilage to the subchondral plate. Cartilage is avascular and chondrocytes in the superficial zones are believed to derive nutrition from the synovial fluid. Deeper zones likely obtain nutrition from the subchondral bone. (Fig. 2.3.)

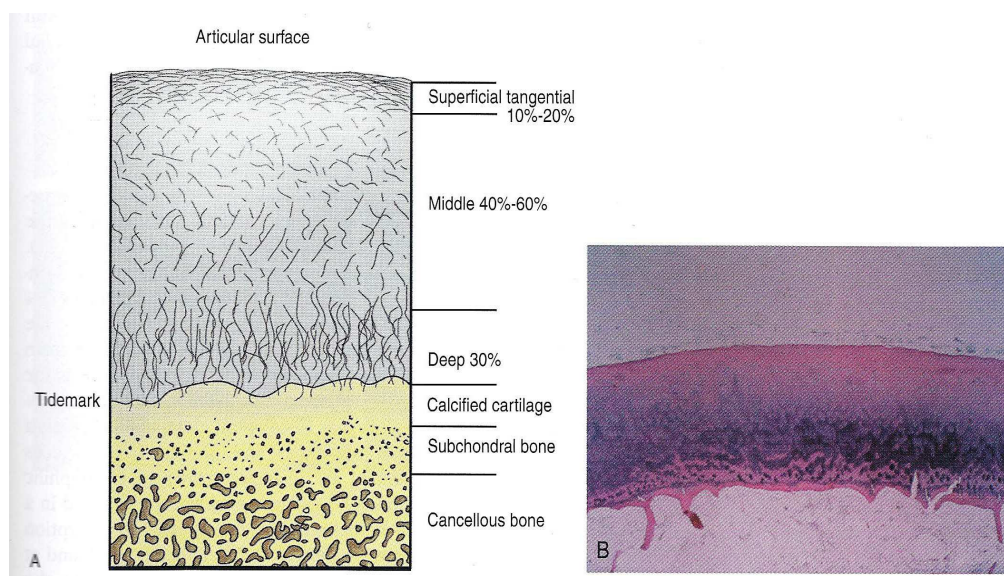


Figure 2.3. A) Diagrammatic representation of the transition from articular cartilage to the bone. B) Normal articular (hyaline) cartilage, composed of water, collagen and proteoglycan. The sparsely cellular smooth superficial zone becomes increasingly cellular in deeper layers. A distinct basophilic line, the mineralization front, can be seen where cartilage becomes calcified.

Examination of gross specimens or arthroscopic visualization reveals normal cartilage to be white, smooth and firm material. Articular cartilage damage or degeneration, termed chondromalacia, can be quite readily identified. These characteristic changes seen during arthroscopic examination have been classified by Outerbridge: grade 0 is normal, white-appearing cartilage; grade I is swelling or softening of an intact cartilage surface; grade II is represented by fissuring and fibrillation over a small area (<1,2 cm); grade III is the same pathological changes over a large area (>1,2 cm); grade IV represent erosion to the subchondral bone and are

indistinguishable from osteoarthritis. Chondral flap tears caused by delamination of the articular cartilage may be also encountered. (Fig. 2.4.) [52]

These changes in the articular cartilage cannot be directly visualized on conventional radiographs but may be seen on magnetic resonance imaging (MRI) studies. However, even MRI is unreliable for detecting early stages of chondromalacia. These may appear as foci or areas of diffuse abnormal signal with a normal surface. Grad III or IV chondromalacia is visible as thinning, irregularity and fissuring of the cartilage. [52]

Damage to the articular cartilage and joint surface may result indirectly from pathological changes in the subchondral bone. Both osteonecrosis and osteochondritis dissecans (OCD) may lead to destruction of the articular surface. In the knee, OCD tends to occur on the intercondylar aspect of the medial femoral condyle in young people. These lesions may separate from the surface and form a loose body. The base of these lesions will reveal vascular subchondral bone if debrided. Classic radiographic findings include a lucent osseous defect that may have a fragmented or corticated osseous density within the lucency. On MRI studies, increased signal about the defect on T2-weighted images represents joint fluid surrounding the lesion; irregularity of the articular surface may also be noted. Osteonecrosis results in a similar osteochondral fragment but tends to occur in elderly patients on the weightbearing aspect of the medial femoral condyle. In distinction to the lesions in OCD, fragments in osteonecrosis separate from a bed of avascular bone. Again, radiographs may reveal a lucent defect at the involved site, but MRI is more reliable for the evaluation of these defects. A curvilinear area of low signal with variable bone edema is characteristic. Although the articular cartilage is initially normal, both processes may lead to detachment of osteochondral loose bodies, fragmentation and collapse of the articular surface, resulting in degenerative changes.

The menisci are two crescentic fibrocartilage structures that serve to deepen the articular surfaces of the tibia for reception of the femoral condyles. Each meniscus covers approximately the peripheral two-thirds of the corresponding articular surface of the tibia. The peripheral border of each meniscus is thick, convex and attached to the capsule of the joint; the opposite border tapers to a thin, free edge. The proximal surface of the menisci are concave and are in contact with the femoral condyles; the distal surfaces are flat and rest on the tibial plateau.

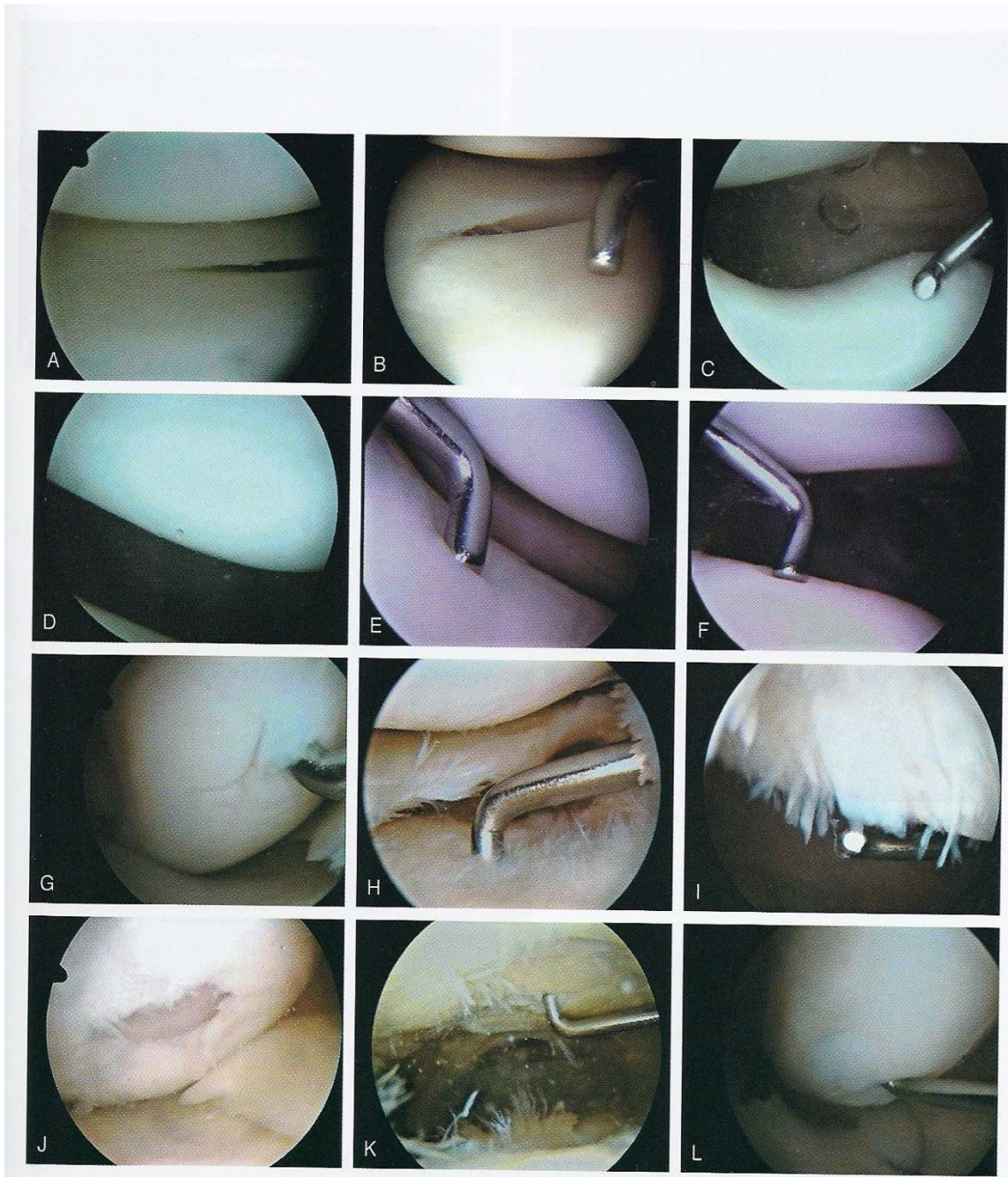


Figure 2.4. Arthroscopic views of articular cartilage. Normal white, smooth articular cartilage (Outerbridge grade 0) in the medial (A), lateral (B) and patellofemoral compartments (C and D). Softening of the articular surface of the lateral tibial plateau (E) and patellofemoral articulation (F) with indentation at the probe tip (Outerbridge grade 1) is noted. (G) A small fissure and fibrillation of the medial femoral condyle (Outerbridge grade 2). Extensive fibrillation of the articular cartilage involving the tibial plateau (H) and patella (I) (Outerbridge grade 3). Erosion of articular cartilage to subchondral bone involving the medial femoral condyle (J) and patella (K) (Outerbridge grade 4). Arthroscopic view of a chondral flap tear (L); the probe tip is deep to a flap of delaminated articular cartilage on the medial femoral condyle.

The menisci perform several important functions, including (1) load transmission across the joint, (2) enhancement articular conformity, (3) distribution of synovial fluid across the articular surface and (4) prevention of soft-tissue impingement during joint motion. The medial meniscus also confers some stability to the joint in the presence of ACL insufficiency where the posterior horn acts as a wedge to help reduce anterior tibial translation. However, the lateral meniscus does not perform a similar function. The rapid progression of degenerative changes, first observed by Fairbank, that occur as a result of complete meniscectomy have been well documented. These changes include (1) osteophyte formation on the femoral condyle projecting over the site of meniscectomy, (2) flattening of the femoral condyle and (3) narrowing of the joint space on the involved compartment.[52]

3. IMAGING OF THE KNEE

There are nowadays many methods for investigation the knee. Each method has its advantages and disadvantages. With some methods it can be better shown the osseous structures, with others the soft tissues or the effusions. In this chapter there will be presented the methods that exist till now, what can we see with the help of these methods and all that, to show the need of developing a new method for detecting the cartilage injuries.

3.1. Radiographic examination of the knee

A routine radiographic examination of the knee consists of standard anteroposterior (AP) and lateral and tangential axial ("sunrise") views. Other supplemental views include the tunnel view and the flexed, weightbearing posteroanterior (PA) view. [52]

Normal radiographic findings

Soft tissues

The soft tissues of the knee are optimally demonstrated with low kilovoltage. On the lateral view, one can see the quadriceps, patellar tendons and the suprapatellar pouch. These soft tissue structures are normally straight, are of uniform thickness and are sharply demarcated posteriorly by fat. The soft tissues demonstrated on the AP view are the medial and lateral supporting ligaments; however, they have no distinguishing radiographic characteristics unless they are calcified.

Osseous structures

The osseous structures of the knee include the bones and their articulations. Radiographically, the mineralization alignment, integrity and articulation of the bones are examined. The bones of the knee are the distal femur, proximal tibia and fibula, patella and on occasion, a fabella and/or cyamella. The fabella is a sesamoid bone in the lateral head of the gastrocnemius and is identical on the lateral view posterior to the distal femur; on the AP view it is super imposed on the lateral femoral condyle. The cyamella is a sesamoid bone in the popliteus tendon and it is identified on the AP and oblique views in the groove in the lateral aspect of the lateral femoral condyle.

Three joint compartments comprise the knee joint: the medial and lateral femoral tibial compartments and the patello-femoral compartment. Alignment and joint space width of the medial and lateral compartments are best assessed on the AP view, whereas the patello-femoral compartment is most optimally assessed on the Merchant view. The width of the lateral joint compartment is normally wider than that of the medial compartment; this asymmetry should not be misinterpreted as cartilage loss. (Figure 3.1., 3.2. and 3.3.) [52]

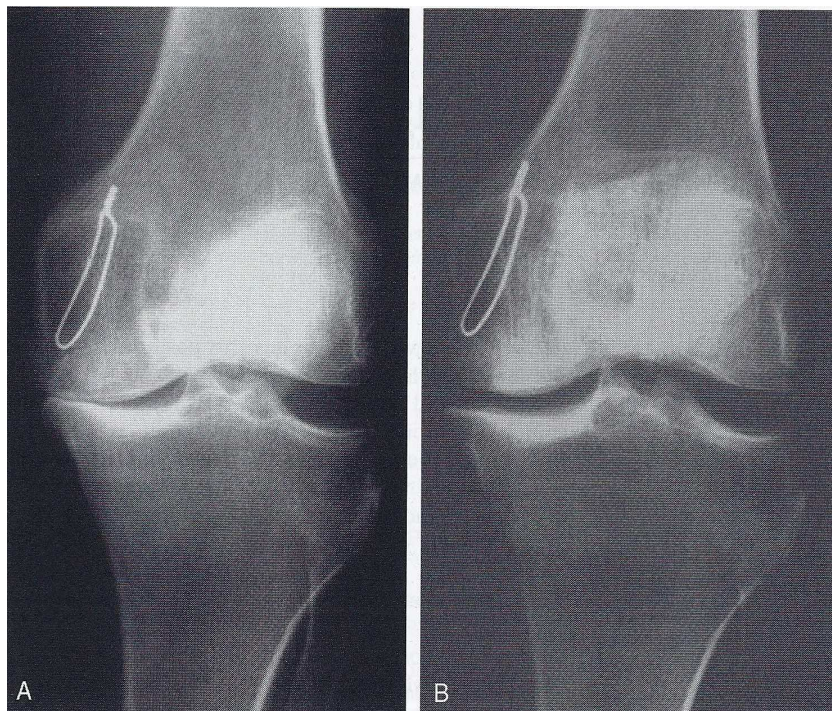


Figure 3.1. Anteroposterior supine versus weightbearing. The severe medial joint space narrowing is much more apparent on the weightbearing view (A) than on the supine view (B).

Special Views

Some radiographic techniques have special applications. Although these are not routinely obtained in the evaluation of patients with knee problems, in certain conditions these individual views may be indicated.

Obliques

Oblique radiographs of the knee are usually not necessary. They have limited usefulness for evaluating possible nondisplaced and/or stress fractures about the knee. They can conceivably also be helpful for evaluation of conditions such as osteochondritis dissecans or Salter fractures of the distal femoral or proximal tibial

physes. Two views are described, a lateral oblique and a medial oblique, each taken 45 degrees from the AP plane.

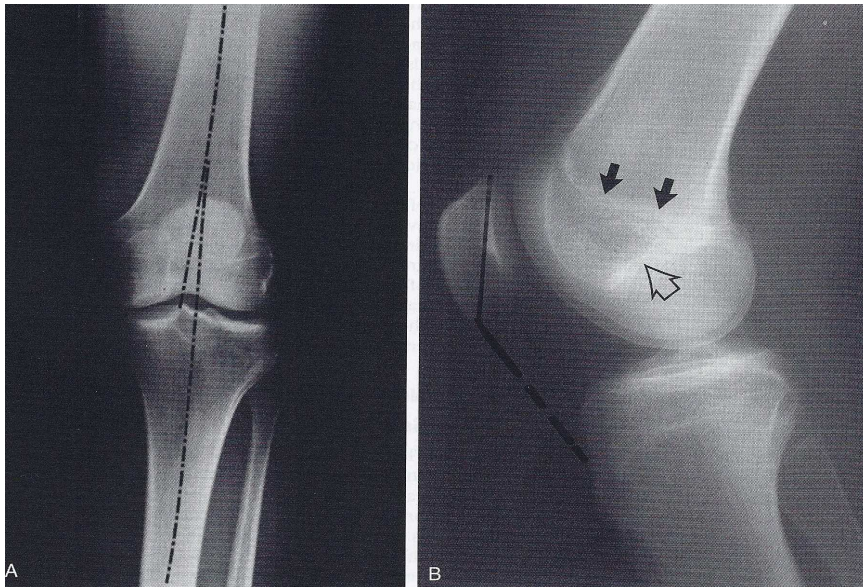


Figure 3.2. A) Normal anteroposterior view of the knee. The osseous structures are normally mineralized and the articular cortices are smooth. The femoral tibial alignment is in 7° of valgus. The lateral compartment is normally slightly wider than the medial compartment. B) Lateral view of the knee. Blumensaat's line (open arrow) represents the roof of the intercondylar notch. The physeal scar is indicated by the solid arrows. The patella is commonly located between these two lines, with the lower pole approximately at the level of Blumensaat's line. The Insall-Salvati ratio is a more accurate method of assessing patellar height; the length of the patellar tendon divided by the greatest diagonal length of the patella should be equivalent (0,8 to 1,2).

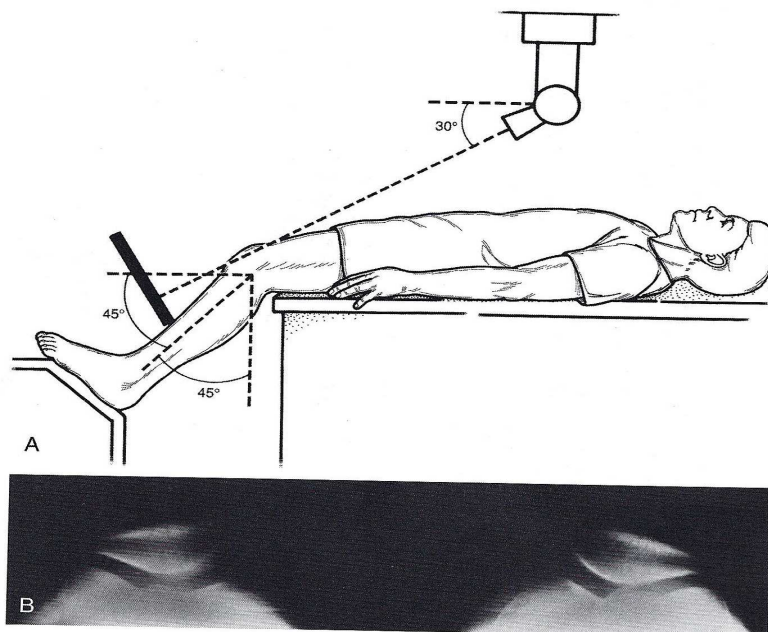


Figure 3.3. Merchant's view. A) Technique. B) Normal Merchant's view. Patellofemoral alignment is normal bilaterally and the osseous articular cortices are normal.

Notch view

The notch view radiograph is included in some routine knee series. It is a non-weight-bearing view taken in the AP plane with the knee flexed approximately 60 degrees. This view is most often used for evaluation of osteochondritis dissecans, osteonecrosis or loose bodies.

Stress views

Stress radiographs are those obtained while an examiner applies a force in certain direction to the knee. These could conceivably be of use in evaluation medial collateral ligament (MCL) or lateral collateral ligament (LCL) injuries, but their most common use is for evaluating occult growth plate fractures around the knee. It should be noted that obtaining stress radiographs of the knee in the setting of a possible growth plate injury is controversial. Although these types of radiographs may better delineate the fracture pattern, some believe that, by performing this radiographs, additional trauma is being inflicted on the growth plate and may adversely affect the eventual healing response of the fracture. Another use of stress fracture is to evaluate the amount of translation between the femur and tibia in knees with ACL or PCL injury. This can be useful for evaluating the success of operative procedures or in correlation with arthrometer measurements.

Patological findings

Soft tissues

Radiographically, the most common abnormality in the knee is an oval, soft tissue density posterior to the quadriceps tendon. It indicates an abnormality distension of the suprapatellar pouch by either joint infusion or synovial hypertrophic tissue. A joint infusion may be synovial fluid, blood or pus.

When a joint infusion is present in a patient with a clinically suspected occult fracture, a „cross-table“ lateral view is often helpful. This view is obtained with the patient supine, the cassette perpendicular to the table top and the central x-ray beam perpendicular to the cassette. A fracture that involves an articular surface bleeds into the joint, this blood contains bone marrow fat. Because fat has a lower specific gravity than blood, it separates from the blood and layers on top of it analogous to oil floating on water. The sharpe interface between the low density of fat and the soft tissue density of blood can be distinguished radiographically on this view, the so-called „fat fluid level“.

Popliteal (Baker's) cysts often present as a soft tissue mass in the popliteal fossa. They are almost always accompanied by a joint effusion and represent communication of the synovial cavity with a bursa/recess at the postero-medial aspect of the knee. The communication of the knee between the joint and this recess exists between the tendon of the medial head of the gastrocnemius and the semimembranosus. Plain films are insensitive for diagnosing popliteal cysts, as the soft tissue density of the gastrocnemius muscles obscures their visualization. The cyst and communication with the joint can be accurately diagnosed most cost-effectively on ultrasonography and can also be clearly delineated on MRI.

Calcifications

Calcification of the knee can be extra-articular or intra-articular and the cause of these calcifications can often be determined by fairly specific distinguishing characteristics. Causes of extra-articular calcifications include normal anatomic structures (fabella, cyamella), tendon and ligament calcification (Pellegrini-Stieda disease – calcification around the medial collateral ligament; Osgood-Schlatter disease – calcification at the tibial tubercle insertion of the patellar tendon; Sinding-Larsen-Johansson disease – calcification of the patellar attachment of the patellar tendon; myositis ossificans – ossification in the soft tissue), calcified bursitis, tendon calcification/ossification, calcified neoplasm (extra-articular; intra-articular calcification: within the articular cartilage or meniscal cartilage – chondrocalcinosis, calcified loose bodies, and calcification in the infra-patellar fat pad – Hoffa's disease), aneurysm, and tumoral calcinosis.[52]

Avulsion fractures

Originally described in the 1879 and otherwise known as the lateral capsular sign, a Segond fracture is an avulsion lesion of the lateral aspect of the tibia. This can be seen on the AP radiograph or the flexion weight-bearing view. It is significant because it has a high level of association with ACL disruption.

3.2. Radionuclide imaging

Radionuclides may be used to image abnormalities of the knee that are not visible on radiographs. Radionuclide imaging is based on differences in uptake of radionuclides containing radioisotopes by normal and abnormal tissue because of physiological and biological differences rather than anatomic differences, as with

radiographs. The radioisotope emits gamma energy until it decays to a stable state. Gamma rays are detected by a gamma camera using a sodium iodide crystal. When the crystal absorbs the gamma ray or x-ray, it scintillates; that is, it emits light. This light is converted to an electrical pulse by photomultiplier tubes and is amplified. This sequence of events allows creation of an image based on the intensity and distribution of radioactivity in the body. Lead collimators focus the image and increase the resolution by absorbing scattered radiation. All-purpose or high resolution collimators are used routinely. Higher resolution and magnification of the image can be obtained by using a pinhole collimator, but this is at the cost of additional scanning time. Routine images on a gamma camera are two-dimensional (planar). Tomographic images can be obtained by rotating the gamma camera in an elliptical or circular arc around the imaged body part. This is known as single photon emission computed tomography (SPECT). Computerized reconstruction of the data allows tomographic images to be obtained in axial, coronal and sagittal planes. Although there are several reports showing increased accuracy of SPECT for diagnosing abnormalities in the knee, SPECT scanning is not used routinely because of additional scanning time required. [52]

Radionuclide bone scanning is highly sensitive in the detection of osseous disorders, but it lacks specificity. Increased vascularity and uptake in the delayed phase of a bone scan can result from infection, fracture, tumor, arthritis and recent surgery as well as other conditions. Correlation of the bone scan with clinical information, radiographs and other diagnostic imaging modalities may be necessary for a diagnosis in many cases. The appearance or pattern of uptake on the bone scan may also be helpful in increasing the specificity. [52]

3.3. Arthrography

In the last decade, arthrography has been nearly completely replaced by MRI and its indications for knee imaging are currently very limited. Arthrography allows visualization of the intra-articular structures of a joint by obtaining images following injection of positive contrast material alone (single-contrast) or contrast and air (double-contrast). Before MRI, double-contrast arthrography was the standard imaging study for diagnosis of meniscal tears, cruciate ligament injuries, articular cartilage abnormalities and intra-articular loose bodies. A CT scan performed after the arthrogram (CT-arthrography) provides cross-sectional visualization of surface abnormalities of articular

cartilage, intracapsular abnormalities and periarticular soft tissues. It is ideal for diagnosing chondromalacia patella, thickened synovial plicae and popliteal cysts. [52]

3.4. Ultrasound

Ultrasound of the popliteal fossa is one of the first important applications of the technique in musculoskeletal radiology. A popliteal cyst is demonstrated easily and can be differentiated from an aneurysm of the popliteal artery and a fatty pad in the popliteal fossa. Occasionally a neoplasm of soft tissue may arise at this site and some evaluation of such tumors may be made with ultrasound. The appearance of a popliteal cyst is characterized by an echo-poor mass with smooth, well defined walls and occasional septations. Haemorrhage or infection within the cysts can result in multiple internal echoes. When these cysts are of long standing, actual calcification of contained debris may occur. The presence of a popliteal cyst can be established reliably if it is larger than 1-2 cm in diameter. When such a cyst ruptures, ultrasound investigations may give false negative results due to decompression of the cyst. This error is particularly liable to occur when the cyst initially is rather small. However, with larger cysts this complication can be demonstrated by the poor definition of the inferior border of the cyst and surrounding oedema in the adjacent soft tissue of the calf.

The normal popliteal artery is easily visible, ectasia or formation of an aneurysm being demonstrated as a fusiform swelling in continuity with the artery. The size of the popliteal aneurysm bears little or no direct relationship to the likelihood of complications, unlike, of course, the clinical situation with an aortic aneurysm. In addition to popliteal cysts and aneurysms, ultrasound is useful in the assessment of less common masses of the lower extremities, including haematomas, abscesses and neoplasms. A localized mass may be differentiated from diffuse oedema by its internal characteristics.

More recently ultrasound has been used to assess the thickness and integrity of the articular cartilage of the femoral condyles. In patients with arthritis a decreased thickness of cartilage may be shown, as well as blurring or obliteration of the normal sharp margins of the cartilage. The normal menisci may be visualized with ultrasound and reports of demonstrations of tears have appeared recently in the literature. [114]

3.5. Magnetic resonance imaging (MRI)

Magnetic resonance imaging (MRI) has revolutionized diagnostic imaging of the musculoskeletal system. Non-invasive direct visualization of bone, marrow and supporting soft tissue structures are exquisitely and reproducibly obtained with this technology. The MRI examination is well tolerated by patients and the procedure has been widely accepted by referring physicians. The major limitations continue to be the high cost involved in the purchase, installation and maintenance of a system, as well as the limited access in certain geographic areas.

MRI is a tomographic, multiplanar imaging technique, with the ability to display outstanding soft tissue contrast. Striking anatomic sections throughout the human body can be obtained in any projection desired. With a firm understanding of the relevant anatomy or a handy cross-sectional atlas, MRI can be used very simply and effectively as an anatomic imaging device to demonstrate the location of an abnormality. [27]

The MR signal is based on four separate components: the hydrogen proton density of a given tissue; two unique magnetic relaxation times called T1 and T2; and motion or flow. Hydrogen proton density (PD) most closely resembles standard x-ray film acquisition, in which electron density to a large extent determines how the resultant film will appear. Through the interactions of photoelectric effect and Compton scattering, the x-ray photons interact with the electrons of any tissue placed into the beam and the final image will reflect that tissue's electron density. With MRI, PD is a requirement for imaging, but not the most important variable. A tissue with a very low PD will appear quite dark on all pulsing sequences; yet, a tissue with a high PD can appear bright, dark or intermediate. Clearly, other important variables contribute to the MR signal intensity and these are the relaxation times called T1 and T2.

Safety

There is a select group of patients who may be severely injured if placed into an MR scanner. In almost all cases this is not a result of the scan process itself, but of the strong magnetic field. The magnetic field is constant and cannot be turned on or off with the turn of a switch. Patients who should not be scanned are those with intracerebral aneurysm clips, cardiac pacemakers and cochlear implants. If the type of vascular clip or implant is known, available published lists will indicate possible deflection of the appliance in a strong magnetic field. Only those aneurysm clips and appliances tested with no magnetic deflection should be placed into the scanner. Cardiac

pacemakers are contraindicated for two reasons. First, a current may be induced in the pacing wire which may cause fibrillation or thermal injury. Second, the device may be damaged or rendered permanently inoperable, requiring replacement. Another contraindication is a metallic foreign body in the eye. If there is any history of possible metal in the eye, it is best to obtain orbital x-ray films. If metal is within the globe, the patient cannot be scanned. At least one case of unilateral blindness has been reported when a 2x 3,5 mm intraocular metal fragment dislodged and caused a vitreous hemorrhage. Prosthetic heart valves are generally safe, although the Starr-Edwards Pre 6000 valve should not be scanned at field strengths above 0,35 T because of magnetic deflection. Internal orthopedic implants and hardware such as fixation plates, screws, wires, rods and total joints replacements are made from non-ferromagnetic materials and are safe for MRI. An additional concern with large metallic implants such as total joint replacements is adjacent tissue heating, which has been shown to be relatively insignificant with current MR scanning techniques. Shrapnel is also generally safe, although if located within or adjacent to vital structures such as the spine or central nervous system, those patients should not be scanned.

3.5.1. Bone disorders

Osteonecrosis

Osteonecrosis, or avascular necrosis, is the death of marrow and bone cells as the result of ischemia. The cause of such ischemia varies with the clinical setting. For instance, fractures involving the femoral condyles or tibial plateau may interrupt the blood supply and produce osteonecrosis. On T1-weighted images, osteonecrosis usually appears as an area of decreased signal intensity reflecting the death of fat cells and infiltration of edema and fibrous elements. T2-weighted images also demonstrate areas of lower signal intensity than normal marrow, occasionally with a surrounding zone of increased signal, which may represent reactive bone. In patients with spontaneous osteonecrosis, a central area of high-signal intensity within the necrotic marrow has been described. (Fig. 3.6.)

Osteochondritis dissecans

Osteochondritis dissecans is a disease of children and young adults, usually male, in which a shearing or tangential injury produces an osteochondral fragment. The fragment may remain in situ, dislodge, or become a loose body within the joint.

Osteochondral fragments appear as subarticular; rounded areas of decreased signal intensity, as compared with normal marrow on T1-weighted images. The fragment appearance on T2-weighted images is more variable, ranging from bright to dark. (Fig. 3.7.)

Trauma

MRI has the unique ability to detect early marrow changes associated with injury, with a sensitivity similar to nuclear medicine studies, while providing simultaneous anatomic detail. This includes not only the detection of stress fractures in patients in whom conventional radiographs are normal, but also the description and classification of occult fractures in trauma, which are also radiographically inapparent.

Neoplastic conditions

MRI can be very useful in the evaluation of soft tissue components and intramedullary extent of neoplasms and in monitoring chemotherapeutic responses.

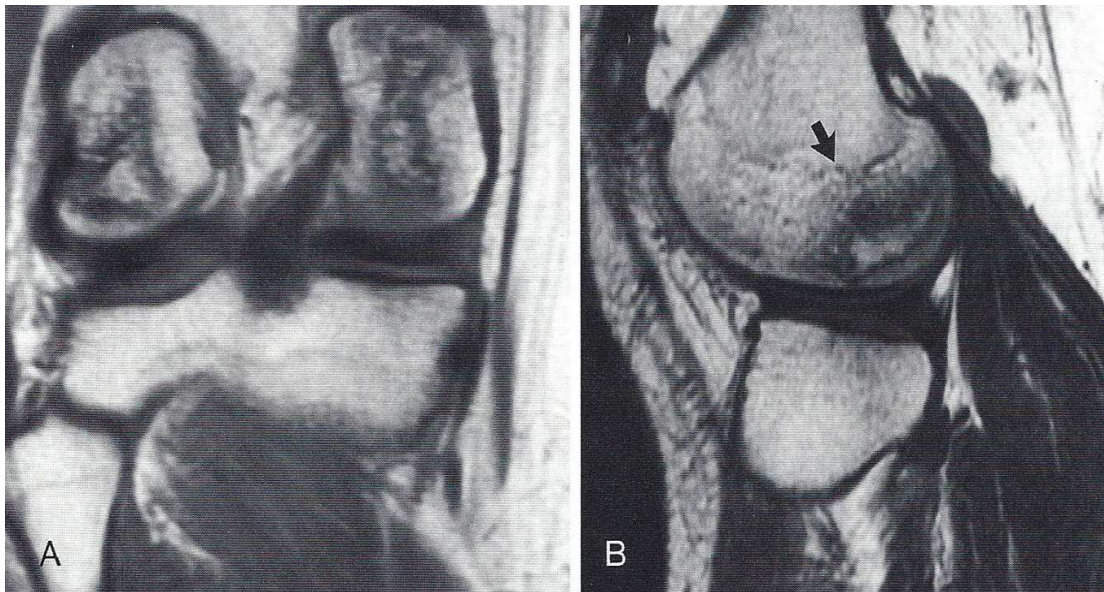


Figure 3.6. Osteonecrosis of the femoral condyles. A) Geographic areas of decreased signal intensity within both the medial and lateral femoral condyles on this coronal-proton-density-weighted image. B) Sagittal image permits localization of the involved area of the posterior (arrow) portion of the femoral condyle.

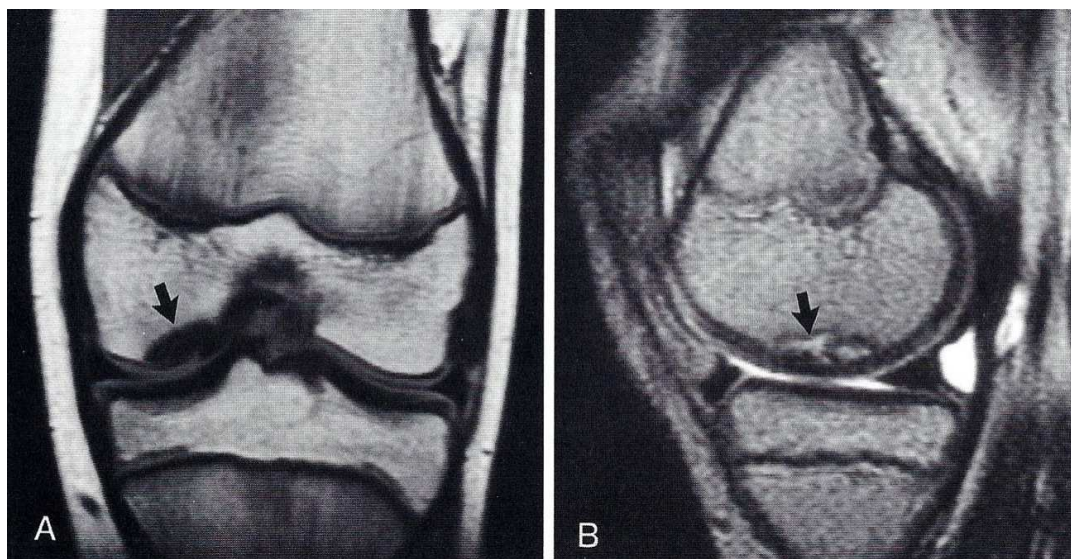


Figure 3.7. Osteochondritis dissecans. A) An osteochondral fragment of the lateral aspect of the medial femoral condyle appears as an area of low signal on this proton-density-weighted image (arrow). B) A sagittal, T2-weighted image of the same lesion shows absence of high signal surrounding the now bright fragment (arrow), indicating that it is stable and has a high probability of healing. The overlying articular cartilage is intact.

3.5.2. Articular disorders

Arthritis

MRI has shown great promise in the evaluation of articular cartilage and synovium. Normal cartilage exhibits at least three zones of signal intensity on MR scans—low signal adjacent to cortical bone, high signal in the midportion and low signal at the synovial surface.

Currently, a popular sequence for the detection of cartilage abnormalities has been fat suppression T1 images in which cartilage appears white against the black background of cortical bone and suppressed bone marrow. Intraarticular injection of either gadolinium or saline has also been suggested by some authors as an adjunct to T1- or T2-weighted sequences, respectively, for detection of cartilage defects as small as 2 to 3 mm.

Synovium is visualized on T1-weighted images as an intermediate intensity with an increase in brightness on T2-weighted images. Unfortunately, synovium may be difficult to visualize because these changes in signal parallel those of adjacent synovial fluid and therefore differentiation between the two may be limited. However, active inflammatory change in synovium demonstrates enhancement on T1-weighted images following the administration of intravenous gadolinium, in contrast to synovial fluid,

which remains dark and may aid in the monitoring of progression or regression of synovial disease.

Osteoarthritis

Hallmarks of osteoarthritis include cartilage defects or thinning, joint space narrowing, osteophyte formation, subchondral cysts and subchondral sclerosis. Cartilage abnormalities are best seen with fat suppression added to T1-weighted or GRASS images in which cartilage appears bright in contrast to the underlying black bone and marrow. Such cartilage abnormalities are usually most severe at the patellofemoral joint and medial femorotibial compartments, with eventual progression to a genu varus deformity caused by the latter. The distribution of osteophytes parallels that of cartilage abnormalities and is seen in continuity with the underlying bone. Subchondral cysts appear as intermediate signal-intensity fluid collections within the subchondral bone on T1-weighted images and as an increased signal intensity equal to synovial fluid on T2-weighted sequences. Accompanying subchondral sclerosis appears dark on both T1- and T2-weighted sequences. In evaluation of the extent and severity of osteoarthritis, MR has been shown to be superior to CT or plain radiographs.

Rheumatoid Arthritis

The diagnosis of this erosive disease of women in their childbearing years is primarily based on serologic studies and plain radiographic examinations. Synovial proliferations, erosions, effusion and cartilage destruction are all traits of rheumatoid arthritis that may be confirmed clinically and by plain radiography. However, recent studies have shown that plain radiographs underestimate the extent of the disease, as compared with MRI. The addition of intravenous gadolinium further helps distinguish active synovitis from chronic synovitis and joint fluid.

3.5.3. Soft tissue disorders and synovial disorders

Cruciate ligaments (a partial from a complete ACL tear, a PCL rupture), collateral ligaments (tear of the medial collateral ligament, the lateral collateral ligament or the popliteus tendon also), menisci, tendons (sartorius, gracilis, semitendinosus, semimembranosus, gastrocnemius, popliteus, biceps femoris and the four distinct muscles of the quadriceps femoris), effusions (joint effusions, whether secondary to trauma or associated with arthritis), popliteal cysts or meniscal cysts, plicae (suprapatellar, mediopatellar and infrapatellar), pigmented villonodular synovitis or synovial osteochondromatosis can be very good detected with the help of MRI. [27]

MRI has a greatest importance in the evaluation of numerous disorders of the knee, from soft tissue, bone, articular, to synovial disorders and its application in the evaluation of the postoperative knee must still discussed.

We see the importance and the great spectrum of the MRI, however this method has its limitations and one of them is the high costs.

4. RELEVANT BIOMECHANICS OF THE KNEE

The knee transmits loads, participates in motion, aids in conservation of momentum and provides a force couple for activities involving the leg. The human knee, the largest and perhaps most complex joint in the body, is a two-joint structure composed of tibiofemoral joint and patellofemoral joint. The knee sustains high forces and moments and is situated between the body's two longest lever arms (the femur and the tibia), making it particularly susceptible to injury. The knee is particularly well suited for demonstrating biomechanical analyses of joints because these analyses can be simplified in the knee and still yield useful data. Although knee motion occurs simultaneously in three planes, the motion in one plane is so great that it accounts for nearly all of the motion. Also, although many muscles produce forces on the knee, at any particular instant one muscle group predominates, generating a force so great that it accounts for most of the muscle force acting on the knee. Thus, basic biomechanical analyses can be limited to motion in one plane and to the force produced by a single muscle group and still give an understanding of knee motion and an estimation of the magnitude of the principal forces and moments on the knee. Advanced biomechanical dynamic analyses of the knee joint that include all soft tissue structures are complex and still under investigation.

Analysis of motion in any joint requires the use of kinematic data. Kinematics is the branch of mechanics that deals with motion of a body without reference to force or mass. Analysis of the forces and moments acting on a joint necessitates the use of both kinematic and kinetic data. Kinetics is the branch of mechanics that deals with the motion of a body under the action of given forces and/or moments. [101]

4.1. Kinematics

Kinematics defines the range of motion and describes the surface motion of a joint in three planes: frontal (coronal or longitudinal), sagittal and transverse (horizontal). Clinical measurements of joint range of motion define the anatomical position as a zero position for measurement. (Fig. 4.1.)

Of the two joints composing the knee, the tibiofemoral joint lends itself particularly well to an analysis of range of joint motion. Analysis of surface joint motion can be performed easily for both the tibiofemoral and the patellofemoral joint.

Any impediment of range of motion or surface joint motion will disturb the normal loading pattern of a joint and bear consequences. [3,4]

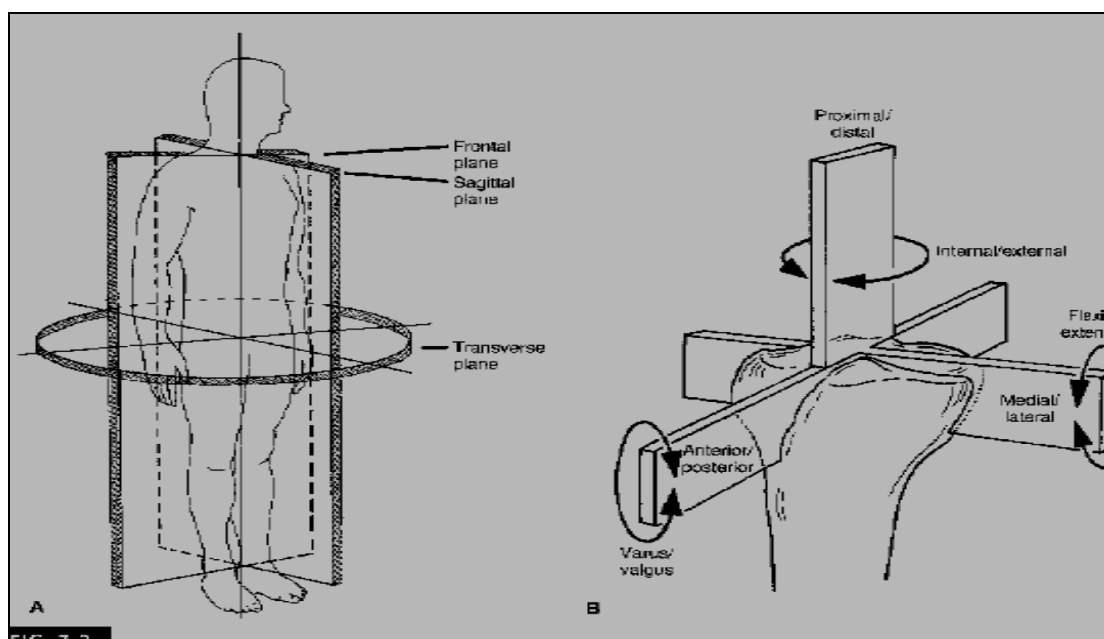


Figure 4.1. A. Frontal, sagittal and transverse planes in the human body; B. Depiction and nomenclature of the six degrees of freedom of knee motion: anterior posterior translation, medial/lateral translation, and proximal distal translation, flexion/extension rotation, internal/external rotation, varus/valgus rotation.

RANGE OF MOTION

The range of motion of any joint can be measured in any plane. Gross measurements can be made with a goniometer, but more specific measurements require the use of more precise methods such as electrogoniometry, roentgenography, stereophotogrammetry, or photographic and video techniques using skeletal pins.

In the tibiofemoral joint, motion takes place in all three planes, but the range of motion is greatest by far in the sagittal plane. Motion in this plane from full extension to full flexion of the knee is from 0° to approximately 140° . [97]

Motion in the transverse plane, internal and external rotation, is influenced by the position of the joint in the sagittal plane. With the knee in full extension, rotation is almost completely restricted by the interlocking of the femoral and tibial condyles, which occurs mainly because the medial femoral condyle is longer than the lateral condyle. The range of rotation increases as the knee is flexed, reaching a maximum at 90° of flexion; with the knee in this position, external rotation ranges from 0° to approximately 45° and internal rotation ranges from 0° to approximately 30° . Beyond

90° of flexion, the range of internal and external rotation decreases, primarily because the soft tissue restrict rotation.

Motion in the frontal plane, abduction and adduction is similarly affected by the amount of joint flexion. Full extension of the knee precludes almost all motion in the frontal plane. Passive abduction and adduction increase with the knee flexion up to 30°, but each reaches a maximum of only a few degrees. With the knee flexed beyond 30°, motion in the frontal plane again decreases because of the limiting function of the soft tissue.

The range of tibiofemoral joint motion required for the performance of various physical activities can be determined from kinematic analysis. Motion in this joint during walking has been measured in all planes. The range of motion in the sagittal plane during level walking was measured with an electrogoniometer by Lamoreaux (1971) and Murray et al. (1964). Full or nearly full extension was noted at the beginning of the stance phase (0% of cycle) at heel strike and at the end of the stance phase before toe-off (around 60% of cycle). Maximum flexion (approximately 60°) was observed during the middle of the swing phase. These measurements are velocity-dependent and must be interpreted with caution. (Fig. 4.2.)

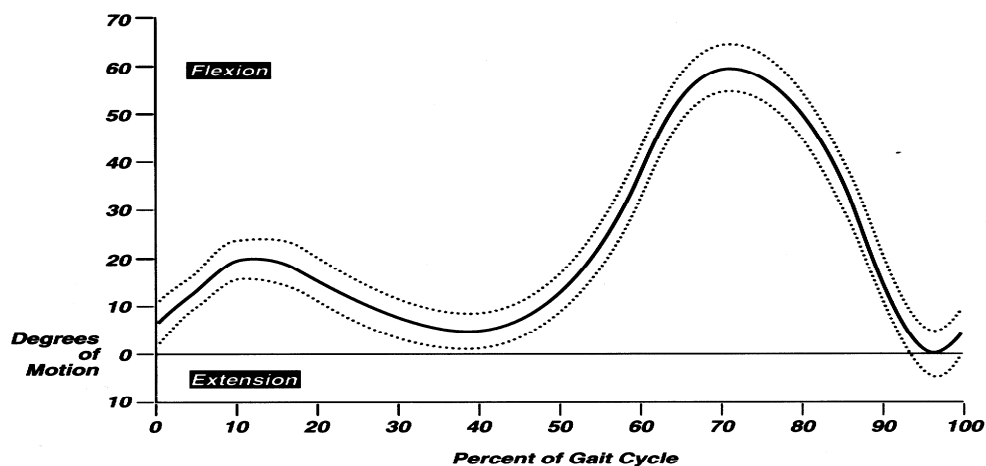


Figure 4.2. Range of motion of the tibiofemoral joint in the sagittal plane during level walking in one gait cycle.

Motion in the transverse plane during walking has been measured by several investigators. Using a photographic technique involving the placement of skeletal pins through the femur and tibia, Levens and associates (1948) found that total rotation of the tibia with respect to the femur ranged from approximately 4 to 13° in 12 subjects

(mean $8,6^\circ$). Greater rotation (mean $13,3^\circ$) was noted by Kettelkamp and coworkers (1970), who used electrogoniometry on 22 subjects. In both studies, external rotation began during knee extension in the stance phase and reached a peak value at the end of the swing phase just before heel strike. Internal rotation was noted during flexion in the swing phase. [101]

SURFACE JOINT MOTION

Surface joint motion, which is the motion between the articulating surfaces of the joint, can be described for any joint in any plane with the use of stereophotogrammetric methods. Because these methods are highly technical and complex, a simpler method, called the instant center technique is used. This method allows surface joint motion to be analyzed in the sagittal and frontal planes, but not in the transverse plane. The instant center technique provides a description of the relative uniplanar motion of two adjacent segments of a body and the direction of displacement of the contact points between these segments.

The skeletal portion of a body segment is called a link. As one link rotates about the other, at any instant there is a point that does not move, that is, a point that has zero velocity. This point constitutes an instantaneous center of motion or instant center. The instant center is found by indentifying the displacement of two points on a link as the link moves from one position to another in relation to an adjacent link, which is considered to be stationary. The points on the moving link in its original position and in its displaced position are designated on a graph and lines are drawn connecting the two sets of points. The perpendicular bisectors of these two lines are then drawn. The intersection of the perpendicular bisectors is the instant center. Clinically, a pathway of the instant center for a joint can be determined by taking successive roentgenograms of the joint in different positions (usually 10° apart) throughout the range of motion in one plane and applying the Reuleaux method for locating the instant center for each interval of motion. When the instant center pathway has been determined for joint motion in one plane, the surface joint motion can be described. For each interval of motion, the point at which the joint surfaces make contact is located on the roentgenograms used for the instant center analysis, and a line is drawn from the instant center to the contact point. A second line drawn at right angles to this line indicates the direction of displacement of the contact points. The direction of displacement of these points throughout the range of motion describes the surface motion in the joint. In most joints, the instant centers lie at

a distance from the joint surface and the line indicating the direction of displacement of the contact points is tangential to the load-bearing surface, demonstrating that one joint surface is gliding on the other (load-bearing) surface. In the case in which the instant center is found on the surface, the joint has a rolling motion and there is no gliding function. Because the instant center technique allows a description of motion in one plane only, it is not useful for describing the surface joint motion if more than 15° of motion takes place in any plane other than the one being measured.

In the knee, surface joint motion occurs between the tibial and femoral condyles and between the femoral condyles and the patella. In the tibiofemoral joint, surface motion takes place in all three planes simultaneously but is considerably less in the transverse and frontal planes. Surface motion in the patellofemoral joint takes place in two planes simultaneously, the frontal and transverse, but is far greater in the frontal plane. [101]

TIBIOFEMORAL JOINT

An example will illustrate the use of the instant center technique to describe the surface motion of the tibiofemoral joint in the sagittal plane. To determine the pathway of the instant center of this joint during a flexion, a lateral roentgenogram is taken of the knee in full extension and successive films are taken at 10° intervals of increased flexion. Care is taken to keep the tibia parallel to the x-ray table and to prevent rotation about the femur. When a patient has limited knee motion, the knee is flexed or extended only as far as the patient can tolerate. [101]

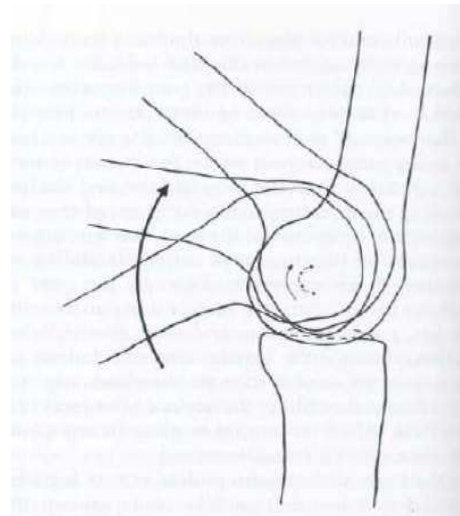
Two points on the femur that are easily identified on all roentgenograms are selected and designated on each roentgenogram. The films are then compared in pairs with the images of the tibiae superimposed on each other. Roentgenograms with marked differences in tibial alignment are not used. Lines are drawn between the points on the femur in the two positions and the perpendicular bisectors of these lines are then drawn. The point at which these perpendicular bisectors intersect is the instant center of the tibiofemoral joint for each 10° interval of motion. The instant center pathway throughout the entire range of knee flexion and extension can then be plotted. In a normal knee, the instant center pathway for the tibiofemoral joint is semicircular. (Fig. 4.3.)

After the instant center pathway has been determined for the tibiofemoral joint, the surface motion can be described. On each set of superimposed roentgenograms the point of contact of the tibiofemoral joint surfaces (the narrowest point in the joint space)

is determined and a line is drawn connecting this point with the instant center. A second line drawn at right angles to this line indicates the direction of displacement of the contact points. In a normal knee, this line is tangential to the surface of the tibia for each interval of motion from full extension to full flexion, demonstrating that the femur is gliding on the tibial condyles. During normal knee motion in the sagittal plane from full extension to full flexion, the instant center pathway moves posteriorly, forcing a combination of rolling and sliding to occur between the articular surface. The unique mechanism prevents the femur rolling off the posterior aspect of the tibia plateau as the knee goes into increased flexion. The mechanism that prevents this roll-off is the link formed between the tibial and femoral attachment sites of the anterior and posterior cruciate ligaments and the osseous geometry of the femoral condyles. (Fig. 4.4.) [61]



Figure 4.3. Locating the instant center



Semicircular instant center pathway for the tibiofemoral joint in a 19-year-old man with a normal knee

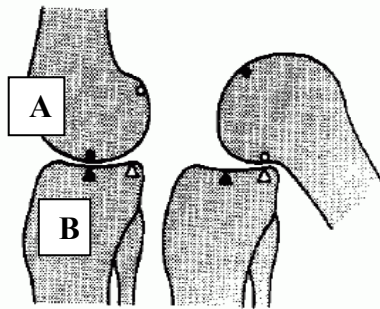


Figure 4.4. In a normal knee, a line drawn from the instant center of the tibiofemoral joint to the tibiofemoral contact point (line A) forms a right angle with a line tangential to the tibial surface (line B). The arrow indicates the direction of displacement of the contact points. Line B is tangential to the tibial surface, indicating that the femur glides on the tibial condyles during the measured interval of motion.

Frankel and associates determined the instant center pathway and analyzed the surface motion of the tibiofemoral joint from 90° of flexion to full extension in 25 normal knees; tangential gliding was noted in all cases. They also determined the instant center pathway for the tibiofemoral joint in 30 knees with internal derangement and found that, in all cases, the instant center was displaced from the normal position during some portion of the motion examined. If the knee is extended and flexed about an abnormal instant center pathway, the tibiofemoral joint surfaces do not glide tangentially throughout the range of motion but become either distracted or compressed. (Fig. 4.2.) Such a knee is analogous to a door with a bent hinge that no longer fits into the door jamb. If the knee is continually forced to move about a displaced instant center, a gradual adjustment to the situation will be reflected either by stretching of the ligaments and other supporting soft tissues or by the imposition of abnormally high pressure on the articular surfaces. (Fig. 4.5.) [28]

Internal derangements of the tibiofemoral joint may interfere with the so-called screw-home mechanism, which is external rotation during extension of the tibia. The tibiofemoral joint is not a simple hinge joint; it has a spiral, or helicoid motion. The spiral motion of the tibia about the femur during flexion and extension results from the anatomical configuration of the medial femoral condyle; in a normal knee, this condyle is approximately 1,7 cm longer than the lateral condyle. As the tibia moves on the femur from the fully flexed to the fully extended position, it descends and then ascends the curves of the medial femoral condyle and simultaneously rotates externally. This motion is reversed as the tibia moves back into the fully flexed position. This screw-

home mechanism (rotation around the longitudinal axis of the tibia) provides more stability to the knee in any position than would a simple hinge configuration of the tibiofemoral joint. (Fig.4.6.)

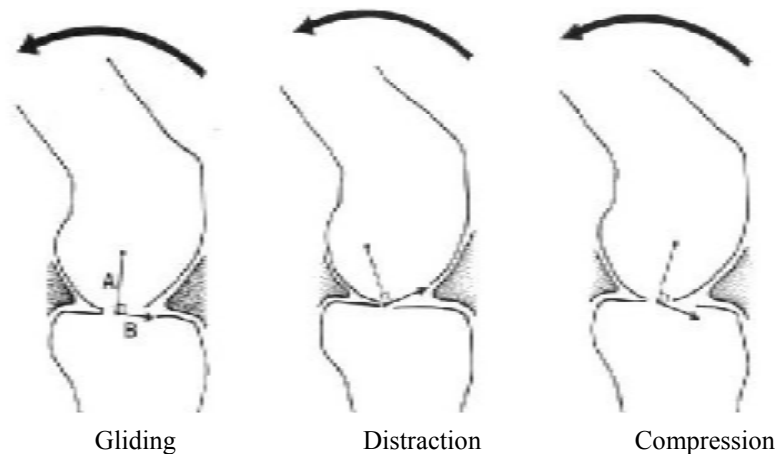


Figure 4.5. Surface motion in two tibiofemoral joints with displaced instant centers. The arrowed line at right angles to the line between the instant center and the tibiofemoral contact points indicates the direction of displacement of the contact points. The small arrow indicates that with further flexion, the tibiofemoral joint will be distracted. With increased flexion, this joint will be compressed.

Matsumoto et al. (2000) investigated the axis of tibia axial rotation and its change with knee flexion angle in 24 fresh-frozen normal knee cadaver specimens ranging in age from 22 to 67 years. The magnitude and location of the longitudinal axis of tibia rotation were measured at 15° increments between 0 and 90° of knee flexion. The magnitude of tibia rotation was 8° and 0° of knee flexion. The tibial rotation increased rapidly as the knee flexion angle increased and reached a maximum of 31° at 30° of knee flexion. It then decreased again with additional flexion. The location of the longitudinal rotational axis was close to the insertion of the anterior cruciate ligament at 0° of flexion. At continuous flexion up to 60°, the rotational axis moved toward the insertion of the posterior cruciate ligament. Between 60 and 90° of flexion, the rotational axis moved anteriorly again. This study showed that the rotational axis remains approximately in the area between the two cruciate ligaments. Any change of direction and tension of the cruciate ligaments and surrounding soft tissue may affect the movement and the location of the longitudinal tibia axis of rotation and thereby affect joint load distribution. [87]

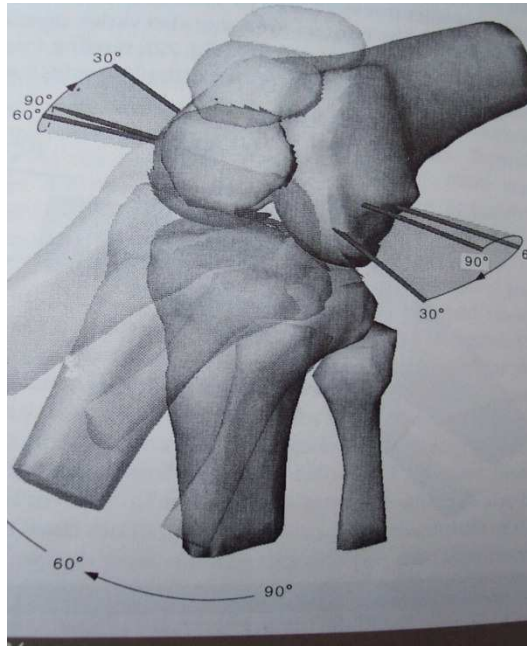


Figure 4.6. Screw-home mechanism of the tibiofemoral joint. During knee extension, the tibia rotates externally. This motion is reversed as the knee is flexed.

A clinical test, the Helfet test (Fig. 4.7.), is often used to determine whether external rotation of the tibiofemoral joint takes place during knee extension, thereby indicating whether the screw-home mechanism is intact. This clinical test is performed with the patient sitting with the knee and hip flexed 90° and the leg hanging free. The medial and lateral borders of the patella are marked on the skin. The tibial tuberosity and the midline of the patella are then designated and the alignment of the tibial tuberosity with the patella is checked. In a normal knee flexed 90° , the tibial tuberosity aligns with the medial half of the patella. The knee is then extended fully and the movement of the tibial tuberosity is observed. In a normal knee, the tibial tuberosity moves laterally during extension and aligns with the lateral half of the patella at full extension. Rotatory motion in a normal knee may be as great as half width of the patella. In a deranged knee, the tibia may not rotate externally during extension. Because of the altered surface motion in such a knee, the tibiofemoral joint will be abnormally compressed if the knee is forced into extension and the joint surfaces may be damaged. [45]

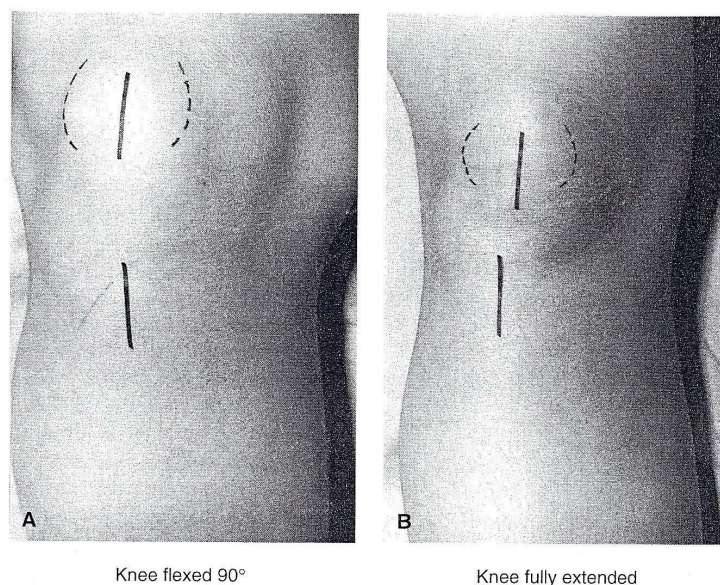


Figure 4.7. Helfet Test. A. In a normal knee flexed 90°, the tibial tuberosity aligns with the medial half of the patella. B. When the knee is fully extended, the tibial tuberosity aligns with the lateral half of the patella.

4.2. Kinetics

Kinetics involves both static and dynamic analysis of the forces and moments acting on a joint. Statics is the study of the forces and moments acting on a body in equilibrium (a body at rest or moving at a constant speed). For a body to be in equilibrium conditions must be met: force (translatory) equilibrium, in which the sum of the forces is zero, and moment (rotatory) equilibrium, in which the sum of the moments is zero. Dynamics is the study of the moments and forces acting on a body in motion (an accelerating or decelerating body). In this case, the forces do not add up to zero, and the body displaces and/or the moments do not add up to zero and the body rotates around an axis perpendicular to the plane of the forces producing the moments. Kinetic analysis allows one to determine the magnitude of the moments and forces on a joint produced by body weight, muscle action, soft tissue resistance, and externally applied loads in any situation, either static or dynamic, and to identify those situations that produce excessively high moments or forces. [101]

4.2.1. Statics of the tibiofemoral joint

Static analysis may be used to determine the forces and moments acting on a joint when no motion takes place or at one instant in time during a dynamic activity such as walking, running or lifting an object. It can be performed for any joint in any

position and under any loading configuration. In such analyses, either graphic or mathematical methods may be used to solve for the unknown forces or moments. A complete static analysis involving all moments and all forces imposed on a joint in three dimensions is complicated. For this reason, a simplified technique is often used. The technique utilizes a free-body diagram and limits the analysis to one plane, to the three main coplanar forces acting on the free-body, and to the main moments acting about the joint under consideration. The minimum magnitudes of the forces and moments are obtained.

An example will illustrate the application of the simplified free-body technique for coplanar forces to the knee. In this case, the technique is used to estimate the minimum magnitude of the joint reaction force acting on the tibiofemoral joint of the weight-bearing leg when the other leg is lifted during stair climbing. The lower leg is considered as a free-body, distinct from the rest of the body, and a diagram of this free body in the stair-climbing situation is drawn. From all forces acting on the free-body, the three main coplanar forces are identified as the ground reaction force (equal to the body weight), the tensile force through the patellar tendon exerted by the quadriceps muscle and the joint reaction force on the tibial plateau. The ground reaction force (W) has a known magnitude (equal to body weight), sense, line of application (point of contact between the foot and the ground). The patellar tendon force (P) has a known sense (away from the knee joint), line of application (along the patellar tendon) and the point of application (point of insertion of the patellar tendon on the tibial tuberosity), but an unknown magnitude. The joint reaction force (J) has a known point of application on the surface of the tibia (the contact point of the joint surfaces between the tibial and femoral condyles, estimated from a röntgenogram of the joint in the proper loading configuration), but an unknown magnitude, sense and line of application. Using vectors calculations and triangles laws the joint reaction force (J) and the patellar tendon force (P) can be calculated. (Calculation Box 1)

It can be seen that the main muscle force has a much greater influence on the magnitude of the joint reaction force than does the ground reaction force produced by body weight. In this example, only the minimum magnitude of the joint reaction force has been calculated. If other muscle forces are considered, such as the force produced by the contraction of the hamstring muscles in stabilizing the knee, the joint reaction force increases.

The next step in the static analysis is analysis of the moments acting around the center of motion of the tibiofemoral joint with the knee in the same position and the loading configuration shown in Calculation Box 1. The moment analysis is used to estimate the minimum magnitude of the moment produced through the patellar tendon, which counterbalances the moment on the lower leg produced by the weight of the body as the subject ascends stairs. (Calculation Box 2) [101]

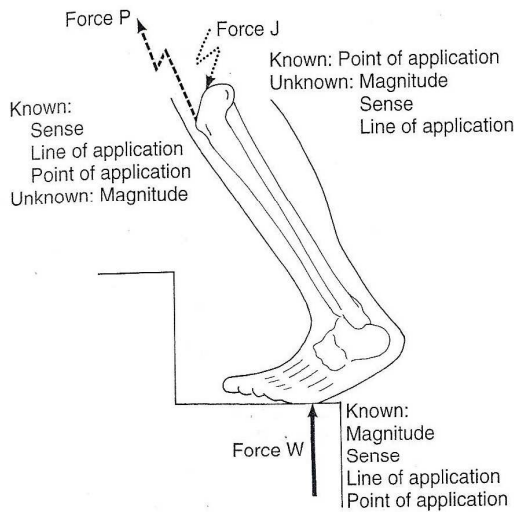
4.2.2. Dynamics of the tibiofemoral joint

Although estimations of the magnitude of the forces and moments imposed on a joint in static situations are useful, most of our activities are of a dynamic nature. Analysis of the forces and moments acting on a joint during motion requires the use of a different technique for solving dynamic problems. As in static analysis, the main forces considered in dynamic analysis are those produced by body weight, muscles, other soft tissues and externally applied loads. Friction forces are negligible in a normal joint and thus not considered here. In dynamic analysis, two factors in addition to those in static analysis must be taken into account: the acceleration of the body part under consideration and the mass moment of inertia of the body part. (The mass moment of inertia is the unit used to express the amount of torque needed to accelerate a body and depends on the shape of the body). [102]

The steps for calculating the minimum magnitudes of the forces acting on a joint at a particular instant in time during a dynamic activity are as follows:

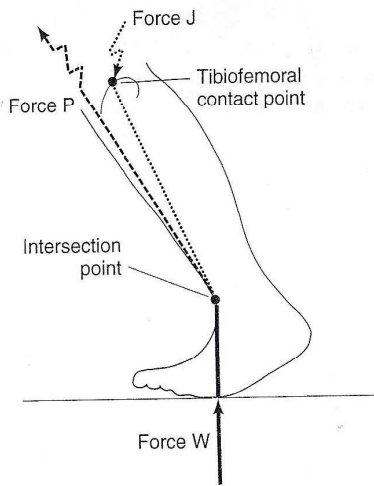
- 1) The anatomical structures are identified: definitions of structures, anatomical landmarks, points of contact of articular surface and lever arms involved in the production of forces for the biomechanical analyses.
- 2) The angular acceleration of the moving body part is determined.
- 3) The mass moment of inertia of the moving body part is determined.
- 4) The torque (moment) acting about the joint is calculated.
- 5) The magnitude of the main muscle force accelerating the body part is calculated.
- 6) The magnitude of the joint reaction force at a particular instant in time is calculated by static analysis.

Free-Body Diagram of the Knee Joint



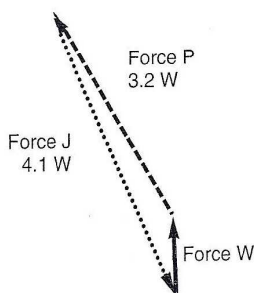
The three main coplanar forces acting on the lower leg: Ground reaction force (W), patellar tendon force (P), and joint reaction force (J) are designated on a free-body diagram of the lower leg while climbing stairs

Calculation Box 1



Because the lower leg is in equilibrium, the lines of application for all three forces intersect at one point. Because the lines of application for two forces (W and P) are known, the line of application for the third force (J) can be determined. The lines of application for forces W and P are extended until they intersect. The line of application for J can then be drawn from its point of application on the tibial surface through the intersection point

Calculation Box 1

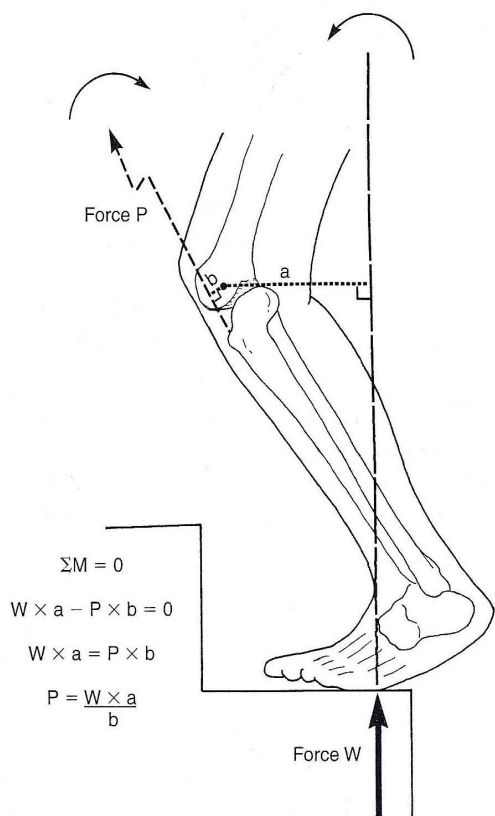


Now that the line of application for J has been determined, it is possible to construct a triangle of forces

First, a vector representing W is drawn. Next, P is drawn from the head of vector W. Then, to close the triangle, force J is drawn from the head of vector W. The point at which forces P and J intersect defines the length of these vectors. Now that the length of all three vectors is known, the magnitude of forces P and J can be scaled from force W, which is equal to body weight. It is determining the number of times the length of force W can be aligned along the force P and J, respectively. In this case, force P is 3.2 times body weight, and force J is 4.1 times body weight.

Calculation Box 2

Free-Body Diagram of the Lower Leg During Stair Climbing



The two main moments acting around the center of motion of the tibiofemoral joint (solid dot) are designated on the free-body diagram of the lower leg during stair climbing (Calculation Box 2).

The flexing moment on the lower leg is the product of the weight of the body² (W , the ground reaction force) and its lever arm (a), which is the perpendicular distance of the force W to the center of motion of the tibiofemoral joint. The counterbalancing extending moment is the product of the quadriceps muscle force through the patellar tendon (P) and its lever arm (b). Because the lower leg is in equilibrium, the sum of these two moments must equal zero ($\Sigma M = 0$).

In this example, the counterclockwise moment is arbitrarily designated as positive ($W \times a - P \times b = 0$). Values for lever arms a and b can be measured from anatomical specimens or on soft tissue imaging or fluoroscopy (Kellis & Baltzopoulos, 1999; Wretenberg et al., 1996), and the magnitude of W can be determined from the body weight of the individual. The magnitude of P can then be found from the moment equilibrium equation:

$$P = \frac{W \times a}{b}$$

²Again the weight of the lower leg is disregarded because it is less than one tenth of body weight.

In the first step, the structures of the body involved in producing forces on the joint are identified. These are the moving body part and the main muscles in that body part that are involved in the production of the motion. Great care must be taken in applying this first step. For example, the lever arms for all major knee muscles change according to the degree of knee flexion and gender.

In joints of the extremities, acceleration of the body part involves a change in joint angle. To determine this angular acceleration of the moving body part, the entire movement of the body part is recorded photographically. Recording can be done with a stroboscopic light and movie camera, with video photogrammetry, with Selspot systems, with stereophotogrammetry, or with other methods. The maximal angular acceleration for a particular motion is calculated. [138, 31, 110]

Next, the mass moment of inertia for the moving body part is determined. Anthropometric data on the body part can be used for this determination. As calculating these data is a complicated procedure, tables are commonly used. The torque about the joint can now be calculated using Newton's second law of motion, which states that

when motion is angular, the torque is a product of the mass moment of inertia of the body part and the angular acceleration of that part :

$T = I\alpha$, where T is the torque expressed in newton meters (Nm), I is the mass moment of inertia expressed in newton meters x seconds squared (Nm sec²), α is the angular acceleration expressed in radians per second squared (r/sec²).

The torque is not only a product of the mass moment of inertia and the angular acceleration of the body part but also a product of the main muscle force accelerating the body part and the perpendicular distance of the force from the center of motion of the joint (lever arms). Thus $T = Fd$, where F is the force expressed in newtons (N) and d is the perpendicular distance expressed in meters (m). Because T is known and d can be measured on the body part from the line of application of the force to the center of motion of the joint, the equation can be solved for F . When F has been calculated, the remaining problem can be solved like a static problem using the simplified free-body technique to determine the minimum magnitude of the joint reaction force acting on the joint at a certain instant in time.

Static analysis can now be performed to determine the minimum magnitude of the joint reaction force on the tibiofemoral joint. The main forces on this joint are identified as the patellar tendon force (P), the gravitational force of the lower leg (T) and the joint reaction force (J). P and T are known vectors. J has an unknown magnitude, sense and line of application. The free-body technique for three coplanar forces is used to solve for J , which is found to be only slightly lower than P .

As is evident from the calculations, the two main factors that influence the magnitude of the forces on a joint in dynamic situations are the acceleration of the body part and its mass moment of inertia. An increase in angular acceleration of the body part will produce a proportional increase in the torque about the joint. Although in the body mass moment of inertia is anatomically set, it can be manipulated externally. For example, it is increased when a weight boot is applied to the foot during rehabilitative exercises of the extensor muscles of the knee. Normally, a joint reaction force of approximately 50% of body weight results when the knee is slowly (with no acceleration forces) extended from 90° of flexion to full extension. In a person weighting 70 kg, this force is approximately 350 N. If a 10-kg weight boot is placed on the foot, it will exert a gravitational force of 100 N. This will increase the joint reaction force by 1,000 N, making this force almost four times greater than it would be without the boot.

Dynamic analysis has been used to investigate the peak magnitudes of the joint reaction forces, muscle forces and ligament forces on the tibiofemoral joint during walking. Morrison (1970) calculated the magnitude of the joint reaction force transmitted through the tibial plateau in male and female subjects during level walking. He simultaneously recorded muscle activity electromyographically to determine which muscles produced the peak magnitudes of this force on the tibial plateau during various stages of the gait cycle (Fig. 4.9.).

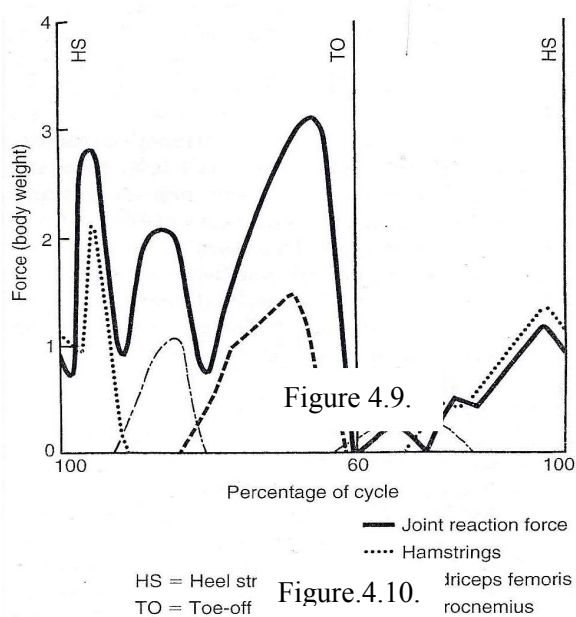
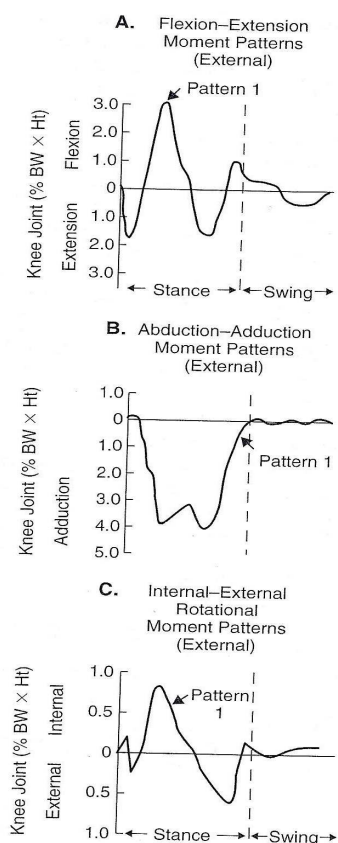


Figure 4.10.

triceps femoris
rocnemius

FIG. 7-15

Joint reaction forces expressed as body weight transmitted through the tibial plateau during walking, one gait cycle (12 subjects). The muscle forces producing the peak magnitudes of this force are also designated. Adapted from Morrison, J.B. (1970). *The mechanics of the knee joint in relation to normal walking*. *J Biomech*, 3, 51.



G. 7-16

Flexion-extension (A), abduction-adduction (B), and internal-external rotation (C) moments produced during one gait cycle in normal subjects. The moments are normalized to each individual body weight X height and expressed as a percentage. Reprinted with permission from Andriacchi, T.P. & Strickland, A.B. (1985). *Gait analysis as a tool to assess joint kinetics*. In N. Berme, A.E. Engin, D.A. Correis, et al. (Eds.), *Biomechanics of Normal and Pathological Human Articulating Joints*. (NATO ASI series, Vol 93, pp. 83-102). Dordrecht, Netherlands: Martinus Nijhoff.

Just after heel strike, the joint reaction force ranged from two to three times body weight and was associated with contraction of the hamstring muscles, which have a decelerating and stabilizing effect on the knee. During knee flexion in the beginning of the stance phase, the joint reaction force was approximately two times body weight and was associated with the contraction of the quadriceps muscle, which acts to prevent

buckling of the knee. The peak joint reaction force occurred during the late stance phase just before toe-off. This force ranged from two to four times body weight, varying among the subjects tested, and was associated with contraction of the gastrocnemius muscle. In the late swing phase, contraction of the hamstring muscles resulted in a joint reaction force approximately equal to body weight. No significant difference was found between the joint reaction force magnitudes for men and women when the values were normalized by dividing them by body weight.

Andriacchi & Strickland (1985) studied the normal moment patterns around the knee joint during level walking for 29 healthy volunteers (15 women and 14 men with an average age of 39 years). Figure 4.9. depicts the flexion-extension, abduction-adduction, and internal-external moments during the stance and swing phase of level walking. The moments are normalized to the individual's body weight and height and are presented as a percentage. The flexion-extension moments during the stance phase are approximately 20 to 30 times larger than the moment produced in the frontal (abduction-adduction) and transverse (internal-external) planes.[4]

An increase in knee joint flexion-extension moment amplitude has been reported at increased walking speeds (Andriacchi & Strickland, 1985; Holden 1997). [4,48] An increase in the production of adduction knee joint moment during stair climbing compared with level walking was reported by Yu (1997). During the gait cycle, the joint reaction force shifts from the medial to the lateral tibial plateau. In the stance phase, when the force reaches its peak value, it is sustained mainly by the medial plateau (adduction moment); in the swing phase, when the force is minimal, it is sustained primarily by the lateral plateau. The contact area of the medial tibial plateau is approximately 50% larger than that of the lateral tibial plateau (Kettelkamp & Jacobs, 1972). Also, the cartilage on this plateau is approximately three times thicker than that on the lateral plateau. The larger surface area and the greater thickness of the medial plateau allow it to more easily sustain the higher forces imposed on it. [65]

In a normal knee, joint reaction forces are sustained by the menisci as well as by articular cartilage. The function of the menisci was investigated by Seedhom (1974), who examined the distribution of stresses in knees of human autopsy subjects with and without menisci. His results suggest that in load-bearing situations, the magnitude of the stresses on the tibiofemoral joint when the menisci have been removed may be as much as three times greater than when these structures are intact. Fukuda et al. (2000) studied in vitro the load-compressive transmission of the knee joint and the role of menisci and

articular cartilage. The load simulated was static and dynamic impact loading. The testing was done in neutral, varus and valgus alignment of the knee joints in 40 fresh-frozen pig knee specimens. The compressive stress on the medial subchondral bone was up to five times higher with the menisci removed. This study points to the importance of the menisci as a structure to absorb load and protect the cartilage and subchondral bone under dynamic conditions. [29,120]

In a normal human knee, stresses are distributed over a wide area of the tibial plateau. If the menisci are removed, the stresses are no longer distributed over such a wide area but instead are limited to a contact area in the center of the plateau. (Fig. 4.11.) Thus, removal of the menisci not only increases the magnitude of the stresses on the cartilage and subchondral bone at the center of the tibial plateau but also diminishes the size and changes the location of the contact area. Over the long term, the high stresses placed on this smaller contact area may be harmful to the exposed cartilage, which is usually soft and fibrillated in that area. The menisci are thought to carry up to 70% of the load across the knee. Movement during knee flexion of the menisci would therefore protect the articulating surfaces while avoiding injury to it. [101]

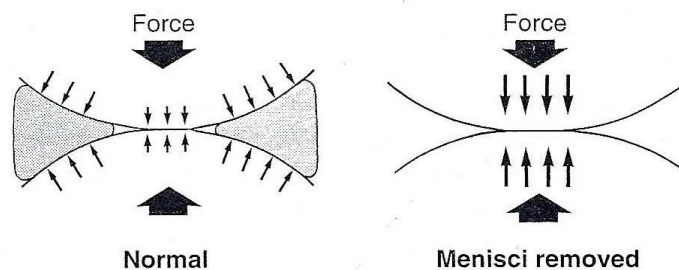


Figure 4.11.

Stress distribution in a normal knee and in a knee with the menisci removed. Removal of the menisci increases the magnitude of stresses on the cartilage of the tibial plateau and changes the size and location of the tibiofemoral contact area. With the menisci intact, the contact area encompasses nearly the entire surface of the tibial plateau. With the menisci removed, the contact area is limited to the center of the tibial plateau.

5. AIM OF THE STUDY

The study was made with the purpose to see if there was a correspondence between the cartilage disorders, the intraoperative views (arthroscopy and the arthroplasty of the knee) and the acoustic emission measurements, performed one day before the surgery. In the same time there were analysed also another parameter, concerning the age, the sex, the length of the femur, the thigh thickness, the body mass index, the anatomical axis of the knee and the correspondence between these parameter and the appearance and the severity of the cartilage injuries. Because there aren't at this moment cheap and standards methods who can determine the early cartilage injuries, this study is supposed (concording with the results) to open new ideas and new advantages in the diagnostic of this often disease, using the acoustic emission measurement system.

6. ACOUSTIC EMISSION MEASUREMENT SYSTEM FOR THE ORTHOPEDICALLY DIAGNOSTIC OF THE KNEE JOINT

Quality control in the orthopedic diagnostic according to DIN EN ISO 9000 ff requires methods of nondestructive process control, which do not harm the patient neither by radiation nor by invasive examinations. To gain an improvement of health economy quality controlled and nondestructive measurements have to be introduced in the diagnostics and the therapy of human joints and bones. There is no non-invasive evaluation method for the state of wear regarding human joints and the cracking tendency of bones yet established.[119]

The analysis of acoustic emission signals allows the prediction of bone rupture far below the fracture load. The evaluation of dry and wet bone samples revealed that it is possible to conclude from crack initiation to the bone strength and thus to predict the probability of bone rupture. Besides the fracture probability of bone acoustic emission allows to assess the tribological status of the knee joint. Simple states of wear without inflammation can be separated from states of wear complicated by inflammation (arthritis). For the assessment of tribological knee function and by the probability of fracture of the femur an adapted Acoustic Emission Measurement System named Bone Diagnostic System (BONDIAS) was developed. This system makes the in vivo analysis of the medical status possible. [26]

A natural center of the surveillance of joints is the analysis of the acoustic emission from joints moving under the typical daily load. Here, the typical loads comprise knee bending, climbing or descending the stairs, but also ergometric examinations. The analysis of acoustic emission from the knee joint clearly reveals cartilage lesions, arthritic degeneration of the knee joint with more or less inflammatory contributions and damage caused by the change of the inclination of the line of thrust. Acoustic emission from the knee (Fig. 5.1.) is registered by a sensor which is fixed by tapes to the skin over the medial condyle of the femur (Fig. 5.2.) during application of the natural load. [26, 118,119, 139]

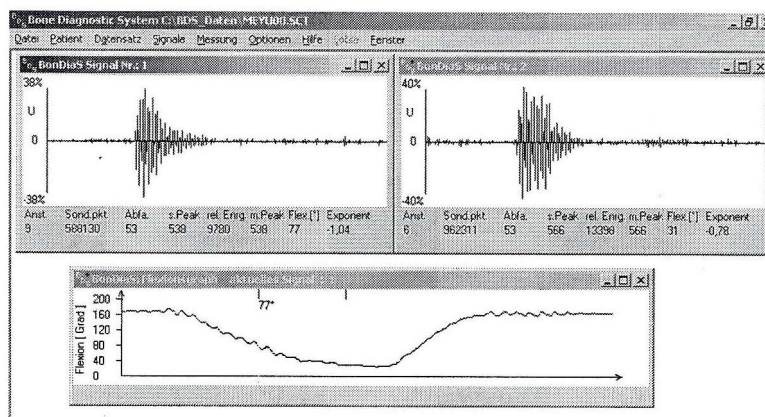


Figure 5.1. Acoustic emission from a knee joint during knee bending, correlated to the angle of knee flexion.

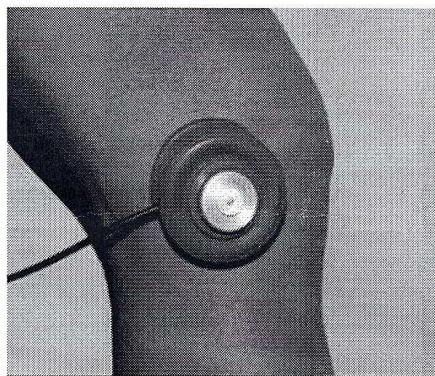


Figure 5.2. Position of an acoustic emission sensor at the medial femoral condyle during the measurement

The acoustic emission is registered over time and correlated to the angle of knee flexion. The kinetics of load and motion can reveal non stationary characteristics which can be typical of certain diseases. Knowing the kinetics of load and motion, the acoustic emission offers potential causes for the measurement phenomena. Whether the medial or the lateral femoral condyle or both are damaged can be tested by changes of the distribution of load and by the concomitant registration of the emission.

The acoustic emission analysis allows for a multifaceted assessment of joint defects depending on the range of knee flexion medial or lateral condyles can be changed thereby.

A short rise time of the acoustic emission characteristic for cartilage defects is correlated to a low signal damping by the cartilage layers. If in that case a cartilage lesion can be verified such a signal is really indicative of a low thickness of the cartilage

layer in the damaged area. To reach this diagnosis the individual damping characteristics of the knee cartilage have to be assessed. This information is drawn from a simple test. The analyzed patient is standing relaxed by on the two legs and then he quickly raises one leg. The fast increase in load of the loaded leg initiates reactions also in the additionally loaded knee cartilage. Acoustic emission typical of normal cartilage or of arthritis with more or less inflammatory contribution and of cartilage lesions are demonstrated in figures 5.3. to 5.5.

Figure 5.3. demonstrates the acoustic emission from a knee joint caused by cartilage deformation due to the sudden change from a two legs stand to a one leg stand. The intermittent cartilage deformation is of visco-elastic nature. The graph of acoustic emission over time shows a correlation to the thickness of the deformed cartilage. Short signal duration is indicative of a thin cartilage layer.

Acoustic emission from a cartilage lesion is shown in Fig. 5.4. Articulating cartilaginous counterparts literally “fall” into a cartilage lesion. In reality this process has to be considered as a sliding one. Sliding into the lesion – indicated by region 1 – over the ingoing visco-elastic edge of the cartilage lesion is accompanied by a low energy transfer. The concomitant acoustic emission is of low energy and amplitude. Sliding out of the lesion, however, as shown in region 2, the outgoing edge of the lesion is strongly deformed. A higher volume of the cartilage is deformed visco-elastically with high energy. This is accompanied by acoustic emission with a high rise time representing both the sequence of motion and the deformation process of the cartilage. The latter is responsible also for this type of amplitude descent. [42,77,130,131,137]

The acoustic emission from an arthritic defect is represented in Fig. 5.5. Arthritic defects are characterized by different events in the course of acoustic emission. This can be a signal typical of cartilage lesions where needle like signal peaks are superimposed. These signal peaks are usually due to stick-slip effects or to the interaction of bone structures in the contact areas. [25,26,]

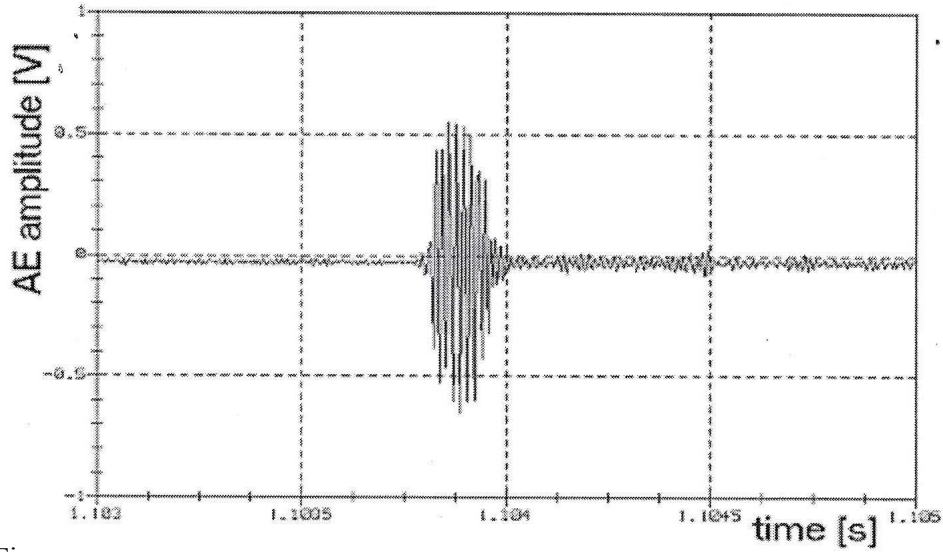


Figure 5.3. Acoustic emission from healthy knee joint cartilage deformation after the sudden change from a two legs stand to a one leg stand.

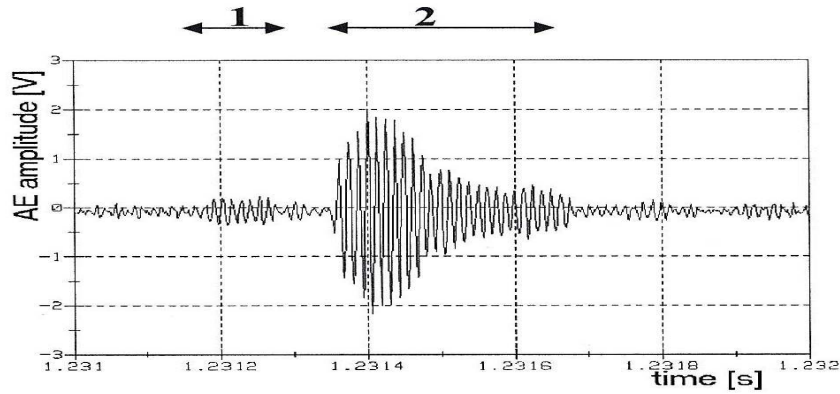


Figure 5.4. Acoustic emission from a cartilage

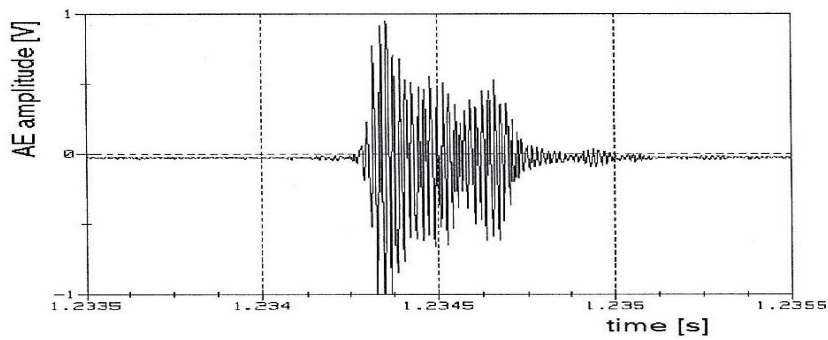


Figure 5.5. Acoustic emission from an arthritic defect

MEASUREMENT SYSTEM BONDIAS

The measurement system BONDIAS has been developed for the automated assessment and evaluation of the acoustic emission from the human femur and knee joint for the orthopedic diagnosis. Knee bending of a patient will release acoustic emission in high temporal resolution and well correlated to the angle of knee flexion. However, the physician is not left alone with a bundle of data and the task to evaluate the acoustic emission. He will get the relevant information concerning:

~ arthritic lesions in the knee joint: well characterized with acoustic emission, singular events without a follow up of further emission

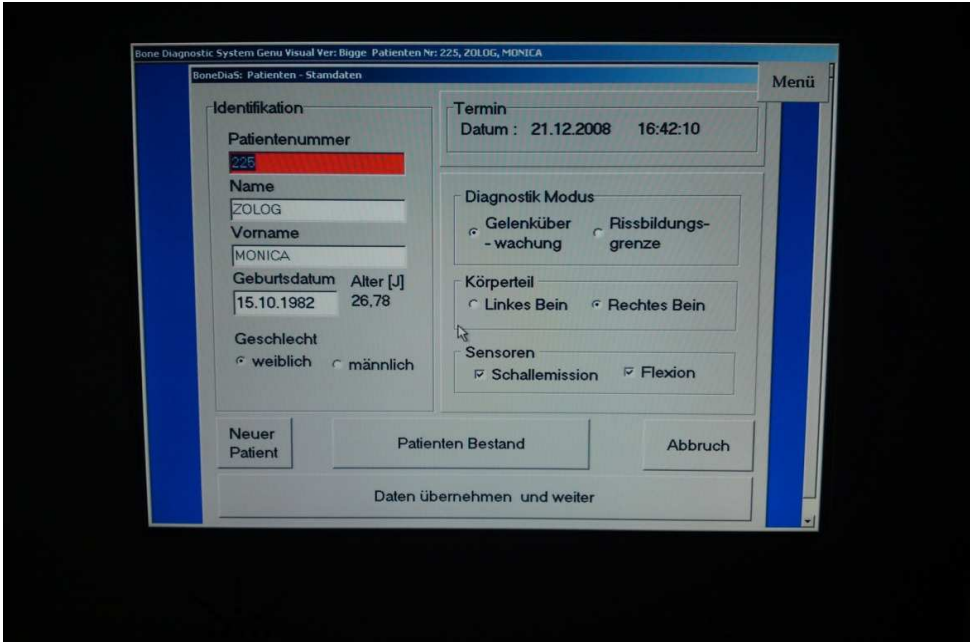
~ acoustic emission due to elevated intraarticular friction caused by cartilage lesions, inappropriate surface roughness, a lack of synovial fluid or other defects : a plethora of continuous emission

~ crack initiation in the femur: a burst type of acoustic emission followed by continuous emission, which is typical of relaxation phenomena in the crack bands

The energy and the frequency of signals are mostly indicative of the originating events and important characteristics for the evaluation of defects. [26]

How does BONDIAS acoustic measurement function?

The system is connected to 220-240V. The system is opening directly the program we need. We type in menu program the personal data of the patients, name, date of birth, sex, if the measurement is for the femur or knee joint, then the side, right or left (Fig.5.6.).



The screenshot displays the 'BoneDias: Patienten - Standarden' window. The title bar indicates 'Bone Diagnostic System Genu Visual Ver: Bigge Patienten Nr: 225, ZOLOG, MONICA'. The window is divided into several sections:

- Identifikation:** Includes fields for 'Patientennummer' (with a redacted value), 'Name' (ZOLOG), 'Vorname' (MONICA), 'Geburtsdatum' (15.10.1982), 'Alter [J]' (26,78), and 'Geschlecht' (radio buttons for 'weiblich' and 'männlich').
- Termin:** 'Datum : 21.12.2008 16:42:10'.
- Diagnostik Modus:** Radio buttons for 'Gelenküberwachungs' and 'Rissbildungsgrenze'.
- Körperteil:** Radio buttons for 'Linkes Bein' and 'Rechtes Bein'.
- Sensoren:** Checkboxes for 'Schallemission' and 'Flexion'.

At the bottom, there are buttons for 'Neuer Patient', 'Patienten Bestand', and 'Abbruch', along with a 'Daten übernehmen und weiter' button.

Figure 5.6. Identification data of the patients

After that there will be introduced information about the knee joint pathology, if the arthritic lesions, cartilage injuries are already known and where is the pain, in patella region, medial or lateral femoral condyle, medial or lateral joint, medial or lateral head of the tibia, or head of the fibula.(Fig. 5.7. and 5.8.). There will be also introduced at which grade of flexion the pain appears and how strong is this pain, mild, medium or strong.

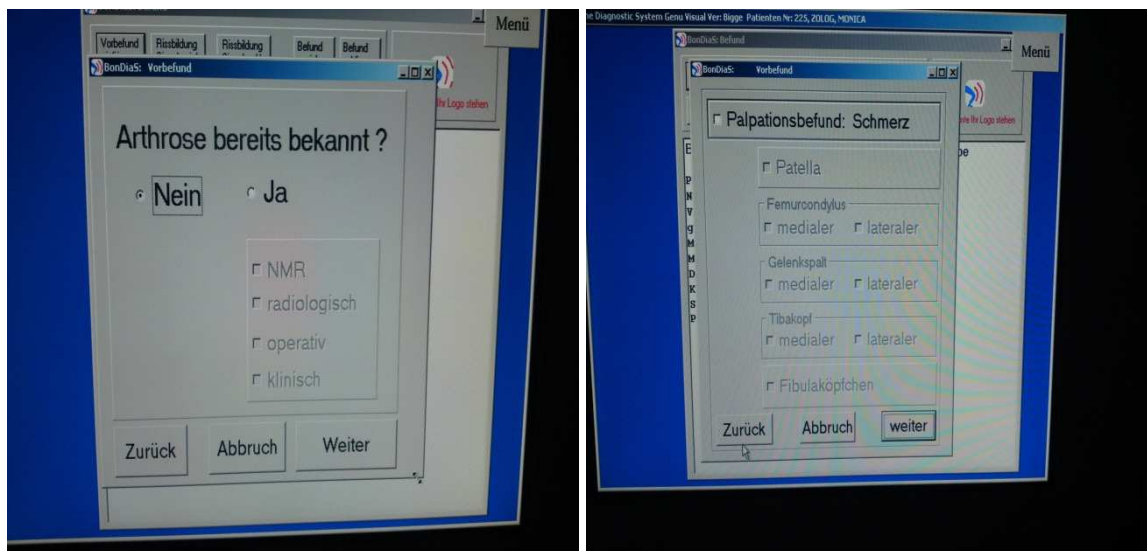
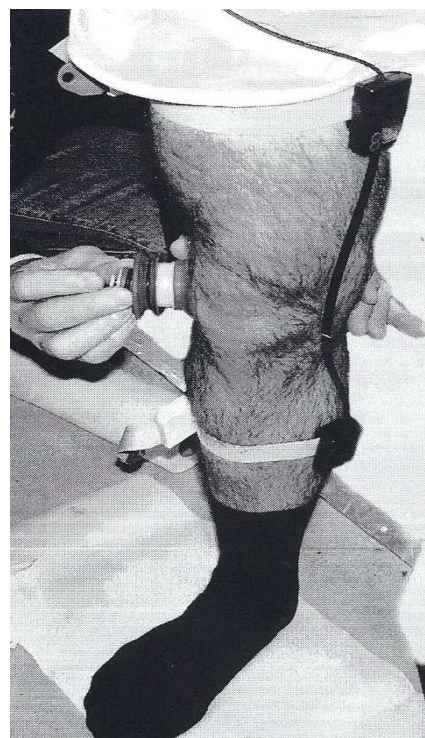


Figure 5.7.-5.8. Introducing information about the knee joint pathology

The transducer head will be then attached with a special glue on the patient knee. The patient's knee has to be shaved, because the hair can interfere with the measurement. A vacuum pump will make void and will keep the transducer head attached to the skin. For acoustic emission measurement of the knee, the transducer head will be attached on the lateral knee joint. The flexion measurement guiding line will have to be at the medial side of the knee and smooth anteriorly flexed. (Fig.5.9.)

Figure 5.9. Attaching the transducer head on the patient knee



After that, the measurement will be done. This will take 10 seconds and the patient has to do three knee squats, slowly and regularly. After the measurement we can analyse the crack initiation in the femur or the cartilage lesions, what, from these both is wished in the beginning. There are for these both pathological lesions specific signal types. (Fig. 5.10. and Fig. 5.11.) The measurement can also indicate at which angle of flexion appears the lesion.

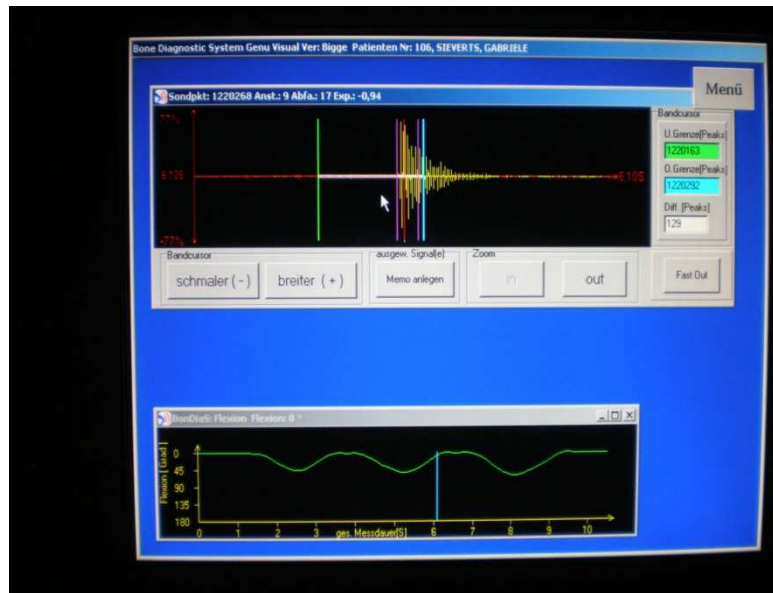


Figure 5.10. Example for a signal of crack initiation in the femur

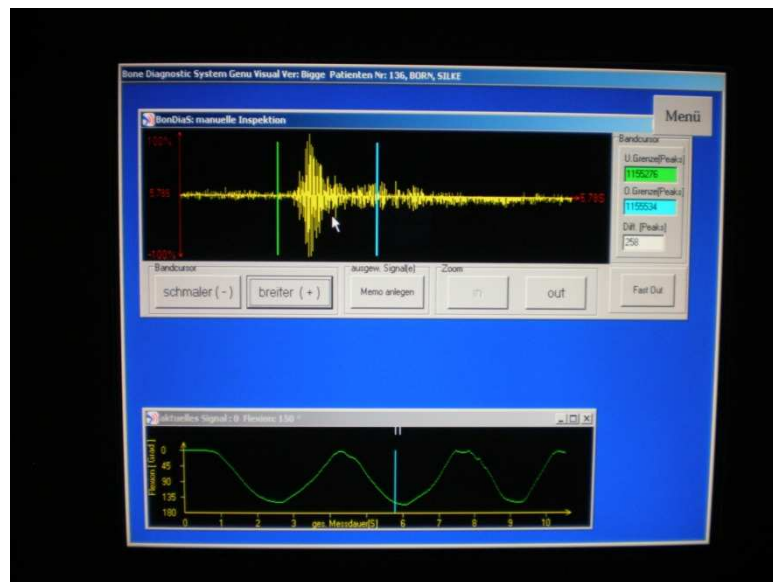


Figure 5.11. Example for a signal of cartilage lesion of the knee

Each measurement is registered and saved under a number and the name of the patient and can be open and analysed each time. It can be also saved on an USB Stick and transferred on a computer. The measurement shows the three knee squats, how deep they are, how regularly and at which angle appear the signals. With a touching screen function the signal can be enlarged and in detail analysed.

7. MATERIAL AND METHODS

In a period of time of 14 Months, from May 2008 till June 2009 there were analysed in Elisabeth Klinik Olsberg Bigge, clinic for orthopedics in Nordrheinwestfallen, Germany a number of 125 patients.

These patients were analysed with the BONEDIAS acoustic measurement system. They were supposed to receive an arthroscopic surgery or an arthrotomy, with total knee replacement. The measurements were made one day before surgery, as the patients were hospitalized and prepared for the surgery. We recruited only the patients who were supposed to receive a surgery because of the possibility to observe by the minimally invasive surgery or by the open surgical procedure the cartilage lesions and where exactly are they localized on the femur condyle. In the end, the measurements were compared with the intra-operative findings.

For every patient was filled a protocol of study, which included the age, the sex, the height, the weight, the body mass index, the femur length of the measured knee, the thickness of the thigh of the measured knee, the knee side, the knee effusion, the axis of the knee, the range of motion of the knee which was subdued to the surgery.

The protocol of study included also the diagnosis, the surgery which was proceed and the acoustic emission correspondence. After the surgery, the surgeon filled also a diagram with the cartilage lesions he observed on the femoral condyles, the location and the classification after Outerbridge of these lesions. The surgery protocols were also used for supplementary details. The diagram with the cartilage lesions and the protocol of study are shown in the figures 6.1. and 6.2.

Protocol of Study

Number of the patient :

Number of the measure :

Name of the patient and date of birth :

Age of the patient : Years

Sex of the patient : M / F

Height : cm

Weight : kg

BMI :

The Length of the femur : cm

Thickness of the thigh : cm (15cm above the knee joint)

Knee side : left /right

Knee effusion : yes / no

Anatomic axis (clinical) : varus^o/ normal / valgus^o

Range of motion of the knee : _ / _ / _ °

Diagnostic :

Operation :

Diagram of the cartilage injury location on femoral condyle and grade of injury after

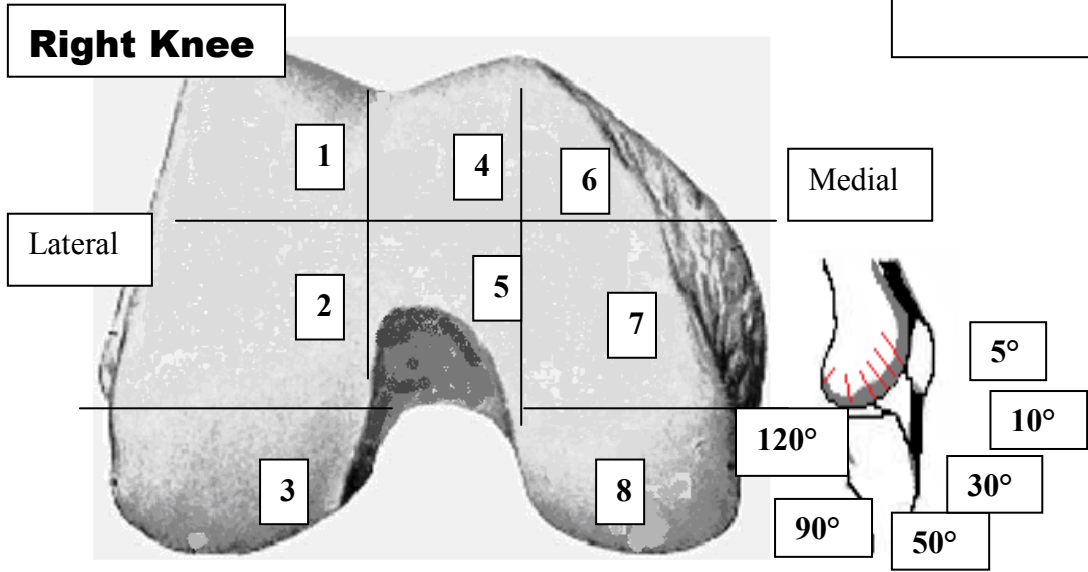
Outerbridge : see attachment

Results of acoustic emission measurement system BONEDIAS :

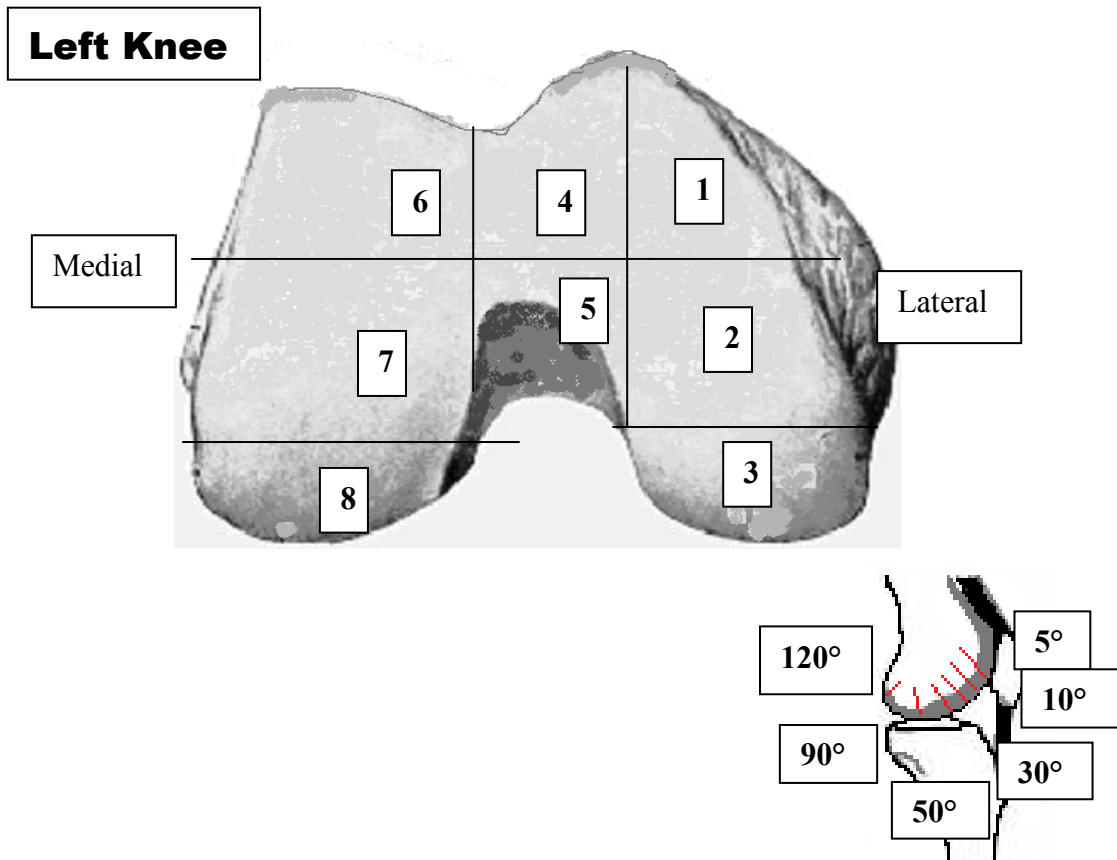
Figure 6.1. Protocol of study

Cartilage Disorders of the Femur Condyle

Patient



Localisation and the grade of injury after Outerbridge :



Localisation and the grade of injury after Outerbridge:

Figure 6.2. The diagram of the cartilage injury location on the femoral condyle and grade of injury after Outerbridge

This protocol of study was completed for every patient. The acoustic emission measurement with the BONEDIAS system were in detail examined, for each patient, the signals, the types of signals and at which grade of flexion these signals appear and a short interpretation was filled in the protocol of study, concerning if there was a correspondence between the signals and the intra-operative findings.

The other characteristics introduced in the protocol of study were made with the purpose of studying if there was a correspondence between all these parameters and the cartilage injuries and indirectly with the findings obtained with the BONEDIAS system.

From the 125 recruited patients, 20 were excluded from the study, although the BONEDIAS measurements have been done, the errors appeared had eventually the following causes:

~ the knee effusion over gr. II could (and was demonstrated also by the measurement) interfere with the measurement and give false results;

~ the patients were not in the state to make three regularly and smoothly knee squats (because of the age, the pains or the incapacity to understand the importance of the regularity of the knee squats)

8. RESULTS

The 105 study subjects had ages between 22 and 84 years old, with an average of 58,46 years old, as shown in Fig. 7.1.

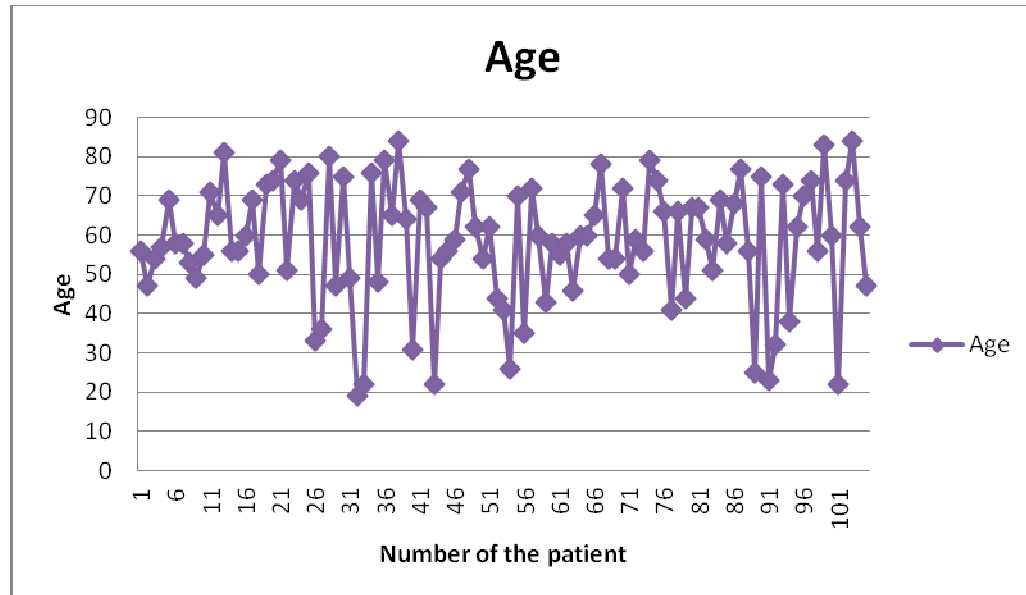


Figure 7.1.

There were 41 men (39%) and 64 women (61%) who were investigated. The distribution on sex is shown in the Fig 7.2.

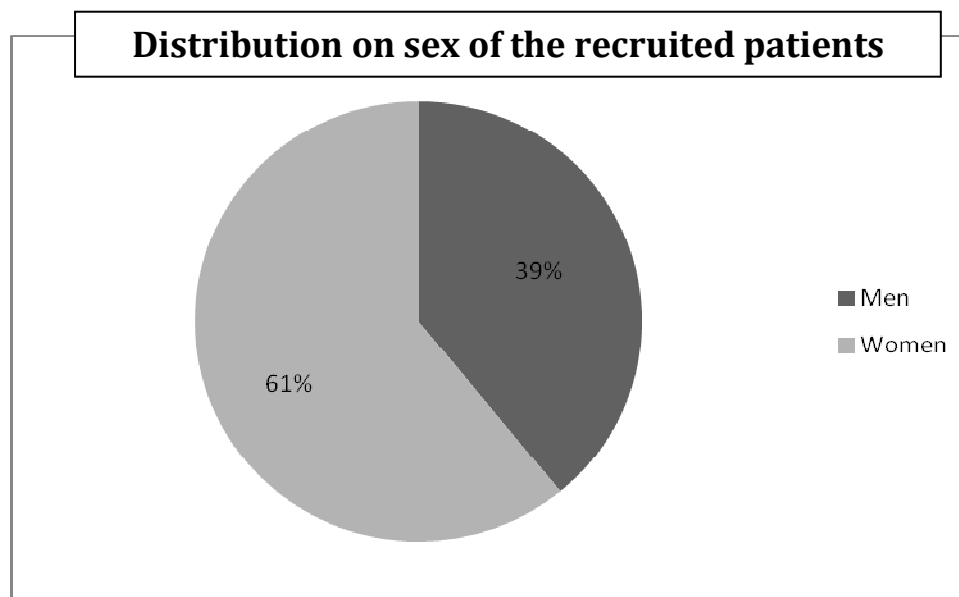


Figure 7.2.

The height and weight of the studied patients were filled in the protocol of study and the body mass index was calculated. The distribution of the patients regarding height, weight and the body mass index is illustrated in Fig. 7.3., 7.4. and 7.5. There were 11 patients with a height ≤ 1.59 m, 37 between 1.60-1.69, 31 between 1.70-1.79 and 26 patients with a height over 1.80. There were 26 subjects between 50-69 kg, 43 between 70-89 kg and 36 over 90 kg.

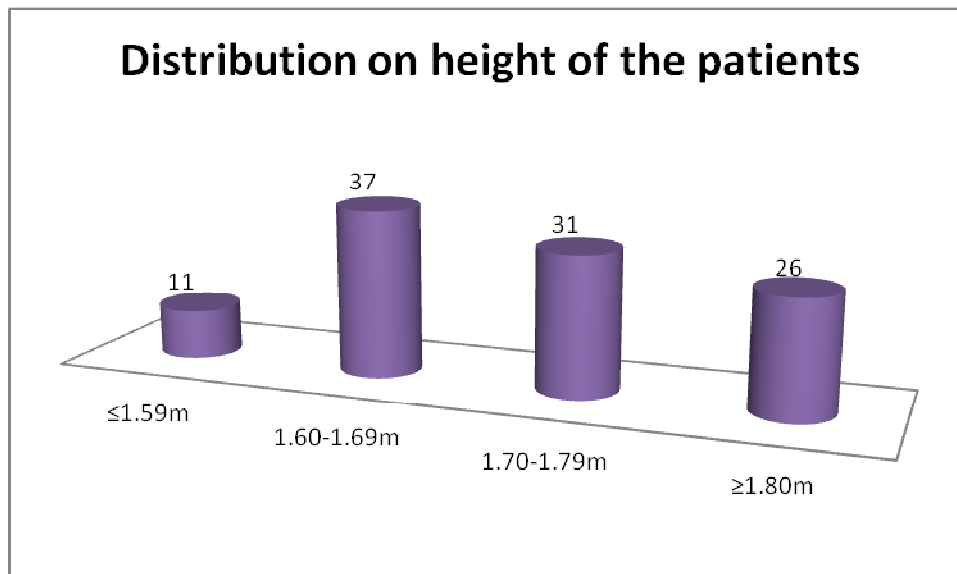


Figure 7.3.

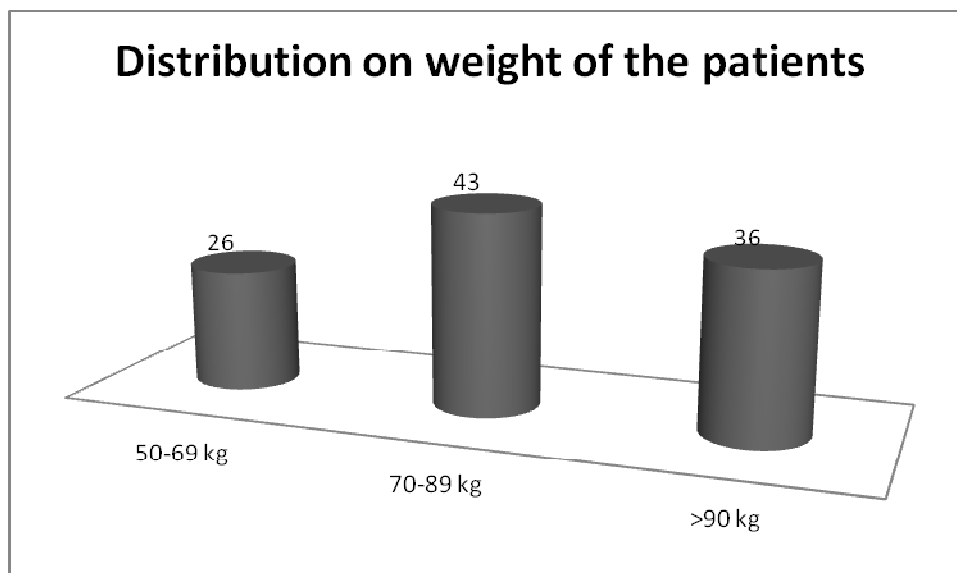


Figure 7.4.

Concerning the body mass index, there was no patient with underweight (BMI ≤ 18.5), 28% were with normal weight (BMI = 18.5-24.9), 44% with overweight

(BMI=25-29.9) and 28 % obese (BMI \geq 30). The body mass index was calculated after the known formula BMI = kg/m².

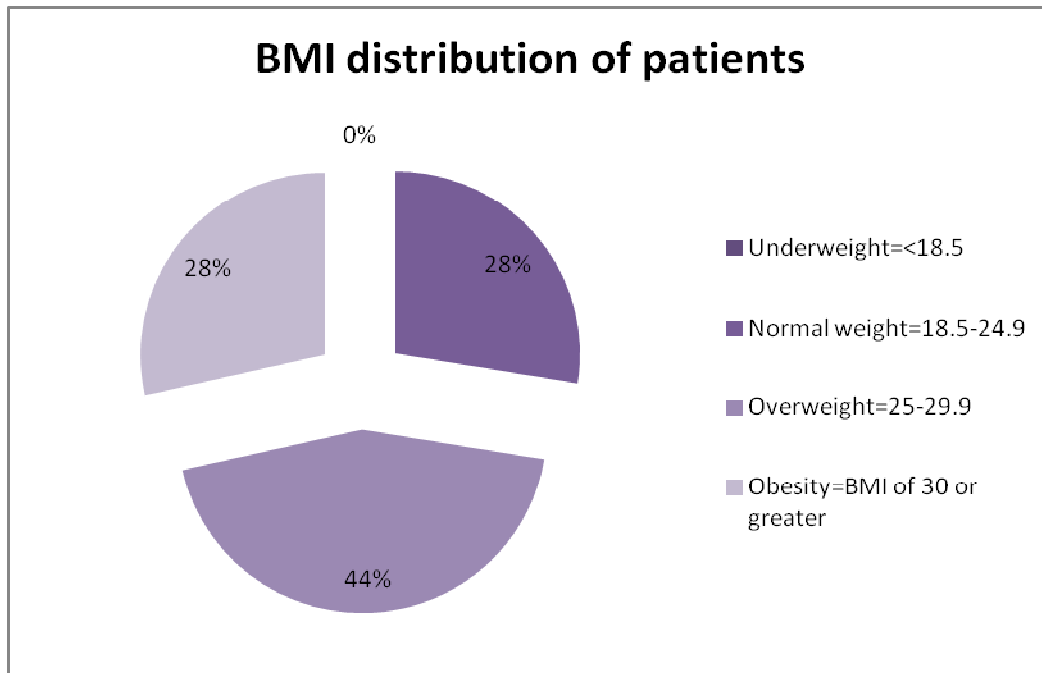


Figure 7.5.

The femur length and the thigh thickness were also measured. The knee side and the axis were introduced as study parameters and the results are shown in the next figures. There were 7 knees with a femur length between 30-40 cm (7%) , 75 between 40-50 cm (71%) and 23 over 50 cm (22%). 27 (26%) patients had a thigh thickness between 40-50 cm, 58 (55%)between 50-60 cm and 20 subjects (19%) over 60 cm.

There were analysed 44 left knees (42%) and 61 right knees (58%).

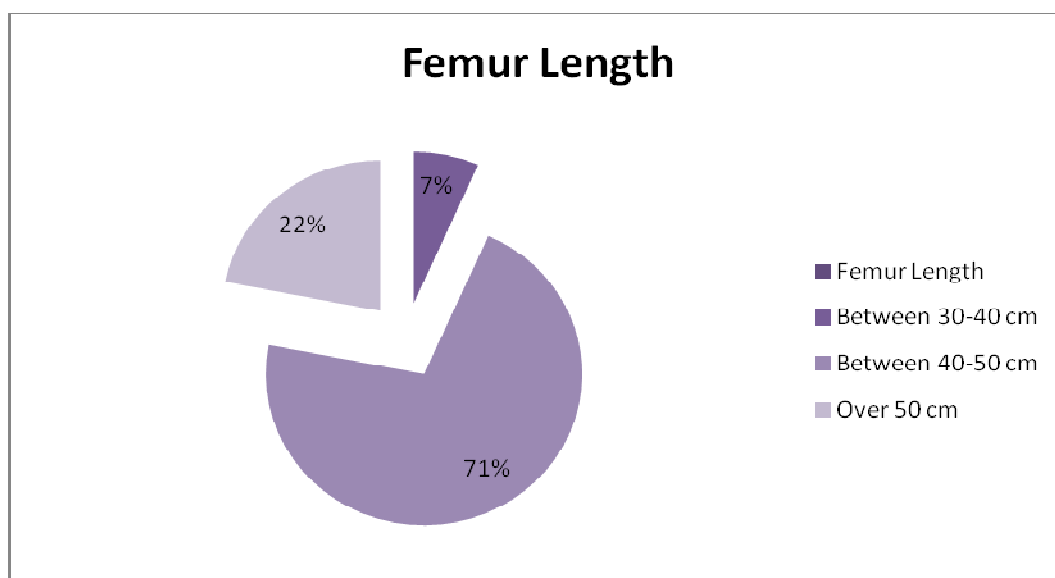


Figure 7.6.

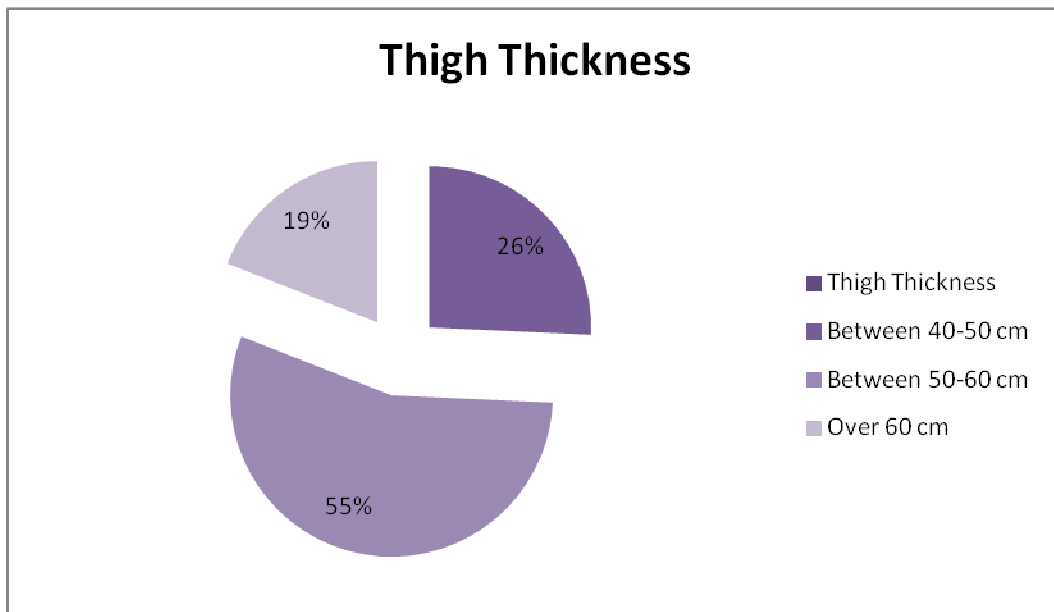


Figure 7.7.

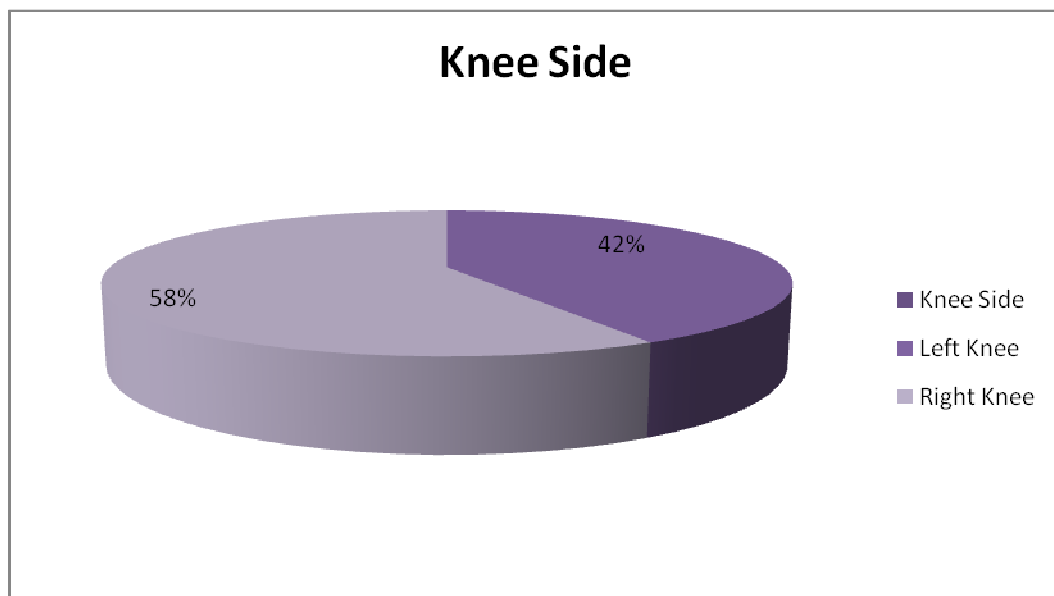


Figure 7.8.

There were observed 59 knees with a normal clinical anatomical axis, 17 knees with valgus axis, 11 till 5° valgus, 4 between $5-10^\circ$ and 2 over 10° valgus and 29 knees with varus, 9 with varus till 5° , 18 between $5-10^\circ$ and 2 over 10° varus. The patients with knee effusion were excluded from the study because of interferences with the measurement. A effusion grade I was accepted, because of good results by the acoustic emission measurements. The results are represented below.

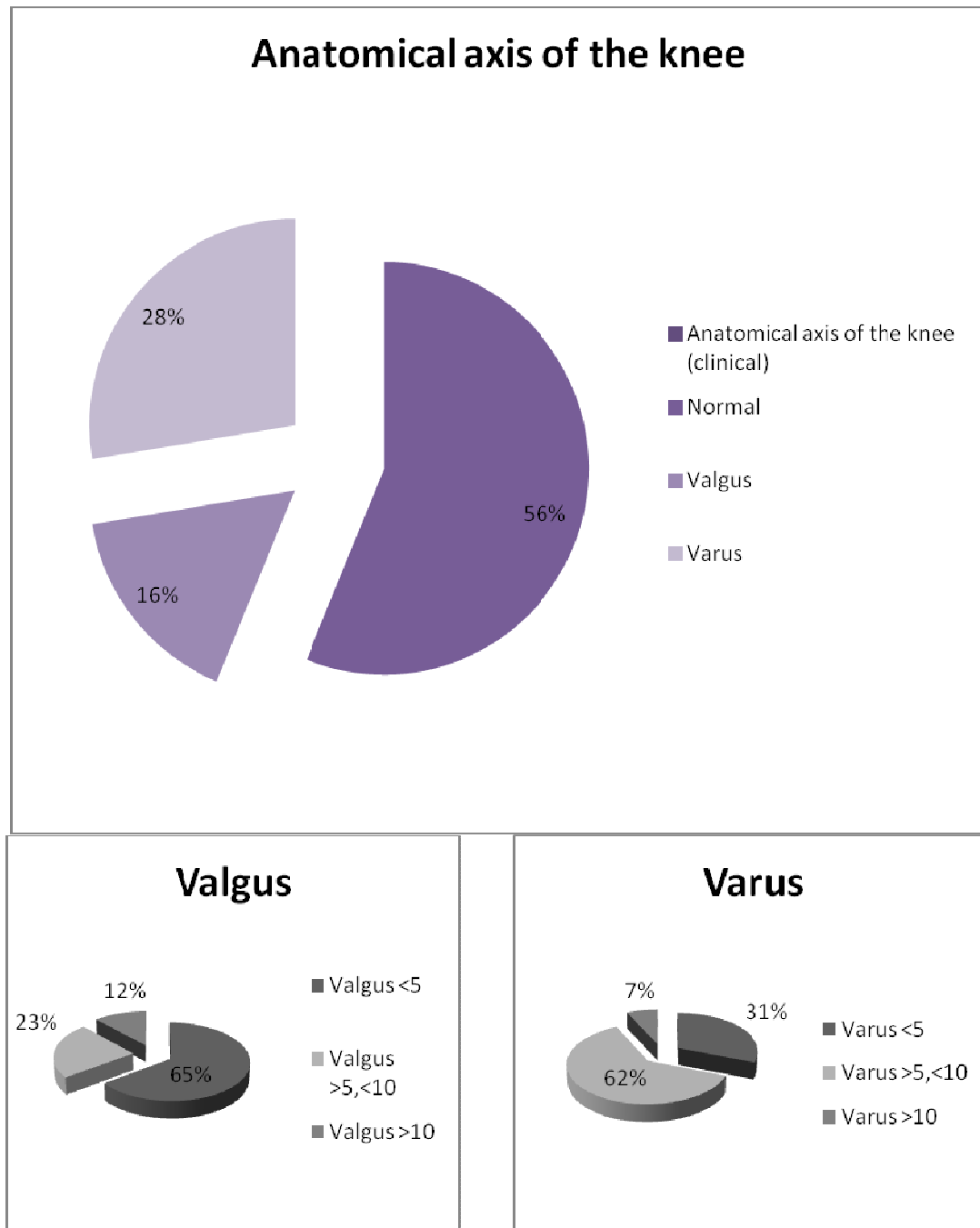


Figure 7.9.

From 105 patients, 55 received an arthroscopy and 50 a total knee replacement. After the classification of Outerbridge, grade 0 is normal, white-appearing cartilage, grade I swelling or softening of an intact cartilage surface, grade II represented by fissuring and fibrillation over a small area (<1,2 cm), grade III with the same pathological changes over a large area (>1,2 cm) and grade IV with erosion to the subchondral bone, indistinguishable from osteoarthritis we distinguished

chondromalacia grade 0 at 6 of the recruited patients, grade I at 4 patients, grade II at 6 patients, grade III at 18 subjects and grade IV at 71 patients. There were a few patients who had solitary lesions of grade II, III or IV, the most of them had combined lesions and the lesion of upper grade was taking in study.

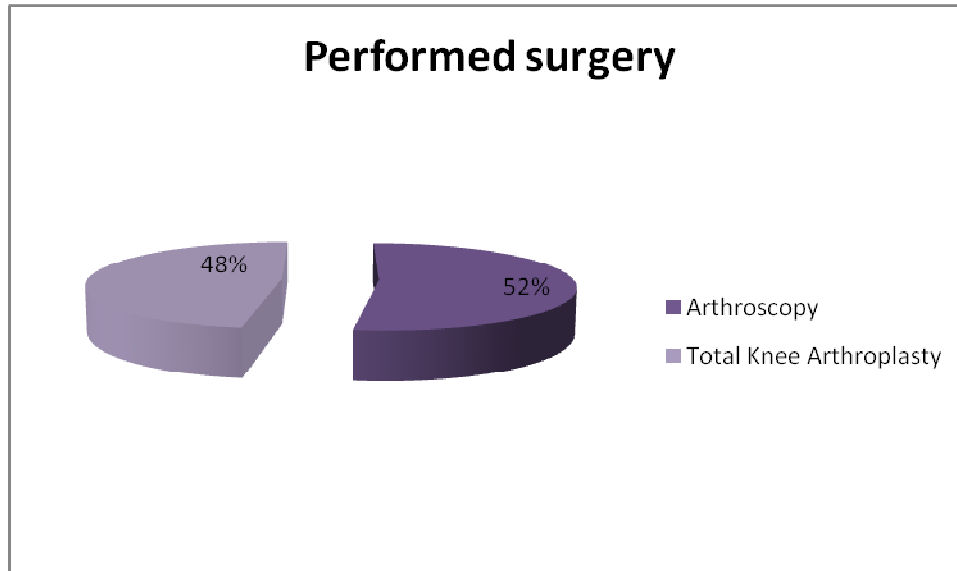


Figure 7.10.

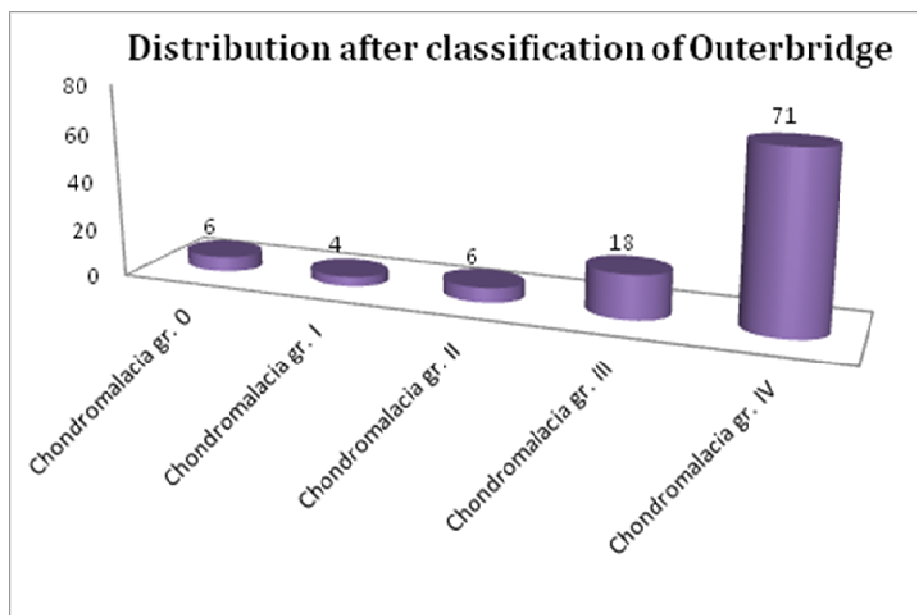


Figure 7.11.

From the signals obtained from the knee we could differentiate : signals for the crack initiation in the femur in 10 cases, signals for the cartilage lesion of the knee in 68 cases, the combination of those two signals in 15 cases and no signals or no typically signals in 12 cases.

Signals obtained with the BONDIAS acoustic measurement system

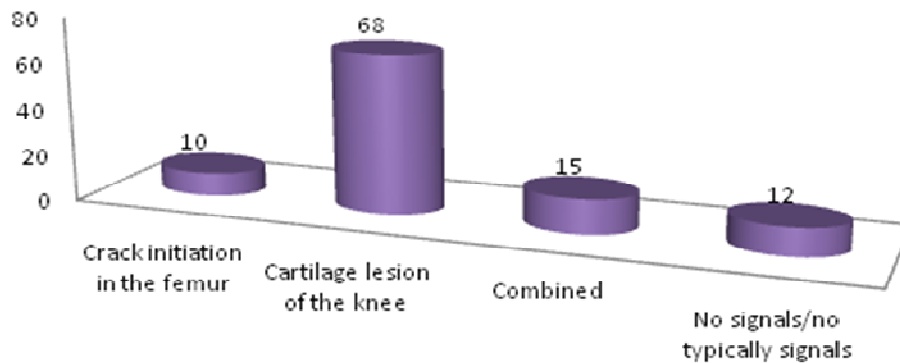


Figure 7.12.

It was analysed and studied if there were a correspondence between
 ~ the age and the sex of the subjects, the length of the femur, the thigh thickness, the BMI, the anatomical axis of the knee and the appearance and severity of the cartilage lesions

~ the obtained signals with BONDIAS system and the intra-operative findings

The statistical analysis was performed using Microsoft Office Excel and the WINKS Statistical Data Analysis Program.

The relation between the age (VAR1) and the severity of cartilage injuries (VAR2) is shown in the next sequences and the next figure.

For these data,

the Mean(SD) of VAR1 for VAR2 = 0,00 is 34,5(11,2205), N= 6,

the Mean(SD) of VAR1 for VAR2 = 1,00 is 37,5(15,1767), N= 4,

the Mean(SD) of VAR1 for VAR2 = 2,00 is 48,1667(17,9044), N= 6,

the Mean(SD) of VAR1 for VAR2 = 3,00 is 51,3889(16,3136), N= 18,

and the Mean(SD) of VAR1 for VAR2 = 4,00 is 64,338(11,1008), N= 71.

(Results must be interpreted in the context of the practical {i.e. clinical} implications of any observed differences.)

There can be observed that the severity of cartilage injuries increase with the age, as advanced with the age the patients are, increases the grade of cartilage disorders.

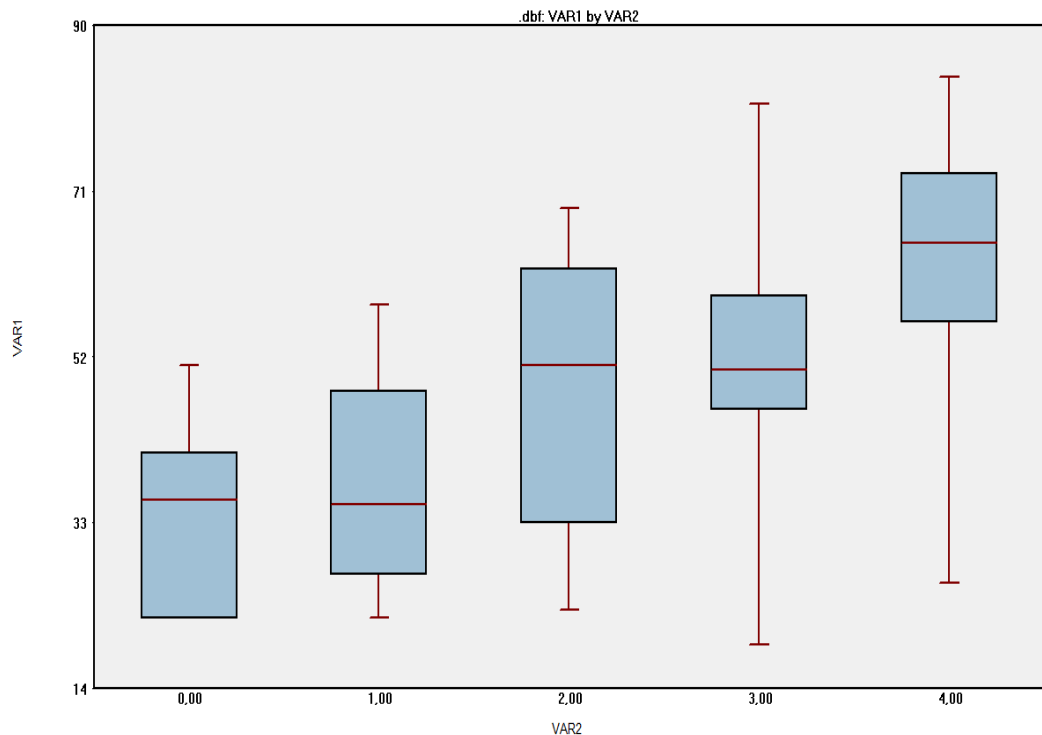


Figure 7.13. Relation between age(VAR1) and cartilage injuries after Outerbridge(VAR2).

Regarding the sex of the patients and the anatomical axis of the knee, there could not be found correspondences between the any of the both variable and the appearance and severity of the cartilage disorders.

The relation between the length of the femur and the cartilage injuries was not offering any similarities. (VAR1=length of the femur, VAR2=grade of injuries after Outerbridge).

For these data,

the Mean(SD) of VAR1 for VAR2 = 0,00 is 48,5(6,1237), N= 6,

the Mean(SD) of VAR1 for VAR2 = 1,00 is 50,5(5,4467), N= 4,

the Mean(SD) of VAR1 for VAR2 = 2,00 is 49,8333(6,6458), N= 6,

the Mean(SD) of VAR1 for VAR2 = 3,00 is 50,5556(5,8533), N= 18,

and the Mean(SD) of VAR1 for VAR2 = 4,00 is 45,507(5,2505), N= 71.

(Results must be interpreted in the context of the practical {i.e. clinical} implications of any observed differences.)

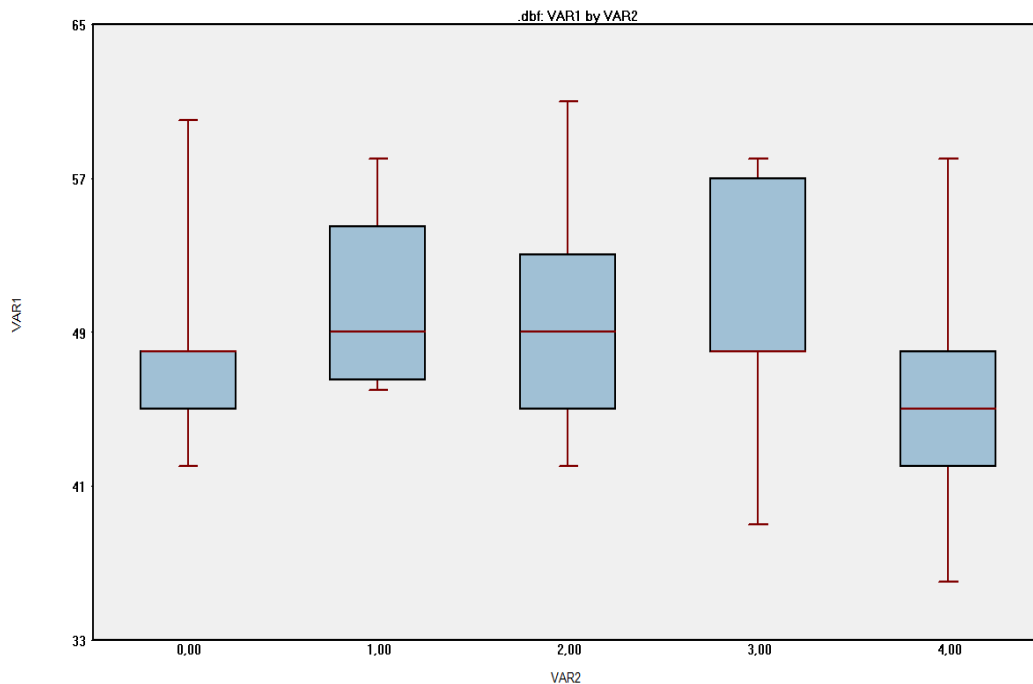


Figure 7.14. Relation between femur length(VAR1) and severity of cartilage injuries(VAR2).

Afterwards it was analysed if there is a correlation between the thigh thickness and the grade of cartilage injuries. A directly correlation could not be noted neither in this case, a great thickness of the thigh being observed also at patients with no cartilage injuries, and also at those with arthritic defects.

For these data,

the Mean(SD) of VAR1 for VAR2 = 0,00 is 54,0(8,7407), N= 6,

the Mean(SD) of VAR1 for VAR2 = 1,00 is 50,25(4,6458), N= 4,

the Mean(SD) of VAR1 for VAR2 = 2,00 is 51,0(,8944), N= 6,

the Mean(SD) of VAR1 for VAR2 = 3,00 is 54,0556(5,8256), N= 18,

and the Mean(SD) of VAR1 for VAR2 = 4,00 is 54,8169(7,1939), N= 71.

(Results must be interpreted in the context of the practical {i.e. clinical} implications of any observed differences.)

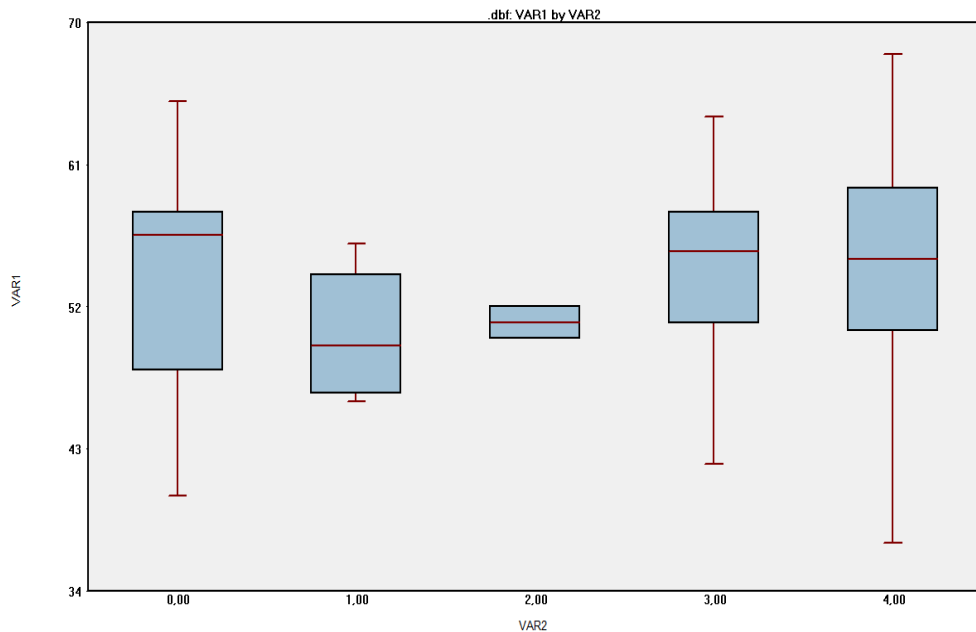


Figure 7.15. Correlation between thigh thickness(VAR1) and the severity of cartilage injuries (VAR2).

The correspondence between the Body Mass Index (VAR1) and the cartilage damage severity (VAR2) is shown below. A direct correlation could not be observed, although the severe IV^o injuries appeared by subjects with high body mass index, the most of them obese.

For these data,

the Mean(SD) of VAR1 for VAR2 = 0,00 is 26,265(5,1394), N= 6,

the Mean(SD) of VAR1 for VAR2 = 1,00 is 25,3075(3,6038), N= 4,

the Mean(SD) of VAR1 for VAR2 = 2,00 is 24,9917(3,7559), N= 6,

the Mean(SD) of VAR1 for VAR2 = 3,00 is 27,4783(4,0058), N= 18,

and the Mean(SD) of VAR1 for VAR2 = 4,00 is 28,7654(4,6820), N= 71.

(Results must be interpreted in the context of the practical {i.e. clinical} implications of any observed differences.)

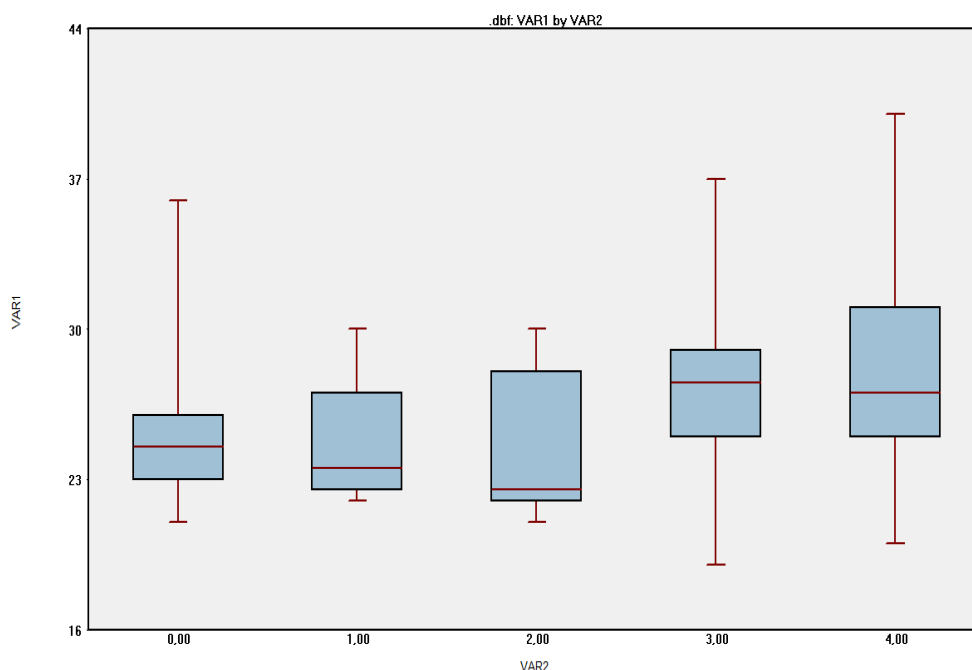


Figure 7.16. Correspondence between BMI (VAR1) and Outerbridge cartilage damage (VAR2)

To answer the second question, a diagram was filled for each patient (after the arthroscopically intervention or after the open surgery), where the lesions were schematically drawn, the location, the area and with the help of the diagram below, it could be noted at which grade of flexion the lesion appears.

The patients with grade 0 and I of cartilage lesions after Outerbridge, because of the similarity, and not obvious differences of cartilage lesions, were analysed together, when they were compared with the acoustic signals.

10 patients with chondromalacia gr. 0 and I had the following results with the BONDIAS system: by 5 measurements no signals were obtained (one patient had a medial meniscus lesion, one patient had a lateral meniscus ganglion, one patient had jumper's knee, two had a plica syndrom, none of them had articular cartilage disorders), so we could interpret as a 50% correspondence. The other 5 measurements were with no typically signals or with signals of cartilage lesions, so we could not assess as similarity with the intra-operative findings (Figure 7.21.).

From 6 patients with chondromalacia gr. II, 3 had signals by the measurement who corresponded with the intraoperative findings (Figure 7.22.). An example is shown below (Figure 7.17. and 7.18.). There were a II° lesion, on the medial femurcondyle, in

the located area and the signal, typically for a cartilage lesion appeared at 119° of flexion.

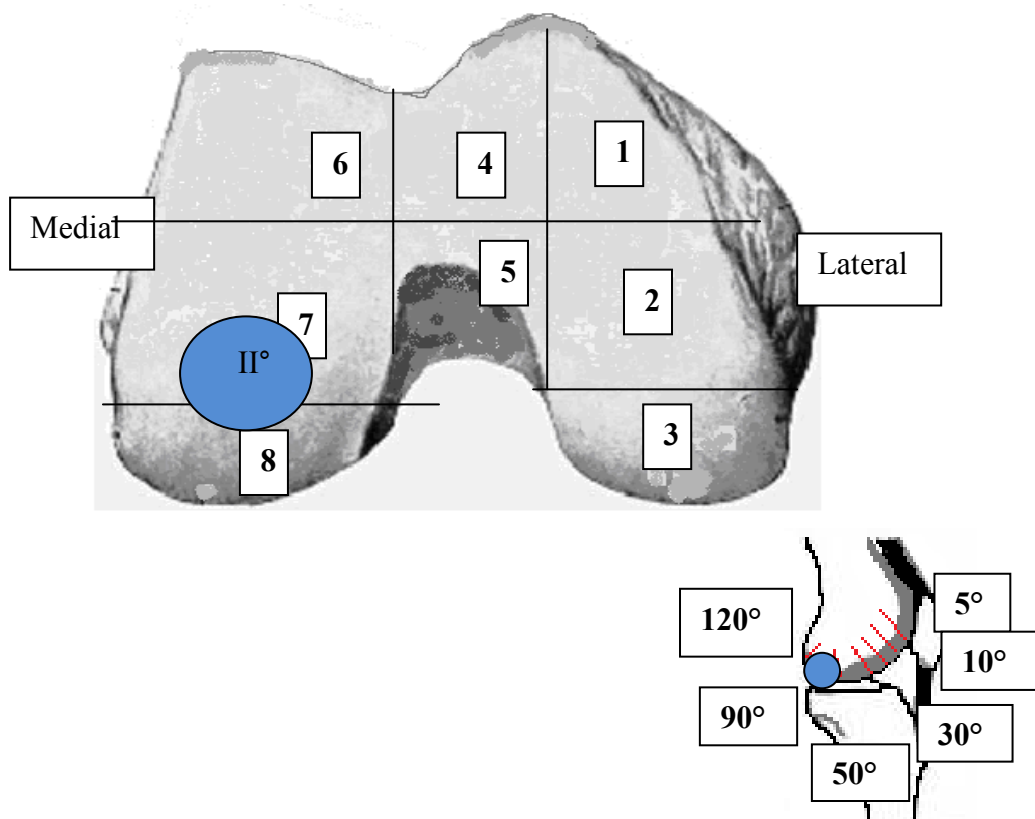


Figure 7.17.

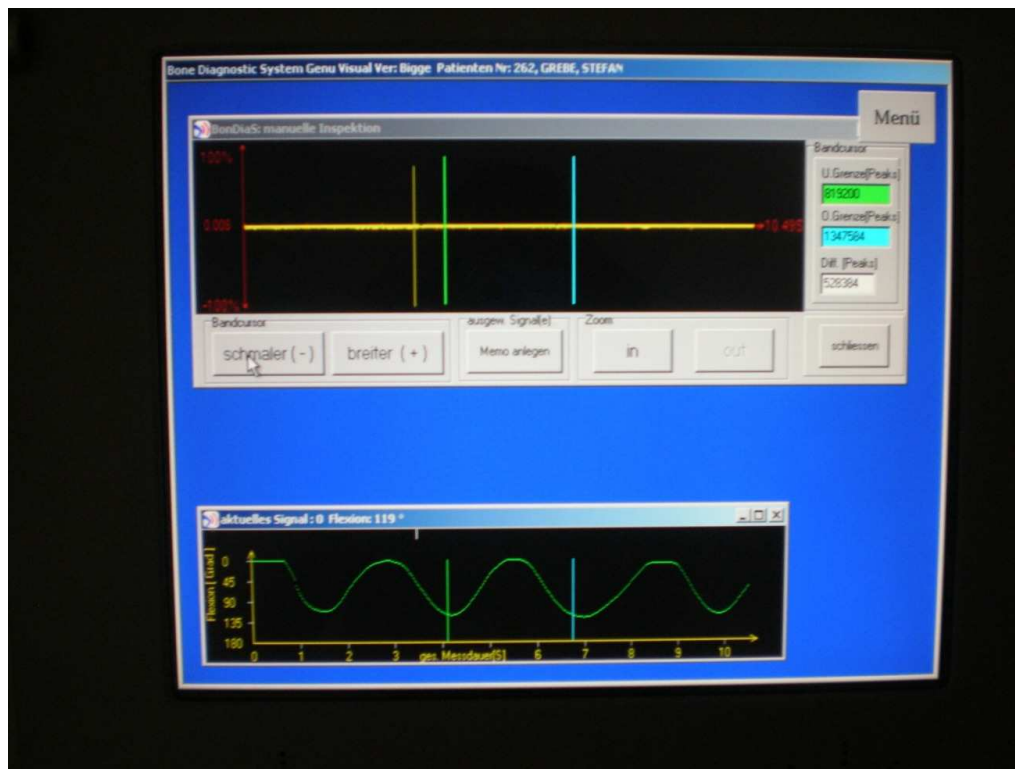


Figure 7.18.

From 18 patients with chondromalacia III°, 12 correspondences (67%) are observed and 6 measurements (33%) that did not shown similarities (Fig. 7.23.). By the patients with chondromalacia IV°, most of them were with big areas of cartilage injuries, receiving a total knee arthroplasty. The signals were multiple and were combined signals of crack initiation in the femur with cartilage lesion signals. There were also patients with isolated IV° cartilage defects. An example is showed in the next images. A signal of cartilage lesion appeared at 42° of flexion, corresponded with the IV° injury in the trochlear groove (Fig. 7.19. and 7.20.). For the patients with chondromalacia IV° (71) there were 45, where the signals were multiple, showing that the friction produced because of the lesions was high. Only in 17 cases with isolated IV° disorders was detected a correspondence between the grade of lesion and the its location. Considering that the 45 measurements showed also signs of cartilage lesions or crack initiation of femur, we evaluated these signals as corresponded with the intra-operative findings. In 9 cases there were not similarities found (Fig. 7.24.).

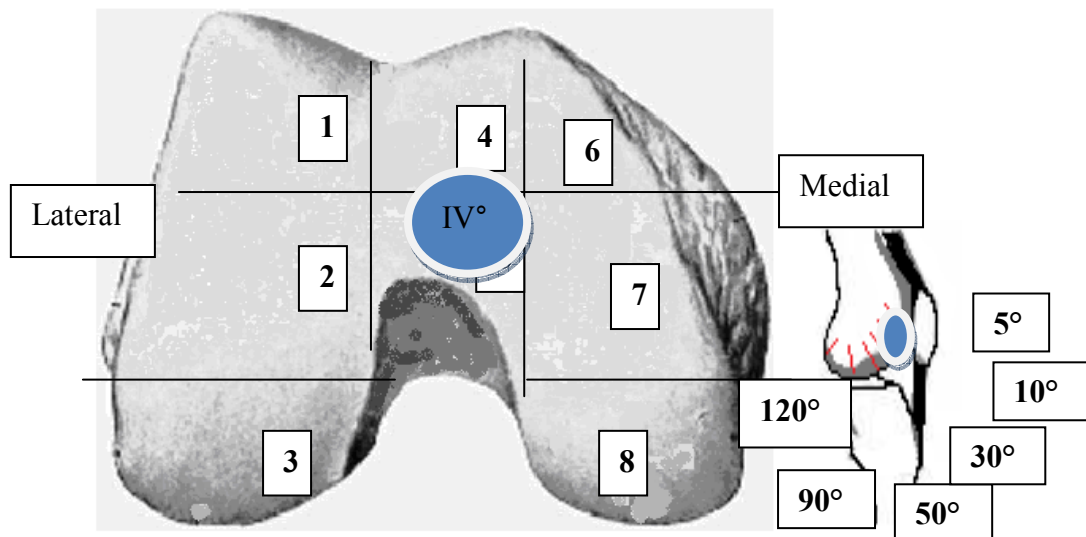


Figure 7.19.

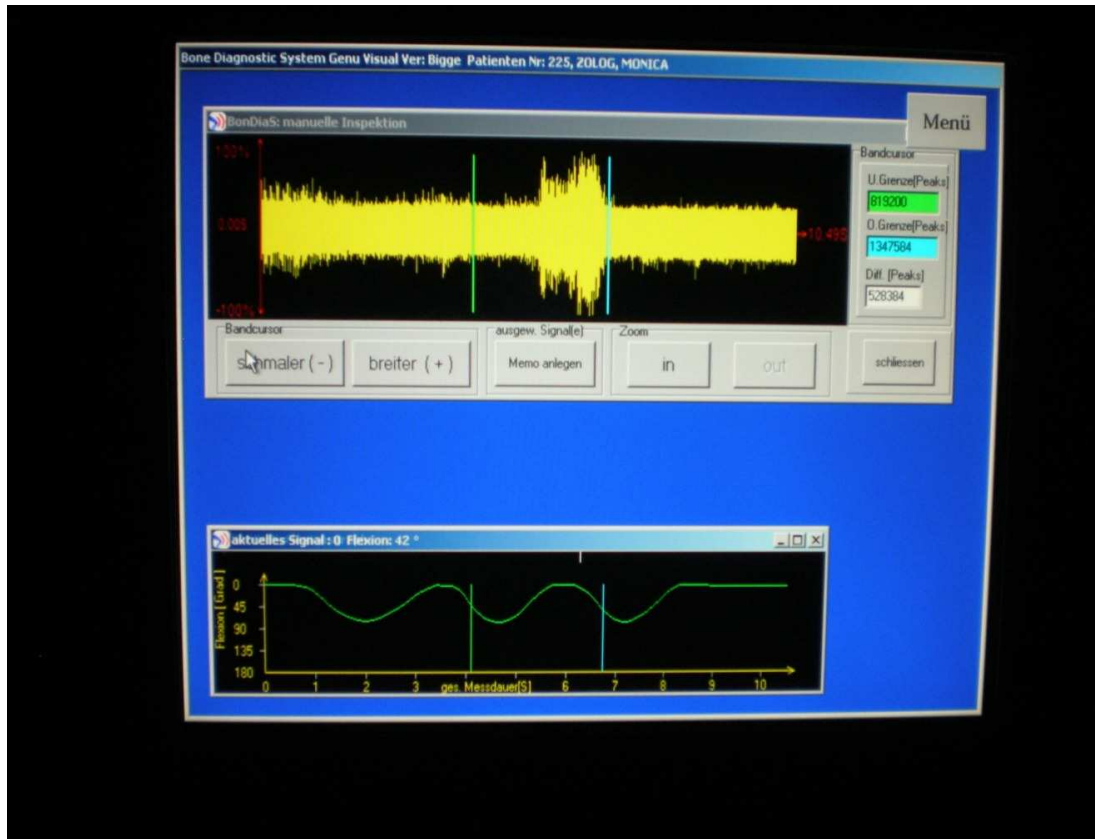


Figure 7.20.

The results are represented schematically in the next figures (7.21.,7.22.,7.23. and 7.24.).

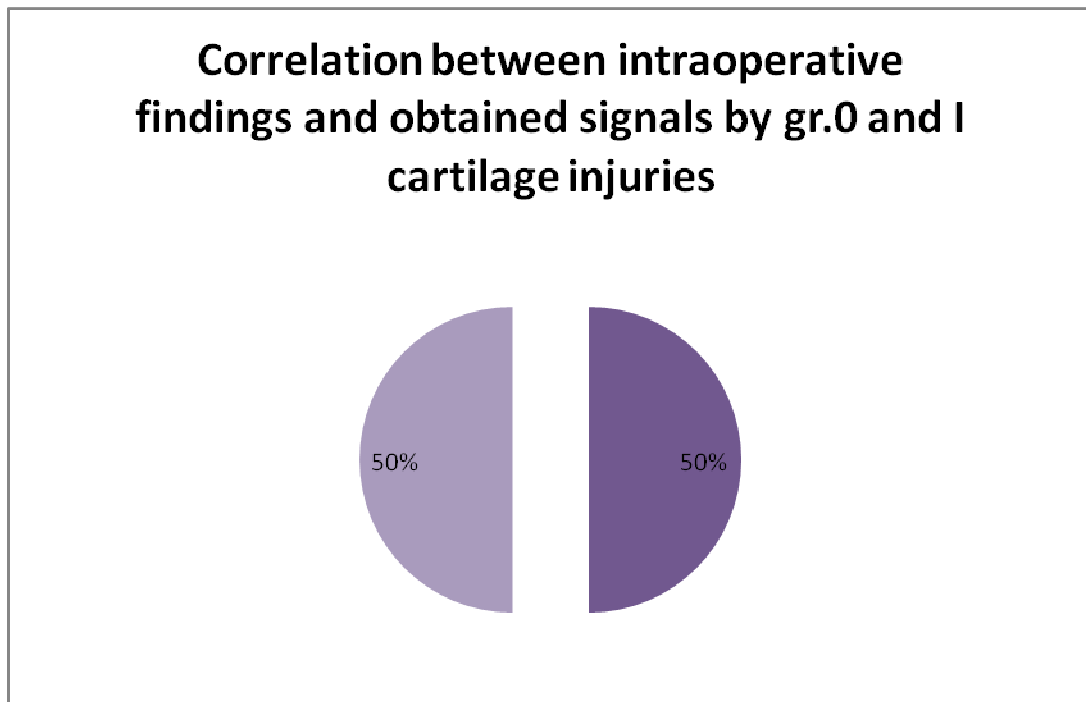


Figure 7.21.

Correlation between intraoperative findings and obtained signals by gr. II cartilage injuries

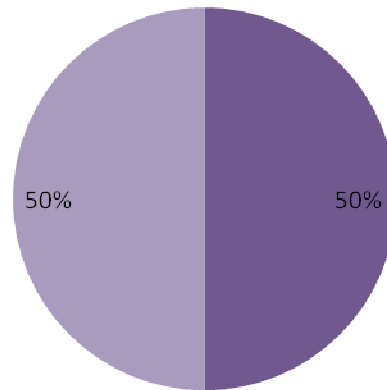


Figure 7.22.

Correlation between intraoperative findings and obtained signals by gr. III cartilage injuries

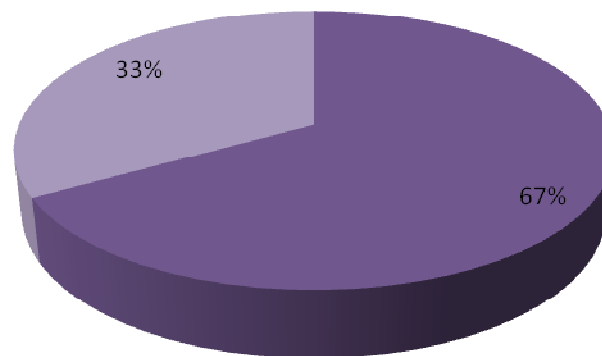


Figure 7.23.

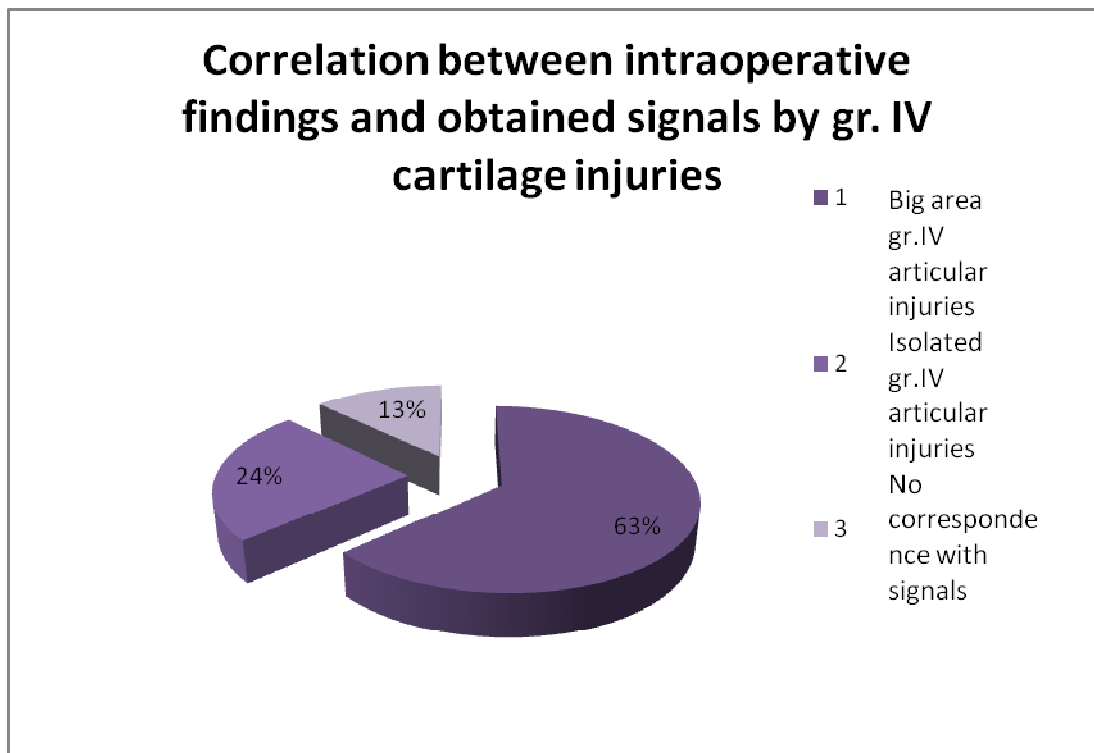


Figure 7.24.

9. DISCUSSIONS

BONEDIAS acoustic measurement system was developed in the last three years and there is no other similar device on market at this moment. Tribology, the science and technology of interacting surface in relative motion brings new perspectives in diagnostic of articulation diseases. Acoustic signals are used till now in stethoscopy and phonocardiography and there are good chances to be implemented also in the study of articulation pathology.

BONEDIAS acoustic measurement system is a non-invasive and cheap method (in analogy with the other invasive – x-ray, or expansive – magnetic resonance imaging, methods). It doesn't harm at all the patients, the only minimal problem would be a lack of understanding and for some patients (for example obese or with a not so good mobility) a difficulty to proceed slowly and regularly the knee squats. The system is also an easy method for the doctor, the nurse or technical assistant, whoever makes the measurement. The learning process takes a few minutes only. The measurement is also reproducible, it can be made many times and changes can be observed and interpreted in a period of time or before or after a surgery.

An important observation is that there are typically signals for cartilage lesions because of the friction process in the articulation, so that we can interpret objective these lesions, when the signals appear. The signals because of the crack initiation in the femur appeared with the knee squats are also typically, so they give us also important information.

The knee is the largest synovial joint in the body, it is a modified hinge joint and its biomechanic is not simple. The flexion and extension at this joint differ from those of a true hinge as the axis about which the movement occurs is not fixed, but translates upwards and forwards during extension and backwards and downwards during flexion. The knee joint possesses limited inherent stability from the bony architecture. The lack of conformity between bony surfaces allow 6° of freedom of motion about the knee including translation in 3 planes (medio-lateral, antero-posterior, proximo-distal) and rotation in 3 planes (flexion/extension, internal/external, varus/valgus). During normal knee motion in the sagittal plane from full extension to full flexion, the instant center pathway moves posteriorly, forcing a combination of rolling and sliding to occur between the articular surface. The unique mechanism prevents the femur rolling off the posterior aspect of the tibia plateau as the knee goes into increased flexion. The

mechanism that prevents this roll-off is the link formed between the tibial and femoral attachment sites of the anterior and posterior cruciate ligaments and the osseous geometry of the femoral condyles. With increased flexion, the tibio-femoral joint will be compressed. In a knee with cartilage lesions, the femoral condyles will glide in a defect zone and they will glide out from the defect zone. This will be registered, more or less, with the help of acoustic signals that are initialized because of the crack/contact in tibio-femoral joint. There are still others components involved in the biomechanics of the knee, the cruciate ligaments, the collateral ligaments, the posterior capsule, the hamstrings, gastrocnemius muscles, the menisci. How much influence they have in appearance of these acoustic signals, this is not yet really defined and at this moments not able to be interpreted objective. The acoustic emission of the frictional behavior, however, allows an evaluation of the state of cartilage degeneration. The method indicates acoustically active defects in the human joint.

A study with 125 knee recordings was performed in 1999 (Hans Joachim Schwalbe, Guido Bamfaste, Ralf Peter Franke). Hence an apparatus for testing the wear in the knee joint was developed, which makes it possible to simulate a more or less physiological roll-glide friction. A qualitative differentiation between damaged and undamaged joints has been achieved. Artificially set defects cause typical acoustic emissions in a reproducible form. Clinical tests with this acoustic emission analytical system which were performed in parallel to the commonly used diagnostic methods, showed that the analysis emission allows a differentiation of joint defects and their consequences. The technique used was also the acoustic emission analysis. Acoustic emission is based on the phenomenon that under load stored energy is released spontaneously by crack initiation and propagation. This is the so called type of acoustic emission. Friction processes, too, cause acoustic emission. But the series of pulses are in the slope of the individual acoustic signal. This is the continuous form of acoustic emission. In the case, that the cracking is accompanied by friction in already existing crack banks, a continuous acoustic emission with low amplitude and energy overlaps the burst signal. The frictional behavior and the gliding mechanism in human joints, while moving under load, can be discriminated and analysed thanks to a well distinguishable form of emission. This form of acoustic emission, corresponding to the physiological roll-glide motion of a human knee joint with known lesions under well defined load. The long rise time of the acoustic signal is obvious. The slope of the signal does not follow an exponential course. The measuring device has to be adapted to

the characteristic signals of acoustic emission generated by crack initiation and propagation or by frictional behavior of articulation surfaces with regard to the surrounding noise. It turned out to be favourable to select from the broadband acoustic emission signal a band of frequencies where the difference of the signal amplitude and the interfering noise amplitude is as large as possible. In the study of Prof. Schwalbe a resonance frequency of the transducer of 100Hz was chosen. The transducer was fixed directly on the bone in the fracture- and friction-tests of the explanted bones or directly on the surface of the skin in the in-vivo-tests of patients. The transducer was an undamped piezoelectric converter, connected to an amplifier with an integrated impedance converter. The amplified acoustic signal was filtered by a band-pass within the resonant frequency band of the transducer. Depending on its intensity the signal was further amplified and then evaluated according to the test query. For a comparison between artificial damage in knee joints, a field test was carried out among volunteers of the faculty members and students of the Technical College Gießen Friedberg and patients with well known joints defects of the orthopaedic clinic Passauer Wolf. It was demonstrated that acoustic emission is reproducible and that there were a correlation between the extent of the damage and the acoustic emission, that an evaluation of the state of wear and friction of human joints under physical strain is possible. [26]

Studies and works about the acoustic emission role in the diagnostic of bone diseases were made also in the United States in 2001, where a non-invasive bone condition data acquisition system performed sensitive and reliable clinical data acquisition, localization and classification of bone disease, particularly osteoporosis. The bone condition data acquisition system measured a correlation between a wideband acoustic emission signature and a spatially localized bone microarchitecture, which was used to determine fracture risk. The bone condition data acquisition system included processors and memory for analyzing acoustic emission signals from bone tissue to generate information-bearing attributes, for extracting a set of times-of-arrival and a feature vector from the attributes, for utilizing the set of times-of-arrival to derive the locations of the acoustic emission events and for responding to the feature vector to classify the bone using a neural network and a nearest neighbor rule processor. [78] This study was made with a provisional patent 6,213,958 (“acoustic emission stimulation of biological tissue structures”, Winder), which was filed with the U.S. Patent and Trademark Office, which described an ultrasound device that employed nonlinear acoustics to stimulate biological tissue (such as bone tissue), for producing

acoustic emissions. The use of nonlinear acoustics in an ultrasound projector is a key requirement for developing a commercially viable acoustic emission monitoring device for medical applications. This technology was used with this patent to create a diagnostic system for acoustic emission monitoring. The proposed systems approach employs an acoustic model originally developed (and successfully used by the author) for various military sonar applications. There was a substantial scientific evidence suggesting that acoustic emission monitoring can be used to describe the strength and quality of bone tissue. This will provide a means for early detection, localization and characterization of metabolic bone disease and bone cancer. The ultimate goal was to build a database of acoustic fingerprints of specific pathological bone conditions, such as osteoporosis. The foundation of acoustic emission physics is based on what is referred to as the “Kaiser Effect” and the “Felicity Effect”. The Kaiser Principle states that materials present acoustic emission only under unprecedented stress. Acoustic emission are attributed to frictional rubbing of grains against each other in polycrystalline materials and also from intergranular fractures. The Kaiser Effect states that many materials show low levels of acoustic emission beginning at very low stress levels, all the way through to final failure. The Kaiser Effect has been tested to be valid for various materials, including metals, woods and other mineral composites. The Felicity Effect is the exception to the Kaiser Principle. It states that when an acoustic emission occurs at stresses lower than the peak stress of the previous acoustic emission, it typically indicates significant permanent damage in the material.

U.S. Patent 6,213,958 (“Methods and apparatus for the acoustic emission monitoring detection, localization and classification of metabolic bone disease”, Winder, 2001) described a diagnostic system to detect, localize and characterize the acoustic emission produced by applying noninvasive mechanical stimulation to the musculoskeletal system. These wideband acoustic emission were extremely rich with information on tissue composition and structure that has not been at that time explored by investigators. Although it was not known with 100% certainty whether the acoustic emission method actually works for bone tissue, all the work performed for the past twenty-five years in the field of acoustic emission materials testing overwhelmingly supports the concept. Acoustic emission monitoring has been investigated by several researchers in the 1970’s as a diagnostic tool for osteoporosis. Hanagud, Clinton and associates [42] showed that the acoustic emission rate from cattle femurs subjects to bending loads is greater for low density specimens as compared to those with normal

density. These emissions were detected well before the actual bone failure. In a fairly study, Leichter and associates [77,78] examined the acoustic emission from cancellous bone under compression. They also found that the post-yield acoustic emission rates were significantly higher in both osteoporotic and osteoarthritic bone specimens, compared to normal bone. In an earlier study, Katz and Yoon [60] related ultrasonic wave propagation measurements to the structure and anisotropic mechanical properties of osteoporotic and osteopetrotic bone. Their results showed that osteoporosis is characterized by increased porosity or decreased density, while osteopetrosis forms calcified cartilage in bone and affects the elastic stiffness and Young's modulus of bone tissue.

Acoustic emission was studied also in Jerusalem Osteoporosis Center, where was investigated the relation between the nature of acoustic emission signals emitted from cancellous bone under compression and the mechanical properties of the tissue. The examined bone specimens were taken from 12 normal, 31 osteoporotic and 6 osteoarthritic femoral heads. The mechanical behavior of the osteoporotic bone specimens was found to be significantly different from that of the normal specimens both in the pre-yield and post-yield ranges. In the osteoarthritic bones only the elastic behavior was significantly different. The rates of acoustic events before yield and beyond it were found to be significantly higher both in the osteoporotic and osteoarthritic bone specimens. The average peak amplitude of the signals was also significantly higher in the diseased bones. Stepwise regression analysis showed that a combination of the acoustic emission parameters could significantly predict some mechanical properties of the bone. The energy absorbed during compression and the ultimate compressive stress of the specimens could be estimated from the rate of pre-yield acoustic events, the average amplitude of the signals and the rate of post-yield events. However, the explanation power of the acoustic emission parameters was only moderate. The nature of acoustic emission signals was thus demonstrated to be a potential tool for assessing bone quality. [77]

A study about the prediction of mechanical properties of healing fractures using acoustic emission was made in Japan in 2000. The objective was to develop a non-destructive method for monitoring fracture healing with acoustic emission. Experimentally produced fractures of the rat femur were tested in tension and in torsion at 4,6,8 and 12 weeks after the fracture. Acoustic emission signals were monitored during mechanical tests. The values for load and torque at the initiation of the acoustic

emission signal were defined as new mechanical parameters. The apparent density and ash density of the fracture site were also measured at each time period. Tensile strength, tensile stiffness, maximum torque and torsional stiffness of the fracture site increased with time. The acoustic emission signal was detected before complete specimen failure. Load and torque for initiation of acoustic emission increased proportionally with increasing mechanical properties. The mineral density, however, reached a plateau at 8 weeks, when callus mechanical strength was approximately 50% of control. Load for initiation of acoustic emission was strongly correlated with the strength, stiffness and failure strain of the callus. Torque for initiation of acoustic emission was highly correlated with the maximum torque and torsional stiffness of the callus. The findings of the study indicated that some mechanical properties of healing fractures could be estimated by monitoring acoustic emission signals. [134]

In Finland there was made a study where there were investigated several novel quantitative biophysical methods, including ultrasound indentation, quantitative ultrasound techniques and magnetic resonance imaging, for diagnosing the degenerative changes of articular cartilage, typical for osteoarthritis. In this study, the combined results of these novel diagnostic methods were compared with histological (Mankin score), compositional (proteoglycan, collagen and water content) and mechanical (dynamic and equilibrium moduli) reference measurements of the same bovine cartilage samples. Receiver operating characteristics analysis was conducted to judge the diagnostic performance of each technique. Indentation and ultrasound techniques provided the most sensitive measures to differentiate samples of intact appearance from early or more advanced degeneration. Furthermore, these techniques were good predictors of tissue composition and mechanical properties. The specificity and sensitivity analyses revealed that the mechano-acoustic methods, when further developed for in vivo use, may provide more sensitive probes for osteoarthritis diagnostics than the prevailing qualitative x-ray and arthroscopic techniques. Noninvasive quantitative MRI measurements showed slightly lower diagnostic performance than mechano-acoustic techniques. The compared methods could possibly also be used for the quantitative monitoring of success of cartilage repair. [68]

Cartilage injuries are a real problem, disease of the joints, in which articular cartilage is degenerated and eventually, worn away. The early changes in cartilage tissue, associated with osteoarthritis, include loss of proteoglycans and degradation of the collagen fibril network (Buckwalter and Mankin, 1997). This leads to softening of

the tissue (Armstrong and Mow, 1982). Softened articular cartilage fails to resist impact forces during normal loading and this endangers this tissue to fissures and fibrillation (Palmoski and Brandt, 1981). Tissue degeneration leads to inflow of water and thereby, to an increase in water content of the tissue. At this stage, cartilage is even more prone to wearing. Besides degenerative changes in cartilage, the underlying bone undergoes a remodeling process that leads to a sclerosis of the subchondral bone (Radin, 1976). [108] The developing cartilage injuries increases pain, restricts exercise and limits physical capability. The earliest degenerative changes may be reversible, changing loading conditions, surgical operation or potentially pharmacological intervention may slow down the progression of cartilage lesions (Buckwalter and Mankin 1997, Freeman 1999). When osteoarthritis progresses to its terminal point, cartilage tissue is almost completely worn away exposing the subchondral bone. Currently, there is no efficient way to re-establish eroded cartilage and, therefore, only palliative treatment or arthroplasty can be used to relieve patients. Therefore, it would be crucial to recognize the very early changes of cartilage injuries to target the treatment efficiently.

Traditionally, the diagnosis of cartilage injuries is based on patients' symptoms and X-ray imaging. The measurement of joint gap narrowing in X-ray images is an indirect way to assess the thickness of articular cartilage between two articulating bones. Unfortunately, the changes visible with this method represent the final stages. Magnetic resonance imaging or arthroscopy are also used to evaluate the integrity of articular cartilage. The costs of these two methods are indeed very high and can be introduced as screening. Further, the emergence of novel surgical methods for repairing damage cartilage has increased the demand for sensitive assessment of the quality of repaired cartilage.

The study below has the advantage of comparing the acoustic emission measurements with intra-operative findings, offering objective results. A correspondence between the age and the sex of the subjects, the length of the femur, the thigh thickness, the BMI, the anatomical axis of the knee and the appearance and severity of the cartilage lesions was studied supplementary. Beside the age of the patients, there were not fine any directly correspondences with the severity of the cartilage lesions and the acoustic emission signals. Important is that over 50% of the obtained acoustic emission signals were coresponded with the intra-operative findings. For the gr. 0, I and II after Outerbridge cartilage injuries, the corespondence, even if the corespondence only 50% was, its more significant, because the lesions in this case

were minimal and were at different grades of flexion. The correlation between the intraoperative findings of grade III and IV cartilage injuries and the acoustic emission signals was over 60%. The lesions were most of them on the big surfaces and were also combined with crack initiation in the femur. Here we can conclude that by severe cartilage disorders, acoustic emission measurement system offers us objective informations about the lesions.

Actually, the problem are not the severe cartilage injuries, where the diagnostic can be achieved also clinically, but the lesions in incipient stadium. For these cases there are till now, none diagnostically methods who can accomplish certain criterion: they should be non-invasive, non-destructive, regarding that these investigations are addressed more the young people and they should be cheap, regarding the always problems of lack of money.

Arthroscopy, the more objective investigation in diagnostic of cartilage injuries, however minimal, is an invasive technique. Will it ever be adopted for determination of early asymptomatic osteoarthritis? Maybe not. At present, each year hundreds of thousands of arthroscopies are performed to patients having problems with their knee. In addition to other pathologies such as meniscal tears, ligament injuries, these patients may also have cartilage lesions, asymptomatic early osteoarthritis or advanced osteoarthritis. These patients seeking relief to their joint problems is the population that might benefit best of the information obtained with the arthroscopic instrument. Could be these cartilage injuries before diagnosed? This was the purpose and the goals of such a study, where non invasive cheap techniques have to be developed to obtain informations and prevent disease. The obtained informations could be used to study risk factors for osteoarthritis development and later, the results of such studies could help to predict osteoarthritis risk as well as to apply appropriate procedures to prevent pregression of osteoarthritis changes. Also, direct mechanical measurements can help in future to judge objectively the results of cartilage repair techniques. Further, monitoring of tissue maturation after repair surgery will help the clinicians to determine optimal amount, pattern and time schedule of external stimulation, such as mechanical loading of the joint with repaired cartilage. For screening healthy, asymptomatic individuals, it is likely that low-cost non-invasive examinations, although not readily available, are needed. The domains where such a system measurement can be implemented is diagnostic, rehabilitation, cartilage repair results, arthroplasty or even skeleton monitoring concerning daily or sportive solicitation.

My personal opinion concerning improving such a system device is the adjustment the sensor (maybe the physicists can develop a circular sensor around the knee), for emphasize the capture of sounds from the articulation and for giving more stability when the knee squats are executed.

The application of tribology and the acoustic emission due to the friction is a domain not deeply explored, but because of the reduced costs and its harmless it should really be investigated more.

10. CONCLUSIONS

Fibrillation of articular surface and depletion of proteoglycans are the structural changes related to early osteoarthritis. These changes make cartilage softer and prone to further degeneration. The aim of the present study was to combine mechanical and acoustic measurements towards quantitative arthroscopic evaluation of cartilage quality.

Osteoarthritis is one of the most important joint diseases and results in considerable economic hardship and a decrease in the quality of life of individuals. One of the first histological signs of osteoarthritis is cartilage tissue softening. After that, occurs cartilage fibrillation and disruption of the collagen network. While early changes without disruption are believed to be reversible, osteoarthritis can only be diagnosed in advanced stages, when regenerative treatment concepts fail.

Several magnetic resonance imaging, computer tomography and arthroscopic methods are under development for sensitive *in vivo* diagnostics of cartilage degeneration and early osteoarthritis (Appleyard et al.,2001; Burstein and Gray, 2003; Cherin et al., 1998; Dashefsky,1987; Hattori et al.,2004; Hermann et al.,1999; Kallioniemi et al.,2007; Kiviranta et al.,2007; Laasanen et al., 2002; Legare et al., 2002; Lvyra et al, 1995; Niederauer et al., 1998; Palmer et al. , 2006; Pellaumail et al.,2002). Arthroscopic indentation measurements have been used to determine the dynamic stiffness of cartilage *in vivo* (Dashefsky, 1987; Lyvra et al.,1999). However, the results obtained with this method include uncertainties, as the effect of unknown tissue thickness on stiffness values cannot be fully eliminated (Hayes et al.,1972).

The mechano-acoustic indentation method, ultrasound indentation, is based on characterizing the mechanical properties of cartilage by compressing. Ultrasound, acoustic emission can be used to characterize the roughness and integrity of cartilage surface (Kaleva et al.,2008; Laasanen et al.,2005; Saarakkala et al.,2004; Töyräs et al.,1999). Quantitative ultrasound measurements of cartilage properties have been shown to provide sensitive and specific measures to detect the early deterioration of cartilage (Brown et al.,2007; Hattori et al.,2005; Kiviranta et al.,2008; Laasanen et al.,2002; Pellaumail et al.,2002).

The purpose of the study below was to determine the early cartilage lesions, to define if there is indeed a correspondence between the signals and the intra-operative findings. The idea is to determine a simply, efficient, cheap and non-invasive method to diagnose the early cartilage injuries, because there isn't such a method till nowadays.

The results obtained, 50% correspondence for the gr. 0, I and II Outerbridge lesions are more important, more significant than the other results, with over 60% correspondence for the advanced osteoarthritis. The obtained acoustic emission signals, corresponding to the intra-arthroscopic findings showed the importance of this method to identify the early cartilage injuries. The method is not perfect and the results (50%) are not really statistically significant, so that we can introduce this method on a large scale, but offers important information that should be used in the future. Also, there isn't a perfect method to compare the acoustic emission signals with the intra-arthroscopic findings. Every patient was analysed separately and with his corresponding measurement compared, that means a lot of time (20 – 30 minutes for the measurement and the other questions and clinical tests and another 15 minutes to analyse the signals and compare them with the intra-operative findings). For a study this can be accepted, but for clinical every day use maybe not. A standard interpretation and analyse method, maybe after clinical large trials, if such a method can be developed, could bring big advantages for the early determination of the cartilage injuries. Microsoft Office Excel and the WINKS Statistical Data Analysis Program could permit a correlation between what was wished to compare, but the developing of a special program for such a study can improve also the results. The adjustment of the sensor that captures the sounds from the articulation could also determinate a higher and accurate level of the measurement and reduce some errors due to the application of this sensor.

In conclusion, the study had offered important informations about the importance of acoustic emission measurements, that can be used for the future studies and with some improvements, this method, cheap and non-invasive, but at this moment a little bit time-consuming, can be helpful in the diagnose of the early cartilage injuries.

11. REFERENCES

- [1] A
- [2] Allum, R., Jones, D., Mowbray, M. A. and Galway, H. R. Triaxial electrogoniometric examination of the pivot shift sign for rotary instability of the knee. *Clin. Orthop. Rel. Res.*, 1984Mar, 144-6
- [3] Andriacchi, T.P.& Birac (1993). Functional ligament testing in the anterior cruciate ligament deficient knee. *Clin Orthop Rel Res*, 288 (March), 40-47
- [4] Andriacchi, T.P. Strickland (1985). Gait analysis as a tool to assess joint kinetics. In N.Berme, A.E.Engin,D.A.Correis. *Biomechanics of Normal and Pathological Human Articulating Joints* (NATO ASI series Vol.93, pp 83-102)
- [5] Adams DJ, Brosche KM, Lewis JL. Effect of specimen thickness on fracture toughness of bovine patellar cartilage. *J. Biomech Eng* 2003, Dec., 125(6):927-9
- [6] B
- [7] Blankevoort, L. Passive motion characteristics of the human knee joint: experiments and computer simulations. PhD thesis, University of Nijmegen, 1991
- [8] Blankevoort, L., Huiskes, R. and de Lange, A. Helical axes of passive knee joint motions. *J. Biomechanics*, 1990, 23(12), 1219-29
- [9] Blankevoort, L., Huiskes, R. and de Lange, A. The envelope of passive knee-joint motion. *J. Biomechanics*, 1988, 21(9), 705-20
- [10] Bull, A. M. J. and Amis, A. A. Letter to the editor—accuracy of an electromagnetic tracking device. *J. Biomechanics*, 1996, 29(6), 791-3.
- [11] Bull, A. M. , Andersen H.N., Basso O., Targett J, Amis A.A. Incidence and mechanism of the pivot shift. An in vitro study. *Clin Orthop Rela Res* (1999), Jun (363), 219-31
- [12] C
- [13] Churchill, D. L., Incavo, S. J., Johnson, C. C. and Beynnon, B. D. The transepicondylar axis approximates the optimal flexion axis of the knee , *Clin Orthop Rela Res*, 1998,Nov,(356), 111-8.
- [14] Cooper, C., Cushnaghan, J., Kirwan, J. R., Dieppe, P. A., Rogers, J., McAlindon, T. and McCrae, S. Radiographic assessment of knee joint in osteoarthritis. *Ann. Rheum. Dis. (UK)*, 1992
- [15] Crowninshield, R., Pope, M. H. and Johnson, R. J. An analytical model of the knee. *J. Biomechanics*, 1976, 9(6), 397-405

[16]D

[17]Dahlkvist, N. J. and Seedhom, B. B. Objective measurement of knee laxity and stiffness with reference to knee injury diagnosis. Part 1: design considerations and apparatus. Proc. Instn Mech. Engrs, Part H, Journal of Engineering in Medicine, 1990, 204(2), 75-82

[18]Dennis, D. A., Komistek, R. D., Hoff, W. A. and Gabriel, S. M. In vivo knee kinematics derived using an inverse perspective technique. Clin. Orthop. Rel. Res., 1996, Okt (331), 107-117

[19]Dimnet, J. The improvement in the results of kinematics of in vivo joints., J. Biomechanics, 1980, 13(8), 653-61

[20]Draganich, L. F., Sathy, M. R. and Reider, B. The effect of thigh and goniometer restraints on the reproducibility of the genucom knee analysis system. Am. J. Sports Med., 1994, Sept-Oct, 22(5), 627-31.

[21]E

[22]Eberhardt, K. B. and Selvik, G. Some aspects of knee joint kinematics in rheumatoid arthritis as studied with Röntgen stereophotogrammetry. Clin. Rheumatol., 1986, Jun, 5(2), 201-9

[23]Eckstein, G. Ateshian, Krishnan, Park. Inhomogeneous cartilage properties enhance superficial interstitial fluid support and frictional properties, but do not provide a homogeneous state of stress, Journal of biomechanical engineering, 2003, Oct, 125(5), 569-77

[24]F

[25]Franke, R.P., Schwalbe H.J., Doerner P., Ziegler B. - Orthopädische Diagnose des menschlichen Femurs und Kniegelenks mit Hilfe der Schallemissionsanalyse

[26]Franke, Dörner, Schwalbe, Ziegler, Acoustic emission measurement system for the orthopedical diagnostics of the human femur and knee joint, 2004

[27]Freddie H. Fu, Christopher D. Harner, Kelly G. Vince - Knee surgery, p.325-350

[28]Frankel, V.H., Burstein, A.H. & Brooks (1971). Biomechanics of internal derangement of the knee. Pathomechanics as determined by analysis of the instant centers of motion. J Bone Joint Surg, 53A, 945

- [29] Fukuda, Y., Takai, S., Yoshino et al (2000). Impact load transmission of the knee joint-influence of leg alignment and the role of meniscus and articular cartilage. *Clinical Biomech*, 15, 516-521
- [30] G
- [31] Gardner, T.R., Ateshian, G.A., Grelsamer (1994). A 6 DOF knee testing device to determine patellar tracking and patellofemoral joint contact area via stereophotogrammetry. *Adv Bioeng ASME BED*, 28, 279-280
- [32] Goh, J. C. H., Lee, P. Y. C. and Bose, K. A cadaver study of the function of the oblique part of vastus medialis. *J. Bone Jt Surg.*, 1995, Mar.77(2), 225-31
- [33] Gollehon, D. L., Torzilli, P. A. and Warren, R. F. The role of the posterolateral and cruciate ligaments in the stability of the human knee. A biomechanical study. *J. Bone Jt Surg.*, 1987, Feb.69(2), 233-42
- [34] Goodfellow, J. and O'Connor, J. The mechanics of the knee and prosthesis design. *J. Bone Jt Surg.*, 1978, Aug.60-B(3), 358-69
- [35] Grood, E. S. and Sunlay, W. J. A joint coordinate system for the clinical description of three-dimensional motions: application to the knee. *Trans. ASME, J. Biomech. Engng*, 1983, May,105(2), 136-44
- [36] Grood, E. S., Stowers, S. F. and Noyes, F. R. Limits of movement in the human knee. Effect of sectioning the posterior cruciate ligament and posterolateral structures. *J. Bone Jt Surg.*, 1988, Jan., 70(1), 88-97
- [37] Grood, E. S., Noyes, F. R., Butler, D. L. and Suntay, W. J. Ligamentous and capsular restraints preventing straight medial and lateral laxity in intact human cadaver knees. *J. Bone Jt Surg.*, 1981, Oct.,63(8), 1257-69
- [38] Growney, E. and Chao, E. Y. Measurement of joint kinematics using ExpertVision system. *Biomed. Sci. Instrum.*, 1991, 27:245-52
- [39] H
- [40] Hinterwimmer S., Krammer M., Krötz M., Glaser C., Baumgart R., Reiser M, Eckstein F. Cartilage atrophy in the knees of patients after seven weeks of partial load bearing. *Arthritis Rheum* 2004, Aug.50 (8), 2516-20
- [41] Herberhold C., Faber S., Stammberger T., Steinlecher M., Putz R., Englmeier KH, Reiser M., Eckstein F. In situ measurement of articular cartilage deformation in intact femoropatellar joints under static loading, *J. Biomech* 1999, Dec 32(12), 1287-95
- [42] Hanagud S., R.G. Clinton and J.P. Lopez, „Acoustic Emission in Bone Substance”, *Proc. Biomech Symp (ASME)*, 1973, p. 79-81

- [43] Hanagud S., G.T.Hannon and R. Clinton, "Acoustic Emission and Diagnosis of Osteoporosis", I.E.E.E. Symp on Ultras, 1974, 77-80
- [44] Hanagud S. and R.G. Clinton, "Acoustic Emission Techniques in the Development of a Diagnostic Tool for Osteoporosis", Ultras Symp Proc, 1975
- [45] Helfet, A.J.(1974). Anatomy and mechanics of movement of the knee joint. In A. Helfet (Ed.) , Disorders of the knee (p.1-17), Philadelphia: J.B. Lippincott
- [46] Hertling, R. Kessler - Management of common musculoskeletal disorders/ Physical therapy principles and methods
- [47] Hollister, A. M., Jatana, S., Singh, A. K., Sullivan, W. W. and Lupichuk, A. G. The axes of rotation of the knee. Clin. Orthop. Rel. Res., 1993, May (290), 259-68
- [48] Holden, J.P., Chou, G.& Stanhope (1997). Changes in knee joint function over a wide range of walking speeds. Clinical Biomech, 12 (6), 375-382.
- [49] Hsieh HH, Walker PS - Stabilizing mechanisms of the loaded and unloaded knee joint. J Bone Joint Surg 58A:87, 1976, Jan 58(1), 87-93
- [50] I
- [51] Inman VT, Rolston HJ, Todd F: Human Walking. Baltimore, Williams & Wilkins, 1981
- [52] Insall. Scott - Surgery of the Knee (Third Edition) p. 13-16, 17-19, 22-24, 95-156
- [53] Ishii, Y., Terajima, K., Terajima, S., Imura, K., Imaizumi, S., Koga, K., Hara, T. and Takahashi, H. E. Three-dimensional kinematics of the human knee with intracortical pin fixation, Clin Orthop Relat Res, 1997, Oct (343), 144-50
- [54] J
- [55] Jacobsen, M. C., Berglund, L. J. and Chao, E. Y. Application of a magnetic tracking device to kinesiological studies. J. Biomechanics, 1988, 21(7), 613-20
- [56] Jevsevar, D. S., Riley, P. O., Hodge, W. A. and Krebs, D. E. Knee kinematics and kinetics during locomotor activities of daily living in subjects with knee arthroplasty and in healthy control subjects. Phys. Ther., 1993, Apr.73(4), 229-39
- [57] Jonsson, H., Kärrholm, J. and Elmqvist, L. G. Kinematics of active knee extension after tear of the anterior cruciate ligament. Am. J. Sports Med., 1989, Nov-Dec, 17(6), 796-802
- [58] K
- [59] Kaiser, J. Erkenntnisse und Folgerungen aus der Messung von Geräuschen bei Zugbeanspruchung von metallischen Werkstoffen. Arch. Eisenhüttenwesen

- [60]Katz J.L. and H.S. Yoon, “The structure and anisotropic mechanical properties of bone”, IEEE Trans on Biomed Engrg, December 1984, 31(12), 878-84
- [61]Kapandji IA: The Physiology of the Joints, Vol.2, p.72-135, Paris:Editions Maloine
- [62]Kärrholm, J., Selvik, G., Elmqvist, L. G., Hansson, L. I. and Jonsson, H. Three-dimensional instability of the anterior cruciate deficient knee. J. Bone Jt Surg., 1988, Nov, 70(5), 777-83
- [63]Kärrholm, J., Elmqvist, L. G., Selvik, G. and Hansson, L. I. Chronic anterolateral instability of the knee. A Röntgen stereophotogrammetric evaluation. Am. J. Sports Med., 1989, Jul-Aug, 17(4),555-63
- [64]Kettelkamp, D. B., Johnson, R. J., Smidt, G. L., Chao, E. Y. and Walker, M. An electrogoniometric study of knee motion in normal gait. J. Bone Jt Surg., 1970, Jun, 52(4), 775-90
- [65]Kettelkamp, D.B.&Jacobs, A.W. (1972). Tibiofemoral contact area determination and implications. J Bone Joint Surg, 54A, 349.
- [66]Kinzel, G. L., Hall Jr, A. S. and Hillberry, B. M. Measurement of the total motion between two body segments. I. Analytical development. J. Biomechanics, 1972, Jan,5(1), 93-105
- [67]Kirstukas, S. J., Lewis, J. L. and Erdman, A. G. 6R instrumented spatial linkages for anatomical joint motion measurement. Part 1: design. Trans. ASME, J. Biomech. Engng, 1992, Feb 114(1), 92-100
- [68]Kiviranta P. et al, “ Comparision of novel clinically applicable methodology for sensitive diagnostic of cartilage degeneration”, European Cell and Materials Vol.13, 2007, Apr 3(13), 46-55
- [69]Kowalk, D. L., Duncan, J. A. and Vaughan, C. L. Abduction-adduction moments at the knee during stair ascent and descent. J. Biomechanics, 1996, 29, 383-8
- [70]Kurosawa, H., Walker, P. S., Abe, S., Garg, A. and Hunter, T. Geometry and motion of the knee for implant and orthotic design. J. Biomechanics, 1985, 18(7),487-99
- [71]Kuster, P.Podsiadlo, Shape of wear particles found in human knee joints and their relationship to osteoarthritis, British Journal of Rheumatology, 1998, Sep,37(9),978-84
- [72]L
- [73]Lafortune, M. A. The use of intra-cortical pins to measure the motion of the knee joint during walking. PhD thesis, Pennsylvania State University, 1984

- [74] Lafortune, M. A., Cavanagh, P. R., Sommer III, H. J. and Kalenak, A. Three-dimensional kinematics of the human knee during walking. *J. Biomechanics*, 1992, Apr.25(4),347-57
- [75] Lahm, M.Uhl – Articular cartilage degeneration after acute subchondral bone damage, *Acta Orthop Scand*, 2004, Dec.75(6), 762-7
- [76] Lane, J. G., Irby, S. E., Kaufman, K., Rangger, C. and Daniel, D. M. The anterior cruciate ligament in controlling axial rotation. An evaluation of its effect. *Am. J. Sports Med.*, 1994, Mar-Apr, 22(2), 289-93
- [77] Leichter et al, “Acoustic emission from trabecular bone during mechanical testing: the effect of osteoporosis and osteoarthritis”, *Proc Inst Mech Eng*, 1990, Vol.204, P.123-127
- [78] Leichter, Bivas, Margulies, Roman, Simkin, US Patent 6213958 Method and apparatus for the acoustic emission monitoring detection, localization and classification of metabolic disease, 2001
- [79] Lewis, J. L. and Lew, W. D. A method for locating an optimal 'fixed' axis of rotation for the human knee joint. *Trans. ASME, J. Biomech. Engng*, 1978,11(8-9),365-77
- [80] Lewis, J. L. and Lew, W. D. A note in the description of articulating joint motion. *J. Biomechanics*, 1977,10(10), 675-8
- [81] Livesay, G. A., Morrow, D. A., Sakane, M., Rudy, T. W., Fu, F. H. and Woo, S. L. Evaluation of the effect of joint constraints on the force distribution within the ACL. *Trans. Orthop. Res. Soc.*, 1997, 15(2), 278-84
- [82] M
- [83] Maquet PGJ: *Biomechanics of the Knee*. Heidelberg, Springer-Verlag, 1976
- [84] Markolf, K. L., Graff-Radford, A. and Amstutz, H. C. In vivo knee stability, a quantitative assessment using an instrumented clinical testing apparatus. *J. Bone Jt Surg.*, 1978, Jul.60(5), 664-74
- [85] Markolf, K. L., Mensch, J. S. and Amstutz, H. C. Stiffness and laxity of the knee—the contributions of the supporting structures. A quantitative in vitro study. *J. Bone Jt Surg.*, 1976, Jul.58(5), 583-94
- [86] Mayer T.,R. Gatchel, P.Polatin, N. Hadler - Occupational musculoskeletal disorders
- [87] Matsumoto, H., Seedhom, B.B., Suda et al. (2000). Axis of tibial rotation and its change with flexion angle. *Clin Orthop*, 371, 178-182.

- [88] McCarty Koopman (Vol. 2) - Arthritis and allied conditions, 1061-1077
- [89] Mensch, J. S. and Amstutz, H. C. Knee morphology as a guide to knee replacement. Clin. Orthop. Rel. Res., 1975, Oct(112), 231-41
- [90] Menschik, A. Mechanik des Kniegelenkes 1. Teil. Z. Orthop., 1974, 112, 481-495
- [91] Menschik, A. Mechanik des Kniegelenkes 2. Teil: Schlussrotation. Z. Orthop., 1975, 113, 388-400
- [92] Migaud, H., Gougeon, F. and Diop, A. In vivo kinematics during level walking and stair climbing after total knee replacements: analysis in 19 patients with unilateral prosthesis. J. Bone Jt Surg., 1995, 81(3), 198-210
- [93] Milne, A. D., Chess, D. G., Johnson, J. A. and King, G. J. W. Accuracy of an electromagnetic tracking device: a study of the optimal operating range and metal interference. J. Biomechanics, 1996, Jun, 29(6), 791-3
- [94] Morrey, Hazel WA- Results of meniscectomy in the knee with anterior cruciate ligament deficiency, Clin Orthop Relat Res, 1993, Jul (292), 232-8
- [95] Morrison, J. B. The mechanics of the knee joint in relation to normal walking. J. Biomechanics, 1970, 3, 51-61
- [96] Meachim G, Fergie IA, Morphological patterns of articular cartilage fibrillation, J Pathol, 1975, Apr., 115(4), 231-40
- [97] Murray, M.P., Drought, A.B., Kory (1964). Walking patterns of normal men. J Bone Joint Surg, 46A, 335
- [98] N
- [99] Nilsson, K. G., Karrholm, J. and Ekelund, L. Knee motion in total knee arthroplasty. A Roentgen stereophotogram-metric analysis of the kinematics of the Tricon-M knee prosthesis. Clin. Orthop. Rel. Res., 1990, Jul., (256), 147-61
- [100] Nilsson, K. G., Kárrholm, J. and Gadegaard, P. Abnormal kinematics of the artificial knee. Roentgen stereophotogrammetric analysis of 10 Miller-Galante and five New Jersey LCS knees. Acta Orthop. Scand., 1991, Oct., 62(5), 440-6
- [101] Nordin Frankel - Basic Biomechanics of the Musculoskeletal System, p.177-201
- [102] Nordin & Özkaya (1999). Fundamentals of Biomechanics: Equilibrium, Motion and Deformation (2nd ed.) New York, Springer Verlag
- [103] P

- [104] Panjabi, M. M., Goel, V. K., Walter, S. D. and Schick, S. Errors in the centre and angle of rotation of a joint: an experimental study. *Trans. ASME, J. Biomech. Engng*, 1982, Aug,104(3), 232-7
- [105] Pennock, G. R. and Clark, K. J. An anatomy-based coordinate system for the description of the kinematic displacements in the human knee. *J. Biomechanics*, 1990, 23(12), 1209-18
- [106] R
- [107] Radcliffe, C. W. Four-bar linkage prosthetic knee mechanisms: kinematics, alignment and prescription criteria. *Prosthet. Orthop. Int.*, 1994, Dec, 18(3), 159-73
- [108] Radin, I.Paul, M.Lowy, A comparison of the dynamic force transmitting properties of subchondral bone and articular cartilage, *The journal of bone and joint surgery*, 1970, Apr, 52(3), 446-56
- [109] Ramakrishnan, H. K. and Kadaba, M. P. On the estimation of joint kinematics during gait. *J. Biomechanics*, 1991, 24(10), 969-77
- [110] Ramsey, D.K.& Wretenberg, P.F. (1999). Biomechanics of the knee: Methodological considerations in the in vivo kinematic analysis of the tibiofemoral and patellofemoral joint. Review paper. *Clinical Biomech*, 14, 595-611.
- [111] Reuben, J. D., Rovick, J. S., Schrage, R. J., Walker, P. S. and Boland, A. L. Three-dimensional dynamic motion analysis of the anterior cruciate ligament deficient knee joint. *Am. J. Sports Med.*, 1989, Jul-Aug,17(4),463-71
- [112] Rheinschmidt, C., van den Bogert, A. J., Nigg, B. M., Lundberg, A. and Murphy, N. Effect of skin movement on the analysis of skeletal knee joint motion during running. *J. Biomechanics*, 1997,Jul,30(7),729-32
- [113] Rhoads, D. D., Noble, P. C., Reuben, J. D. and Tullos, H. S. The effect of femoral component position on the kinematics of total knee arthroplasty. *Clin. Orthop. Rel. Res.*, 1993, Jan(286),122-9
- [114] Rogers (Vol.2) - *Radiology of Skeletal Trauma*, p.2016-2025
- [115] S
- [116] Saarakkala, Quantitative ultrasound imaging of degenerative changes in articular cartilage surface and subchondral bone, *Phys Med Biol* 2006, Oct 21, 51(20), 5333-46
- [117] Saied, E.Cherin, H.Gaucher – Assessment of articular cartilage and subchondral bone: subtle and progressive changes in experimental osteoarthritis using

50MHz ecography in vitro, Journal of bone and mineral research, 1997, Sep,12(9),1378-86

[118] Schwalbe H.-J., R.-P- Franke Orthopädische Diagnostik und Qualitätskontrolle mit Hilfe der Schallemissionsanalyse, 12. Kolloquium Schallemission, DGZfP, 2000, 151-160

[119] Schwalbe, R.P.Franke, Nondestructive and noninvasive observation of friction and wear of human joints and of fracture initiation by acoustic emission, Proc. Instn Mech Engrs Vol 213 Part H, 1999, 41-48

[120] Seedhom, B.B., Dowson, D.& Wright (1974). The load-bearing function of the menisci: A preliminary study. In O.S. Ingwersen et al, The Knee Joint: Recent Advances in Basic Research and Clinical Aspects (p. 37-42), Amsterdam: Excerpta Medica

[121] Shiavi, R., Limbird, T., Frazer, M., Stivers, K., Strauss, A. and Abramovitz, J. Helical motion analysis of the knee. II. Kinematics of uninjured and injured knees during walking and pivoting. J. Biomechanics, 1987, 20(7), 653-65

[122] Shiavi, R., Limbird, T., Frazer, M., Stivers, K., Strauss, A. and Abramovitz, J. Helical motion analysis of the knee. I. Methodology for studying kinematics during locomotion. J. Biomechanics, 1987, 20(5), 459-69

[123] Shoemaker, S. C., Adams, D., Daniel, D. M. and Woo, S. L. Quadriceps/anterior cruciate graft interaction. An in vitro study of joint kinematics and anterior cruciate ligament graft tension. Clin. Orthop. Rel. Res., 1993, Sep(294),379-90

[124] Sommer, H. J. and Miller, N. R. A technique for the calibration of instrumented spatial linkages used for biomechanical kinematic measurements. J. Biomechanics, 1981, 14(2), 91-8

[125] Soudan, K., van Audekercke, R. and Martens, M. Methods, difficulties and inaccuracies in the study of human joint kinematics and pathokinematics by the instant axis concept. Example: the knee joint. J. Biomechanics, 1979, 12(1), 27-33

[126] Smidt, G. L. Biomechanical analysis of knee flexion and extension. J. Biomechanics, 1973, Jan,6(1), 79-92

[127] Strathy, G. M., Chao, E. Y. and Laughman, R. K. Changes in knee function associated with treadmill ambulation. J. Biomechanics, 1983,16(7), 517-22

[128] T

[129] Tomatsu, N.Imai – Experimentally produced fractures of articular cartilage and bone, British Editorial Society of bone and Joint Surgery, 1992,May,74(3),457-62

- [130] Thomas M., Evans J.H. : Acoustic emission from vertebral bodies, *Journal of materials science letters*, 7 (1988), P. 267-269
- [131] Thomas R.A., Yoon H.S., Katz J.L. : Acoustic emission from fresh bovine femora, *IEEE Ultrasonics Symposium Proceedings New York* (1977), P. 237-241
- [132] V
- [133] Van Dijk, R., Huijskes, R. and Selvik, G. Roentgen stereo-photogrammetric methods for the evaluation of the three dimensional kinematic behaviour and cruciate ligament length patterns of the human knee joint. *J. Biomechanics*, 1979,12(9),727-31
- [134] Watanabe Y, S.Takai, Y.Arai, N. Yoshino, Y. Hirasawa, Prediction of mechanical properties of healing fractures using acoustic emission, *Orth Research Society* 2001, Jul, 19(4), 548-53
- [135] Walker, P. S., Shoji, H. and Erkman, M. J. The rotational axis of the knee and its significance to prosthesis design. *Clin. Orthop. Rel. Res.*, 1972,89,160-70
- [136] Walker, P. S., Blunn, G. W., Broome, D. R., Perry, J., Watkins, A., Sathasivam, S., Dewar, M. E. and Paul, J. P. A knee simulating machine for performance evaluation of total knee replacements. *J. Biomechanics*, 1997,Jan,30(1),83-9
- [137] Wright T.M., Volsburgh F., Burstein A.H. : Permanent deformation of compact bone monitored by acoustic emission : *Journal of biomechanics*, Vol 14 (1981), p. 405-409
- [138] Winter, D. A. (1990). In *Biomechanics and Motor Control of Human Behaviour* (2nd ed.). New York: John Wiley & Sons
- [139] Wiercholski K., H.-J- Schwalbe: A review of Friction Forces in Human Joints: *Tribologia* 1/2000 (169), 39-62
- [140] Y
- [141] Yoshioka, Y., Sin, D. and Cooke, T. D. The anatomy and functional axes of the femur. *J. Bone Jt Surg.*, 1987, Jul, 69(6), 873-80
- [142] Yoshioka, Y. and Cooke, T. D. Femoral anteversion: assessment based on functional axes. *J. Orthop. Res.*, 1987,5(1), 86-91
- [143] Yoshioka, Y., Siu, D. W., Scudamore, R. A. and Cooke, T. D. Tibial anatomy and functional axes. *J. Orthop. Res.*, 1989, 7(1), 132-7
- [144] Z

- [145] Zavatsky, A. B. and O'Connor, J. J. A model of human knee ligaments in the sagittal plane. Part 1: response to passive flexion. Proc. Instn Mech. Engrs, Part H, Journal of Engineering in Medicine, 1992, 206(3), 125-34
- [146] Zavatsky, A. B. and O'Connor, J. J. A model of human knee ligaments in the sagittal plane. Part 2: fibre recruitment under load. Proc. Instn Mech. Engrs, Part H, Journal of Engineering in Medicine, 1992, 206(3), 135-45
- [147] Zavatsky, A. B. A kinematic-freedom analysis of a flexed-knee-stance testing rig. J. Biomechanics, 1997, Mar,30(3), 277-80

Acknowledgments

I want to express my gratitude to Priv. Doz. Dr. Stefan Endres who offered me invaluable assistance, support and guidance.

Deepest gratitude to Prof. Dr. Dr. Axel Wilke, due to him I am here, in Germany, in Elisabeth Klinik Bigge, where I received the opportunity to develop myself in my profession.

Special thanks to Prof. Schwalbe und Mr. Ziegler, from Gießen, who invented BONEDIAS System, who shared the literature and helped me with the interpretations of the measurements.

I want to thank all of my colleagues from Elisabeth Klinik Bigge, who completed after the surgery the diagram of the cartilage injury location on the femoral condyle and grade of injury after Outerbridge. Without these diagrams my research would not have been possible.

I want to express also my love and gratitude to my family, my parents and my sister, for their understanding and endless love, through the duration of the study, and not only.

Ehrenwörtliche Erklärung

Ich erkläre ehrenwörtlich, dass ich die dem Fachbereich Medizin Marburg zur Promotionsprüfung eingereichte Arbeit mit dem Titel

“Acoustic Emission Measurement System in Diagnostic of Cartilage Injuries of the Knee”

unter Leitung von Priv. Doz. Dr. med. Stefan Endres mit Unterstützung durch Prof. Schwalbe ohne sonstige Hilfe selbst durchgeführt und bei der Abfassung der Arbeit keine anderen als die in der Dissertation angeführten Hilfsmittel benutzt habe. Ich habe bisher an keinem in- oder ausländischen Medizinischen Fachbereich ein Gesuch um Zulassung zur Promotion eingereicht, noch die vorliegende oder eine andere Arbeit als Dissertation vorgelegt.

Bigge, 11.11.2010

Cristina Zolog

Verzeichnis akademischer Lehrer

Meine akademischen Lehrer waren

in Cluj Napoca: Acalovschi, Anderco, Badea, Bantias, Barsan, Barsu, Benga, Bocsan, Bocu, Borzan, Buzoianu, Capalneanu, Cazacu, Ciuce, M. Cosgarea, R. Cosgarea, Cosman, A. Cristea, V. Cristea, Don, Donca, Duncea, Florian, Georgescu, Gherman, Junie, Lucaciu, Lucan, Lupu, Marginean, Miu, A. Muresan, O. Muresan, Nagy, Oarga, Olinici, Olteanu, Oprea, Paraianu, Perju, Petrov, Plesca-Manea, I. Pop, M. Pop, V. Pop, Popa, Rednic, Rusu, Sampalean, Sfrangeu, Surcel, Talos, Tiganu, Turdeanu, Vladutiu, Zaharie, Zanc.

in Marburg : Prof. Dr. Dr. Axel Wilke , Priv. Doz. Dr. Stefan Endres

CURRICULUM VITAE

Persönliche Daten

Geburtsdatum und – ort: 24. März 1979 in Cluj-Napoca (Klausenburg), Rumänien

Familienstand: ledig

Staatsangehörigkeit: rumänisch

Schulbildung

1985-1993 - Gymnasium (Lyzeum für Natur und Wissenschaft, Klausenburg)

1994-1997 - Lyzeum für Natur und Wissenschaft (Onisifor Ghibu, Klausenburg)

1997 - Abitur

Hochschulausbildung

1997 – Beginn des Studiums der Humanmedizin an der " Iuliu Hatieganu"Universität,
Klausenburg

2003 – Abschluss des Studium und Approbation als Ärztin

Berufliche Laufbahn

2003-2004 – Ärztin im Praktikum Universitätsklinikum Cluj-Napoca
(6 Monate Innere, 6 Monate Chirurgie)

2005-2006 – Assistenzärztin für Kinderchirurgie Universitätsklinikum Cluj-Napoca
Rotation 2005 Kinderchirurgie, 2006 Kinderorthopädie

2007 (Januar-Juli) – Assistenzärztin für Orthopädie und Unfallchirurgie
Universitätsklinikum Cluj-Napoca

31.07.2007 – Approbation als Ärztin an der Bezirksregierung Arnsberg

2007 Juli bis 2009 September – Assistenzärztin für Orthopädie und Unfallchirurgie
Elisabeth Klinik Bigge, Klinikdirektor Prof.Dr.Dr.Axel Wilke

2009 September bis jetzt - Assistenzärztin für Orthopädie und Unfallchirurgie Walburga
Krankenhaus Meschede, unfallchirurgische Abteilung, Chefarzt Dr.med. Detlef Drüppel

Sprachkenntnisse

- Rumänisch: Muttersprache
- Deutsch : fortgeschritten (Zertikat Deutsch, Grundstufe, im Deutsches Kultur Zentrum, Klausenburg, am 10 Juli 2002 bestanden; Mittelstufe Zertifikat im Deutsches Kultur Zentrum, Goethe Institut, am 16.07.07 bestanden)
- Englisch : fortgeschritten
- Französisch und Portugiesisch : mittelstufe

Besonderheiten

2003 – Stipendium in Deutschland, für 3 Monaten , in der orthopädischen Klinik des
Universitätsklinikums Charite (unter der Leitung von Prof.Dr.med.H.Zippel)

2007 Juni – Gastärztin am Salzburger Universitätsklinik, Orthopädie und
Kinderorthopädie Abteilung, unter der Leitung von OA Dr. Franz Landauer